TRW —11176-H593-R0-00

PROJECT TECHNICAL REPORT
TASK E-9H

AN ANALYSIS OF A PREEMPHASIS - DEEMPHASIS
TECHNIQUE FOR LCRU TELEVISION

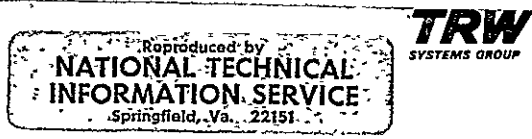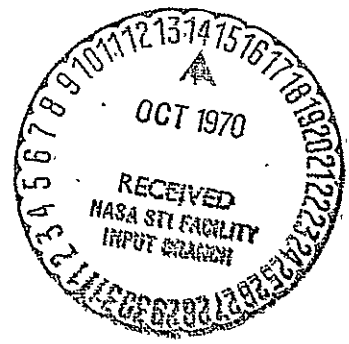NAS 9-8166   5 AUGUST 1970

Prepared for
NATIONAL AERONAUTICS AND SPACE ADMINISTRATION
MANNED SPACECRAFT CENTER
HOUSTON, TEXAS

Prepared by
Communication and Sensor Systems Department
Electronic Systems Laboratory

N70-41059

OCT 1970
RECEIVED
NASA STI FACILITY
INPUT BRANCH

TRW
SYSTEMS GROUP

CF-108606

11176-H593-R0-00

PROJECT TECHNICAL REPORT
TASK E-9H

AN ANALYSIS OF A PREEMPHASIS - DEEMPHASIS
TECHNIQUE FOR LCRU TELEVISION

NAS 9-8166   5 AUGUST 1970

Prepared for
NATIONAL AERONAUTICS AND SPACE ADMINISTRATION
MANNED SPACECRAFT CENTER
HOUSTON, TEXAS

Prepared by
R. J. Panneton

Approved by _____
W. B. Warren, Task Manager

Approved by _____
John DeVillier, Manager
Communication and Sensor
Systems Department

TRW
SYSTEMS GROUP

ACKNOWLEDGMENTS

ABSTRACT

This report investigates the use of preemphasis/deemphasis to improve the performance of the Lunar Communications Relay Unit (LCRU) television system. A theoretical analysis is made of the improvement in video signal-to-noise ratio (SNR) obtained with the use of signal emphasis on an FM channel, above and below threshold. The theoretical development, construction, and testing of preemphasis-deemphasis networks is also presented. Significant performance improvement is demonstrated by total system tests involving visual assessment of video picture quality. Experimental results indicate a minimum 3 dB RF (radio frequency) level improvement, approximately corresponding to a minimum 3.7 dB video SNR improvement, can be achieved using video signal emphasis. Good television picture quality is obtained at -90 dBm, the worst-case total-received RF power level for the LCRU-to-85-foot MSFN (Manned Space Flight Network) station link. In summary, simple preemphasis and deemphasis networks can provide improved LCRU television performance at a modest cost in terms of circuitry. It is recommended, therefore, that video signal preemphasis and deemphasis networks be implemented in the LCRU television system.

CONTENTS

CONTENTS (Continued)

TABLES

ILLUSTRATIONS

Page

ILLUSTRATIONS (Continued)

ILLUSTRATIONS (Continued)

Page

ILLUSTRATIONS (Continued)

NOMENCLATURE

AM	Amplitude modulation
CSM	Command and service module
EKG	Electrocardiogram
EMU	Extravehicular mobility unit
EVA	Extra-vehicular astronaut
EVCS	Extravehicular communications system
FM	Frequency modulation
GCTA	Ground commanded television assembly
LCRU	Lunar communications relay unit
LM	Lunar module
LRV	Lunar roving vehicle
MESA	Modularized equipment storage area
MET	Mobile equipment transporter
MSFN	Manned space flight network
PAM	Pulse amplitude modulation
PLSS	Portable life support subsystem
VHF	Very high frequency

1. INTRODUCTION

During extended lunar explorations on future Apollo missions, there will be times when a loss-of-signal will occur between the lunar module and the lunar surface astronauts. The primary purpose of the Lunar Communications Relay Unit (LCRU) subsystem is to provide a communications relay link between the Manned Space Flight Network (MSFN) and the lunar astronauts when these loss-of-signal conditions occur. A secondary purpose of the LCRU subsystem is to provide downlink transmission of the color television signal during lunar exploration, and also during ascent of the lunar module.

The purpose of this report is to document the recent analytical and experimental work which has been completed in investigating the application of preemphasis/deemphasis techniques to improve the performance of the LCRU color television system. A theoretical analysis is made of the improvement in signal-to-noise ratio gained with the use of signal emphasis on an FM channel, above and below threshold. The theoretical development, construction, and testing of preemphasis-deemphasis networks is also presented.

Section 2 presents mathematical models which may be used to represent a random video signal. The validity of these models has been verified experimentally and the choice of which model should be used for a given application is determined by the general nature of the communication problem and the desired complexity of the solution. In Section 3, two video models are used to calculate the theoretical signal-to-noise ratio improvement due to video emphasis on an FM channel. Also, the signal-to-noise ratio improvement through emphasis at carrier-to-noise power ratios in the nonlinear region of the FM detection process is derived. Section 4 describes the experimental preemphasis and deemphasis networks utilized in the evaluation of the best possible pair of networks for eventual implementation in the lunar communications relay unit color television system. Finally, in Section 5, photographs and experimental data are presented as a result of total system tests utilizing the preemphasis/deemphasis networks cited in Section 4.

1.1 LUNAR COMMUNICATIONS RELAY UNIT SUBSYSTEM

The primary purpose of the Lunar Communications Relay Unit sub-
system is to provide a communications relay link between the Manned
Space Flight Network and the astronauts on the lunar surface when there
is a loss-of-signal between the lunar module (LM) and the lunar surface
astronauts. In particular, the LCRU subsystem will provide a communica-
tions relay for uplink (MSFN to LCRU) and downlink (LCRU to MSFN) voice
and downlink EMU (Extravehicular Mobility Unit) data after loss-of-signal
between the LM and the lunar surface astronauts during extended lunar
exploration on the Apollo J-Missions (Apollo 16-19). A secondary purpose
of the LCRU subsystem is to provide downlink transmission of the color
television signal from the Ground Commanded Television Assembly (GCTA) and
to provide uplink relay of the 70 kHz subcarrier for GCTA commands during
lunar exploration sorties and also during ascent of the lunar module.

Figure 1-1 is a sketch of the LCRU installed on the lunar roving
vehicle (LRV) which is shown in mobile operation on the lunar surface.
The LCRU S-band downlink carrier frequency which will transmit voice,
data, and TV is 2272.5 MHz, while the S-band uplink received carrier
frequency containing voice and commands is at 2101.8 MHz. A LCRU VHF
carrier with frequency 296.8 MHz is used to relay voice information to the
astronauts from the earth. The VHF carrier at 259.7 MHz is used to trans-
mit voice information from EVA-1 (Extra-vehicular Astronaut No. 1) to
EVA-2 (Extra-vehicular Astronaut No. 2) and also to transmit voice/data
to the LCRU for subsequent relay to the MSFN.

The LCRU subsystem itself is to be small, lightweight, and self-
contained so that it can be stowed in the LM modularized equipment storage
area (MESA) and later installed by the crew on the lunar roving vehicle
or on the mobile equipment transporter (MET). The LCRU will be portable
so that in an emergency situation requiring a walk-back to the LM the
astronauts can hand-carry the LCRU while continuing to maintain voice/
data communications. A hardline connection between the LCRU and the GCTA
will supply power and the 70 kHz command subcarrier as well as to receive

2106.4 MHz

2272.5 MHz*

2287.5 MHz

*CSM DATA DUMP

2101.8 MHz

2282.5 MHz

2272.5 MHz

2101.8 MHz

TO AND FROM
LUNAR MODULE

296.8 MHz

259.7 MHz
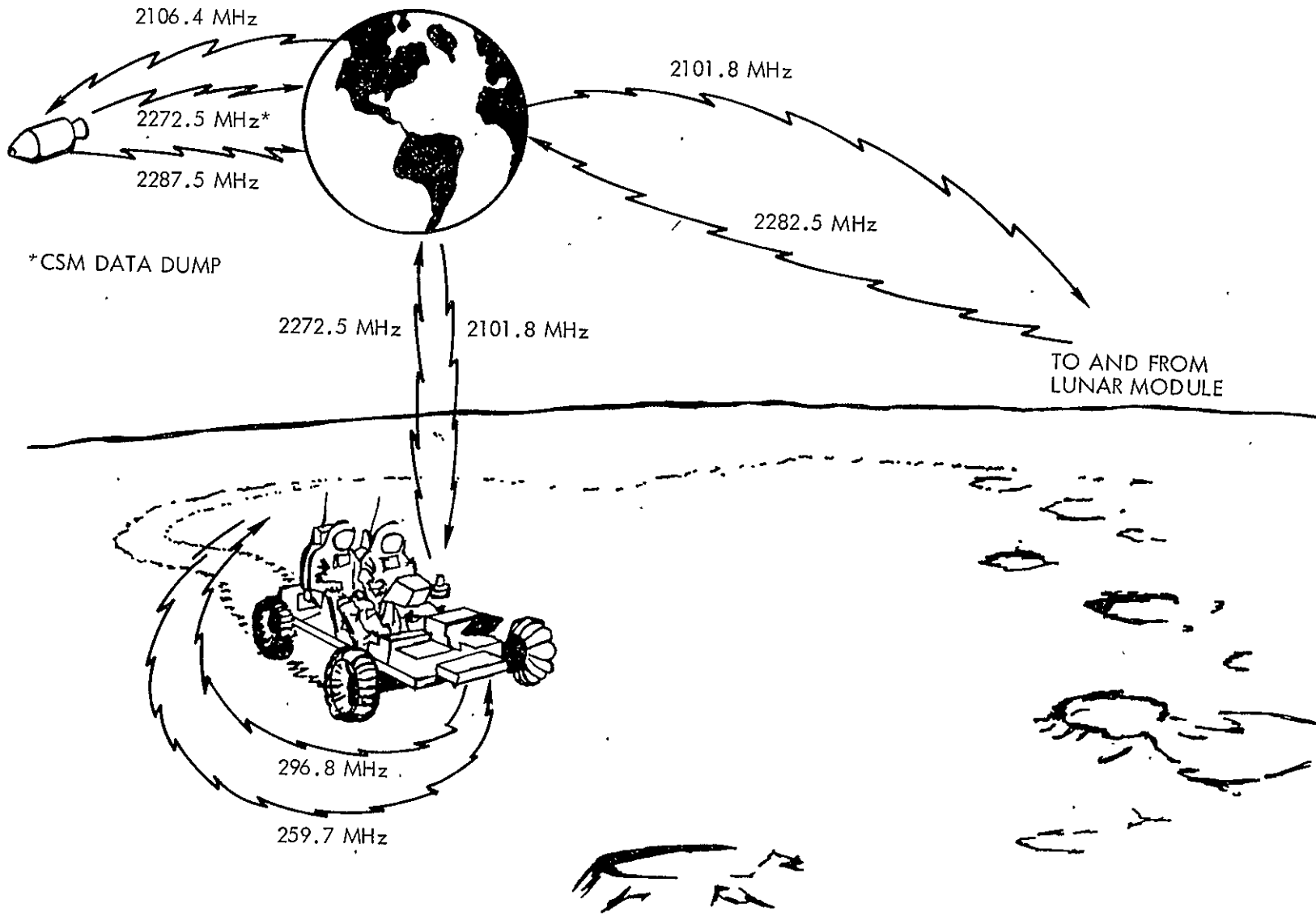
Figure 1-1. LCRU in Mobile Operation on the LRV

the TV video signal. The LCRU will furnish voice/data/TV transmission for as long as three 6-hour sorties. Good voice/data communications is required from the LCRU subsystem to the 85-foot MSFN ground station during mobile operation of the LRV or MET.

Figure 1-2 is a sketch of the LCRU installed on the lunar roving vehicle which is shown in fixed base operation on the lunar surface. Television/voice/data communications between the LCRU and MSFN is obtained with a 23 dB deployable dish antenna and the S-band uplink and downlink carriers, 2101.8 MHz and 2272.5 MHz, respectively. Voice and data information from EVA-2 is transmitted to EVA-1 on a 279.0 MHz VHF carrier. Voice and/or data information from EVA-1 is transmitted to EVA-2 and the LCRU on a 259.7 MHz VHF carrier. Voice information is relayed from the MSFN to the astronauts exploring the lunar surface through the use of a LCRU VHF carrier with frequency 296.8 MHz. The voice/data communication links between the LCRU and MSFN 85-foot dish employ an adjustable helical antenna with 6.5 dB minimum antenna gain over a pattern ±30° off boresight. The color TV downlink capability is provided from fixed base operations (LRV or MET in stationary position). Good television communications performance is required between the LCRU dish and the MSFN 210-foot dish. However, minimally acceptable TV communications is sufficient when using the LCRU dish and the MSFN 85-foot station.

The downlink S-band amplitude-frequency spectrum for the TV/voice mode (FM/FM) is depicted in Figure 1-3. The baseband voice and data signals frequency modulate the 1.25 MHz subcarrier. The composite television baseband signal is then summed with the frequency-modulated 1.25 MHz subcarrier. The resultant sum frequency modulates the S-band 2272.5 MHz carrier. FM/FM mode transmission is hardlined to the LCRU high gain antenna (23 dB dish).

The downlink 1.25 MHz subcarrier amplitude-frequency spectrum for the TV/voice mode (FM/FM) is shown in Figure 1-4. The EVA baseband voice plus the four EMU (Extravehicular Mobility Unit) subcarriers and the LCRU status

2106.4 MHz

2272.5 MHz*

2287.5 MHz

2101.8 MHz

2282.5 MHz

*CSM DATA DUMP

2272.5 MHz   2101.8 MHz

TO AND FROM
LUNAR MODULE

259.7 MHz

296.8 MHz   296.8 MHz

EVA-2

259.7 MHz

EVA-1

279.0 MHz
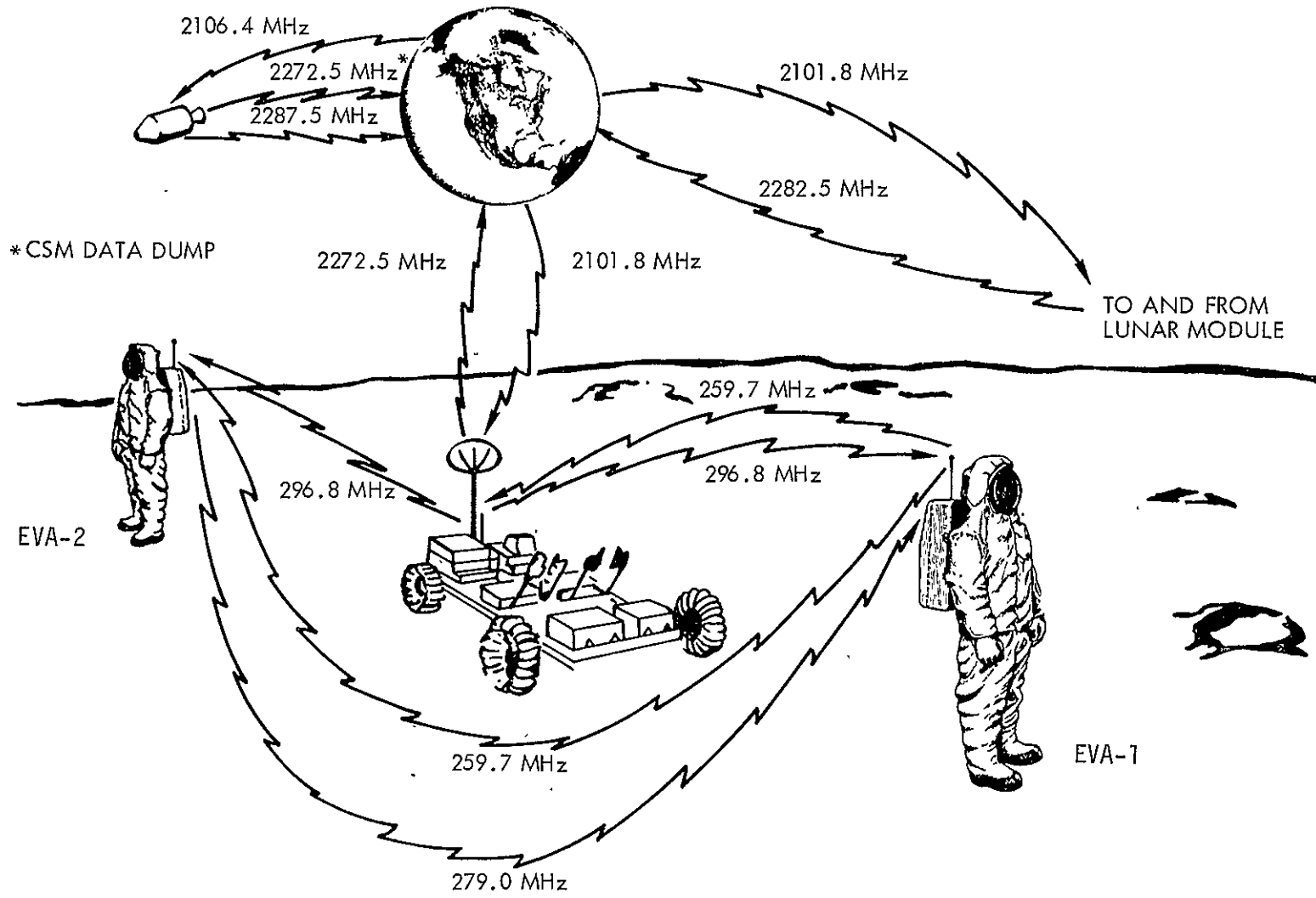
Figure 1-2.   LCRU in Fixed Base Operation on the LRV

DOWNLINK S-BAND SPECTRUM
TV/VOICE MODE (FM/FM)

$f_c - 1.25$ MHz f_c $f_c + 1.25$ MHz
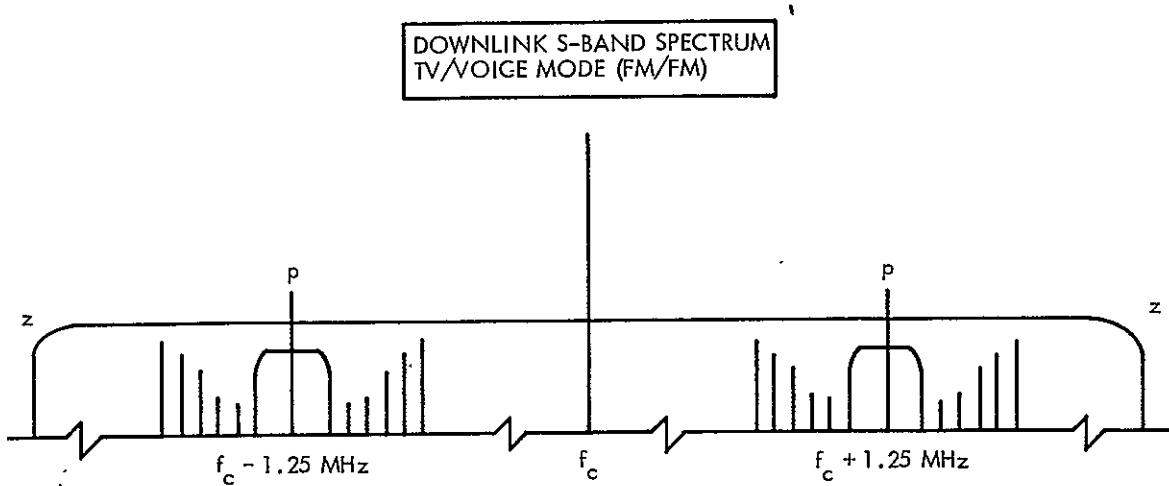
f_c = 2272.5 MHz Carrier (LCRU to MSFN)

p = 1.25 MHz Subcarrier
EVA-1 or EVA-2 Voice, and EMU/ LCRU Data Baseband,
Frequency Modulated onto Subcarrier

z = Color Television Video Baseband

Figure 1-3.   LCRU/MSFN Communication System Downlink
S-Band Amplitude-Frequency Spectrum

DOWNLINK 1.25 MHz SUBCARRIER SPECTRUM
TV/VOICE MODE (FM/FM)
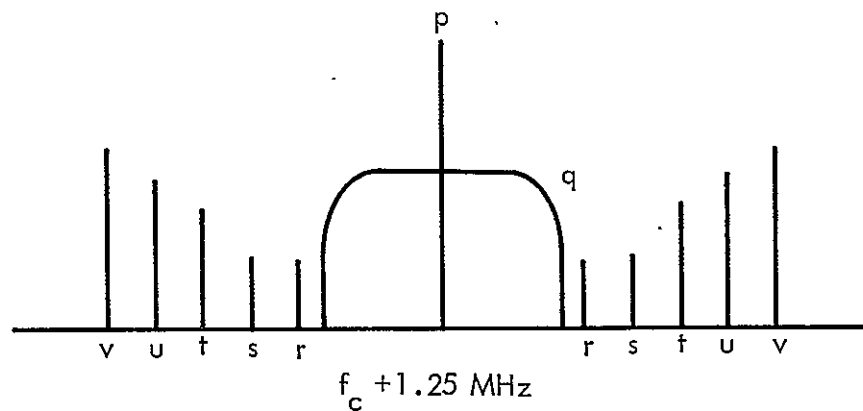
f_c +1.25 MHz

p = 1.25 MHz Subcarrier

q = Baseband Voice, EVA-1 or EVA-2

r = 3.9 kHz Subcarrier, EVA-2 EKG Data

s = 5.4 kHz Subcarrier, EVA-1 EKG Data

t = 7.35 kHz Subcarrier, EVA-2 PLSS Status Data (PAM)

u = 10.5 kHz Subcarrier, EVA-1 PLSS Status Data (PAM)

v = 14.5 kHz Subcarrier, LCRU Status Data (Time Shared)

Figure 1-4. LCRU/MSFN Communication System Downlink 1.25
MHz Subcarrier Amplitude-Frequency Spectrum

data subcarrier frequency-modulate the 1.25 MHz subcarrier. The LCRU status data - baseplate temperature and battery voltage - time share the 14.5 kHz subcarrier frequency modulator.

In Figure 1-5 a block diagram is given of a portion of the LCRU/MSFN communication system. Figure 1-5 shows the signal flow of the EVA-1 voice/data and TV camera signals when input to the LCRU, transmitted to the earth, and then finally recovered in the MSFN ground station receiver.
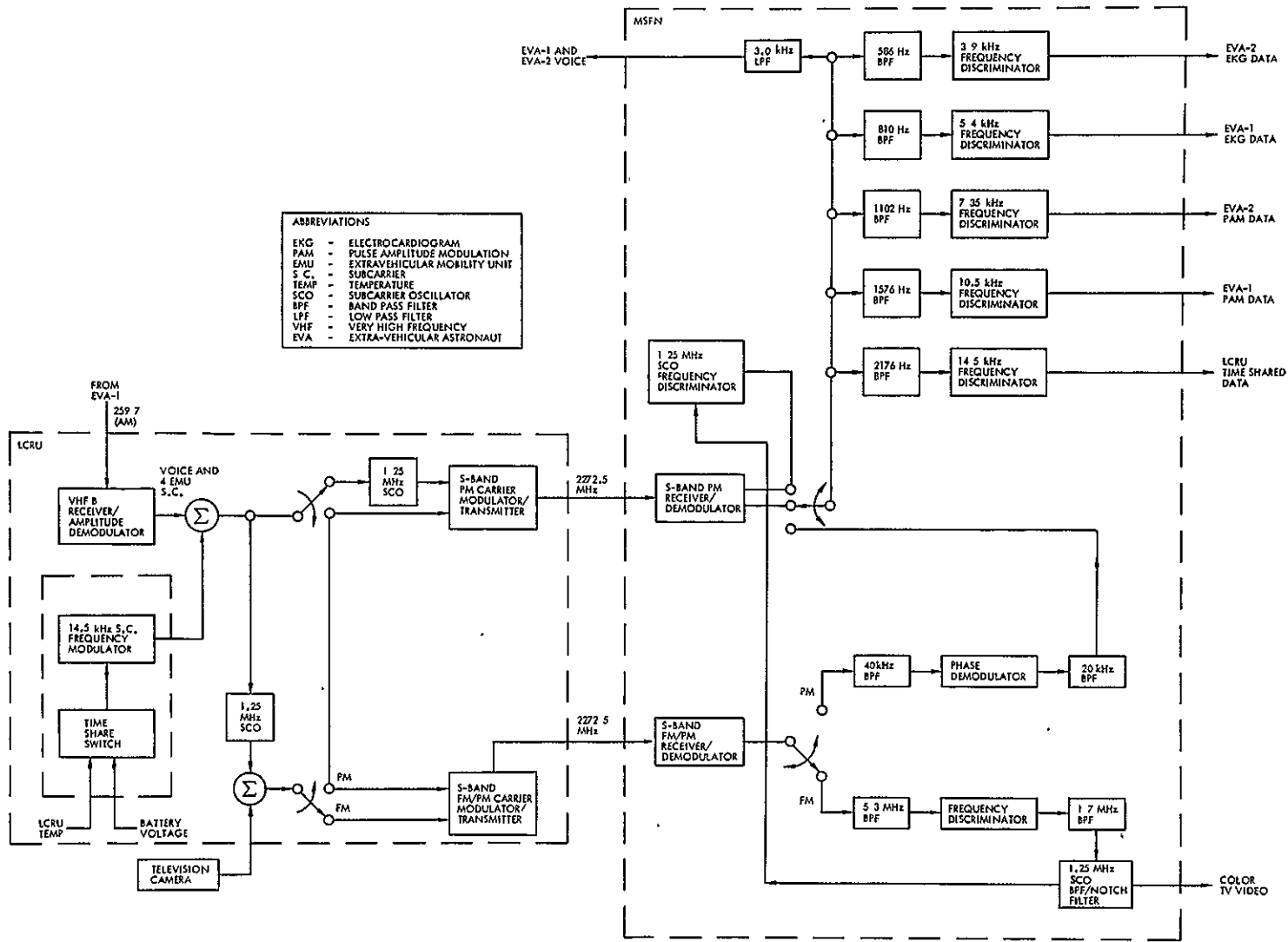
Figure 1-5. Downlink Portion of the LCRU/MSFN Communication System

1.2 APOLLO COLOR TELEVISION SYSTEM

The present Apollo color television system uses a rather unique
method to produce a color signal. The Apollo color camera is basically a
black-and-white camera which has been converted to a field-sequential color
camera by the addition of a rotating color wheel. This technique is very
similar to the old CBS field-sequential system developed for color tele-
vision in the early 1940's. This system was characterized by the use of
color-band filters at the camera and again at the receiver, with only one
camera necessary for viewing a scene and only one picture tube needed at
the receiver. The Apollo color camera, like the old CBS camera, employs
a color filter.wheel to produce a serial color signal.

The field-sequential system uses a rotating filter wheel to expose
the camera's image tube sequentially, at the desired broadcast scan rate,
to the red, blue, and green components of a scene. Thus the need for
complex optical paths and color registration adjustment, such as required
in commercial color cameras, is eliminated. This enables the Apollo color
camera to be light-weight and to require very little power. In addition,
it is capable of operating in the low light levels of the CSM, as well as
in the high light levels of the lunar environment.

Since the output of a field-sequential system is in serial red-blue-
green form, it is not compatible with present broadcast standards. This
requires that a ground station color converter be utilized to change the
sequential color signal to the standard parallel NTSC (National Television
System Committee) color TV format so it can be rebroadcast by commercial
stations.

A general diagram of the Apollo/LCRU color television system (Refer-
ence 1) is shown in Figure 1-6. The image is focused by a zoom lens
through the color filter wheel onto the faceplate of the image tube. To
simplify the problem of synchronization, the scan rate of the wheel, as
the color filters pass in front of the image tube, must be the same as
that of the TV networks, which is 60 fields per second. This was achieved
by dividing the wheel into six sections, with the colors arranged in red-

LUNAR BASE
EQUIPMENT

PARABOLIC
ANTENNA
S-BAND

COLOR
TELEVISION
CAMERA

LCRU S-BAND
FM CARRIER
MODULATOR/
TRANSMITTER

PARABOLIC
ANTENNA

MSFN
RECEIVER

PROCESSING
AMPLIFIER

VIDEO TAPE
RECORDER

VIDEO TAPE
RECORDER

VIDEO
COLOR
CONVERTER

NTSC
COLOR
ENCODER

NTSC
ENCODED
VIDEO
OUTPUT

GROUND STATION
EQUIPMENT

TV
NETWORK
SYNC

COMPOSITE SYNC

COMPOSITE BLANKING

3.58 MHz COLOR BURST

Figure 1-6. Apollo/LCRU Color Television System

blue-green, red-blue-green order, and by driving the wheel at 10 revolutions per second. The motor speed is held constant by the timing of the camera's sync generator.

The field-sequential color signal, which is transmitted by a S-band transmitter in the LCRU, is picked up and amplified by a receiver at the Houston Manned Spacecraft Center. The signal is then clamped in a processing amplifier to restore the d-c component and reestablish the average light value of the reproduced image.

The processed signal is placed into a series of two tape recorders for the purpose of compensating for Doppler shift and presenting real-time information. The sequential color signal is then put into the scan converter that changes the video from the serial color format to the parallel (simultaneous) color format. The scan color converter is a storage and readout device holding the two previous fields in memory and presenting the three fields at once at the output on the incidence of the third field. As the new field is placed into memory the oldest field is erased, updating the information at the field rate. Thus, the three colors are simultaneously read out in the same manner as the output from a standard three-tube NTSC color camera. After video color conversion, the signal is sent to a NTSC color encoder which processes it to form the composite video signal.

2. MODEL OF A VIDEO SIGNAL

When confronted with a communications problem concerning the transmission of video signals, it is often necessary to know the statistical distribution of power in the frequency domain for the signal process. That is, it is desirable to have a model which will satisfactorily characterize the power spectral density of the random video signal. The purpose of this section is to present various mathematical models which may be used to represent a random video signal. The validity of these models has been verified experimentally and the choice of which model should be used for a given application is determined by the general nature of the communication problem and the desired complexity of the solution. In Section 3, two different video models are used to calculate the theoretical signal-to-noise ratio improvement due to video emphasis on a FM channel.

A video signal was modeled and analyzed by L. E. Franks (Reference 2) in 1965 and earlier, in 1934, by Pierre Mertz and Frank Gray (Reference 3). Franks proposed a model for the random picture and derived expressions for the second-order statistical properties of the video signal obtained from a conventional scanning operation on the picture. He found that the properties of typical picture material lead to especially simple, closed form expressions for the power spectral density. The continuous part of the power spectral density is expressed as a product of three factors which show the influence of point-to-point, line-to-line, and frame-to frame correlation. Using parameters of typical picture material, Franks observed that the video spectral components were concentrated near multiples of the line scan and frame scan rates. This conclusion was in agreement with the results determined earlier by Mertz and Gray.

According to Franks' model, the power spectral density for the composite random video signal (Appendix A) is

$$S(f) = (1 - \alpha)G_h(f)G_v(f)G_t(f)$$
$$+ \sum_{\ell=-\infty}^{\infty} |W_\ell|^2 \, \delta(f - \frac{\ell}{NT}) + \overline{d}^2\delta(f)$$

(2-1)

where

$$G_h(f) = (\overline{d^2} - \overline{d}^2)\ \frac{2\lambda_h}{(2\pi f)^2 + \lambda_h^2} \qquad \cdot (2\text{-}2)$$

    = an envelope function representing
horizontal picture correlation

$$G_v(f) = \frac{\sinh \lambda_v T_e}{\cosh \lambda_v T_e - \cos 2\pi T f} \qquad (2\text{-}3)$$

    = a function, periodic 1/T, representing
vertical picture correlation

$$G_t(f) = \frac{\sinh N\lambda_t T}{\cosh N\lambda_t T - \cos 2\pi N T f} \qquad (2\text{-}4)$$

    = a function, periodic 1/NT, representing
frame-to-frame correlation

and

α = relative amount of time occupied by
non-video (synchronizing and blanking)
portion of the signal

$\overline{d}$ = mean value of the picture luminance

$\overline{d^2} - \overline{d}^2$ = variance of the picture luminance

λ_h, λ_v = average number of statistically independent
luminance levels in a unit distance along
the horizontal and vertical directions,
respectively; Poisson rate parameter

describing luminance process in horizontal
and vertical directions, respectively

T_e = time interval equivalent to distance between
adjacent lines at scanner velocity; time
dimension of picture element

T = line scan interval in seconds

λ_t = Poisson rate parameter describing the
luminance of a point at successive frames

N = number of lines per frame

W_ℓ = ℓth Fourier coefficient of the periodic
signal w(t) added to $\bar{d}$ in the blank interval.

Figure 2-1 shows the power spectral density, $\Phi_3(f)$, of a video
signal (without synchronizing and blanking pulses) obtained by repeatedly
scanning a rectangular portion of a randomly moving picture.

$$\Phi_3(f) = G_h(f)G_v(f)G_f(f)$$
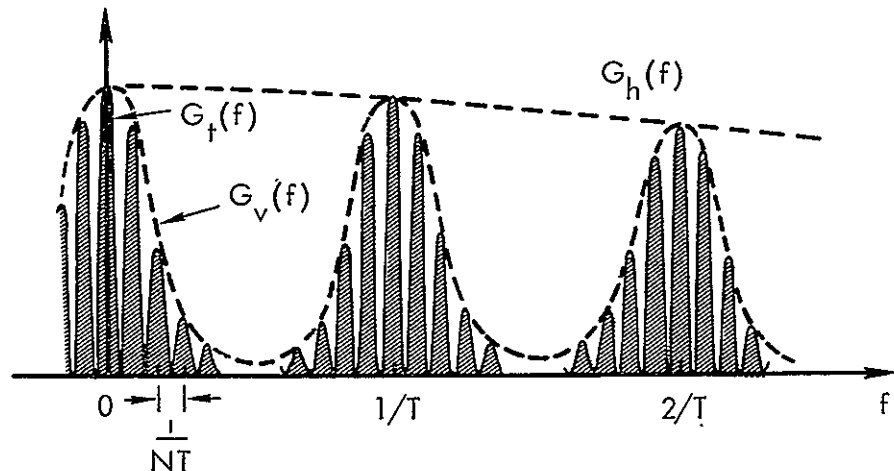
Figure 2-1. Power Spectral Density, $\Phi_3(f)$, of Video Signal Obtained by
Repeated Scanning of Rectangular Portion of Moving Picture

2-3

The picture is considered to have slow variation compared to the frame repetition rate, 1/NT, where vertical scanning is accomplished by N uniformly spaced lines. Because of the slow variation due to motion, frame-to-frame correlation is high. The expression for $\Phi_3(f)$ is given as the product of three functions; an envelope $G_h(f)$ representing horizontal picture correlation, a function $G_v(f)$, periodic 1/T, representing vertical picture correlation, and a function $G_t(f)$, periodic 1/NT, representing frame-to-frame correlation

$$\Phi_3(f) = G_h(f)G_v(f)G_t(f) \qquad (2\text{-}5)$$

As evident from Figure 2-1, the factors $G_v(f)$ and $G_t(f)$ impose a "fine structure" on $\Phi_3(f)$. In considering various smoothed versions of power spectral density, Franks states that it is helpful to note that the average values of $G_v(f)$ and $G_t(f)$ are both unity.

To conserve bandwidth, most practical scanning operations use the line interlacing technique. For the conventional 2:1 interlace scan, the resulting modification of Equation (2-1) is very simple. Since consecutive lines are now twice as far apart, the factor $G_v(f)$ is modified by replacing T_e with $2T_e$. This modification causes the individual peaks in $G_v(f)$, centered at multiples of 1/T, to be broadened to twice their original width. Since the picture is scanned vertically every NT/2 seconds, the $G_t(f)$ factor is modified by replacing N by N/2. This causes a suppression of the terms centered at odd multiples of 1/NT.

2.1 SMOOTHED VERSION

In applications where there is a still picture or where there is extremely slow picture variation due to motion, the frame-to-frame correlation is very high (near unity). This means that the function representing frame-to-frame correlation may be assumed to have unity value. This smoothed version, $(1-\alpha)G_h(f)G_v(f)$, of the continuous part of the video power spectral density is shown in Figure 2-2 and is expressed as [Equation (A-8)]

$$S_m(f) = (1-\alpha)G_h(f)G_v(f) \qquad (2\text{-}6)$$

$$= S_0\left[\frac{1}{1 +\left(\frac{f}{f'}\right)^2}\right] \left[\frac{\cosh \lambda_v T_e - 1}{\cosh \lambda_v T_e - \cos 2\pi Tf}\right] \qquad (2\text{-}7)$$

where

S_0 = spectral density at zero frequency

$$= \frac{2K}{\lambda_h} \frac{\sinh \lambda_v T_e}{\cosh \lambda_v T_e - 1} \qquad (2\text{-}8)$$

K = average video signal power

$$= \int_{-\infty}^{\infty} S_m(f)\, df \qquad (2\text{-}9)$$

$$= (1-\alpha)\ (\overline{d^2} - \overline{d}^2) \qquad (2\text{-}10)$$

f' = the frequency at which $G_h(f)$ has fallen by 3 dB from its zero frequency value, $G_h(0)$

$$= \lambda_h/2\pi \qquad (2\text{-}11)$$

2-5

$$S_m(f) = (1-\alpha)G_h(f)G_v(f)$$
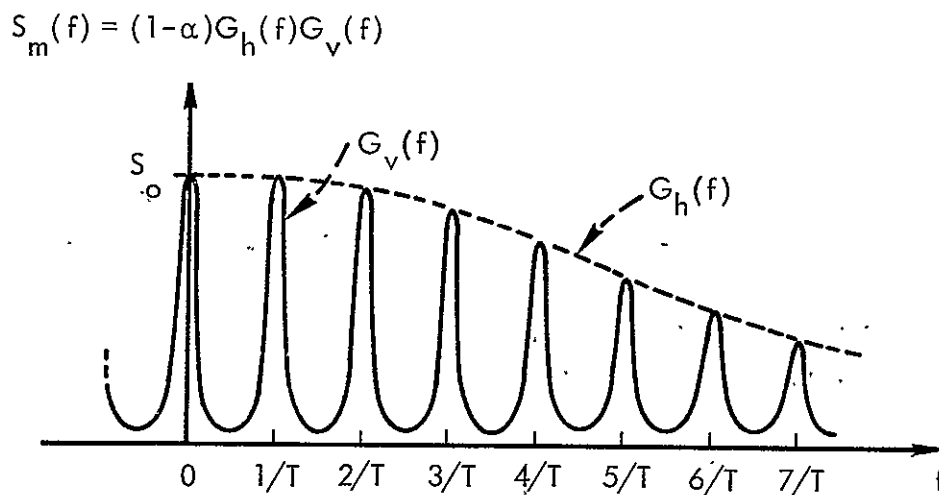
Figure 2-2.   Continuous Part of Power Spectral Density for Typical Video
Signal With Frame Rate Structure Smoothed Out

For purposes of comparison, it is sometimes convenient to assume
that the video picture has the same correlation between picture elements
of dimension T_e in both the horizontal and vertical directions
$(\lambda_h = \lambda_v = \lambda)$. Then the smoothed version of the continuous part of the
video power spectral density for the case of sequential scanning becomes

$$S_m(f) = S_0 \left[\frac{1}{1 + \left(\frac{f}{f'}\right)^2} \right] \left[\frac{\cosh \lambda T_e - 1}{\cosh \lambda T_e - \cos 2\pi T f} \right] \quad (2\text{-}12)$$

where $f' = \lambda/2\pi$. The power spectral density for the case of 2:1 interlace
scanning is obtained from Equation (2-12) by replacing T_e by $2T_e$.

When the assumption is made that $\lambda_h = \lambda_v = \lambda$, the video picture may
be adequately described by, a single correlation coefficient, ρ. For
example, a typical head-and-shoulders view of a person may have a
correlation $\rho = 0.99$, while $\rho = 0.98$ represents a moderately detailed
picture. Even a highly detailed random picture with correlation $\rho = 0.9$

still has its video power extremely concentrated around multiples of the line scan rate, 1/T (References 2, 4 and 5).

2.2 ENVELOPE VERSION

A fundamental problem in the design of any communications system is the determination of the bandwidth necessary for transmission of the required information. In most communications problems, not only is the bandwidth important, but the actual spectral distribution must be known in order to examine the effect of narrowing this bandwidth.

The vertical resolution of a television system is directly proportional to the number of lines in the scanning pattern. The horizontal resolution, however, is a function only of the video channel bandwidth. For example, the maximum number of vertical lines which may be reproduced by a TV system (assuming a fixed number of frames per second) is a function of the bandwidth of that system (Reference 6).

For many problems concerning the transmission of video signals, it is sufficient to model the video spectrum as a slowly changing envelope function with relatively small variation over an interval of width 1/T. In these applications, where only the bandwidth and over-all envelope of the video spectrum are important, the video power spectral density may be expressed as

$$S_e(f) = (1 - \alpha) \, G_h(f) \tag{2-13}$$

$$= S_0 \left[\frac{1}{1 + \left(\frac{f}{f'}\right)^2} \right] \tag{2-14}$$

where S_0 = spectral density at zero frequency

$$- \frac{2K}{\lambda_h} \tag{2-15}$$

K = average video signal power

$$= \int_{-\infty}^{\infty} S_e(f) \, df \qquad (2\text{-}16)$$

$$= (1 - \alpha) \, (\overline{d^2} - \overline{d}^2)$$

f' = the frequency at which $S_e(f)$ has fallen by 3 dB from its zero frequency value, S_o.

$$= \lambda_h / 2\pi \qquad (2\text{-}17)$$

A sketch of this envelope density function is shown in Figure 2-3.
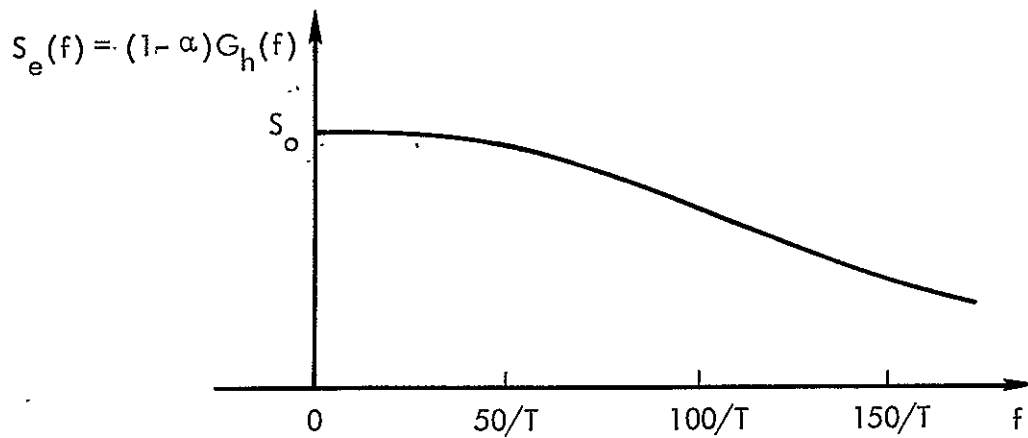
Figure 2-3. Power Spectral Density of Video Signal With Horizontal Picture Correlation

From Equation (A-12) the horizontal correlation coefficient is defined
as

$$\rho_h = e^{-\lambda_h T_e} \qquad (2\text{-}18)$$

or

$$|\ln \rho_h| = \lambda_h T_e \qquad (2\text{-}19)$$

Substituting Equation (2-19) into Equation (2-17) gives the relationship
between the envelope -3 dB frequency, f', and the horizontal picture
correlation, ρ_h. That relationship is

$$f' = \frac{|\ln \rho_h|}{2\pi T_e} \qquad , \qquad (2\text{-}20)$$

where T_e is the picture element scan interval and is a constant for a
given television system. Since ρ_h has the range of values, $0 \le \rho_h \le 1$,
it is seen from inspection of Equation (2-20) that as the correlation
increases, the -3 dB envelope frequency f' decreases. For decreasing
picture correlation the opposite occurs, that is, f' increases.
Intuitively, this makes sense because a highly detailed picture (low
correlation) suggests high frequency content and large video bandwidth,
while a slightly detailed picture (high correlation) suggests low fre-
quency content and thus a small video bandwidth.

3. EMPHASIS OF A VIDEO SIGNAL
ON AN FM CHANNEL

Section 2 described several mathematical models which may be used to represent the power spectrum of a random video signal. Section 3 uses these models in examining the effects of video signal emphasis in an FM transmission system. The effect of emphasis in the FM channel is determined by comparing the signal-to-noise power ratios after FM demodulation with and without emphasis in the channel. While the main discussion of this section is directed to the Apollo TV case (i.e., a TV signal at baseband in a FM transmission system), it is also applicable to other systems employing FM transmission of television.

The application of emphasis in the FM channel for transmission of voice is a well known principle. The same principle also applies to the application of emphasis for FM transmission of television. The preemphasis and deemphasis process is a simple example of a signal-processing scheme which utilizes the different statistical properties of signal and noise to process the signal more efficiently (Reference 7).

The noise-power spectrum at the output of a frequency demodulator is proportional to f^2 for large carrier-to-noise ratio. This spectrum is plotted in Figure 3-1 together with the power density spectrum of a typical video signal and the transfer function of a low-pass filter following the demodulator. The signal density spectrum shown in the figure falls off appreciably for higher frequencies. Video and audio signals typically have spectra of this form where most of the energy is found to be concentrated in the lower-frequency ranges. The relative value of the signal spectrum at $f = \pm f_M$ is quite low, while the relative value of the noise spectrum is quite high at the same frequency. This results in a poor SNR at the high-frequency end of the modulating signal spectrum. It is easily seen that the signal makes very inefficient use of the passband allowed to it, for if the filter bandwidth were to be decreased slightly, a large amount of noise would be eliminated, while losing only a small amount of signal power.
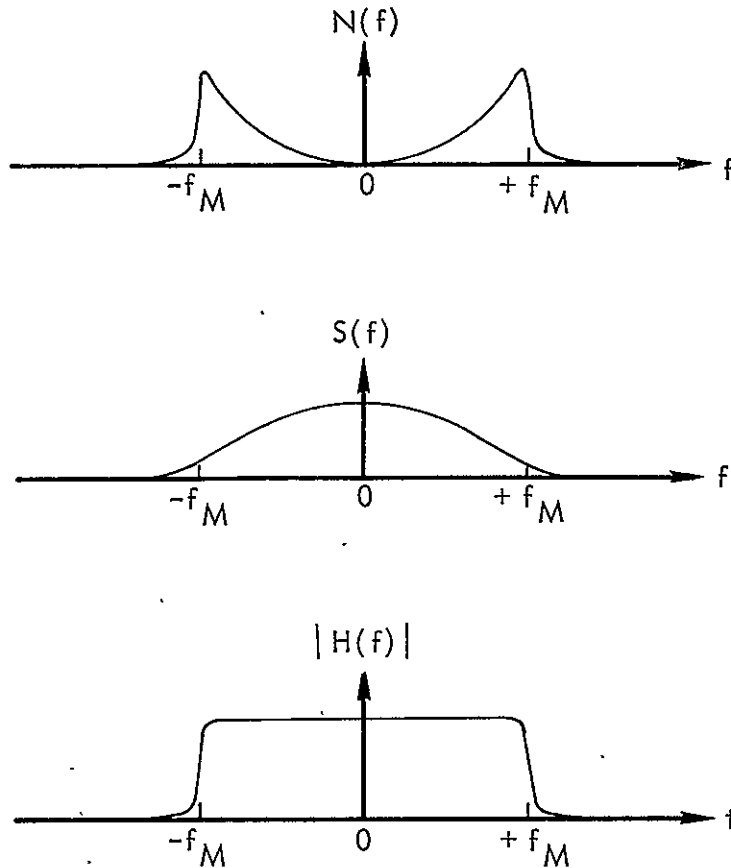
Figure 3-1.   Spectra of Signal and Noise at the Output
of an FM Receiver

Simply reducing the filter bandwidth, however, is not a satisfactory
answer. Although this would considerably reduce the noise power in the
output, while only slightly distorting the signal content, this small
amount of distortion might not be tolerable.

A more satisfactory solution is through the use of signal emphasis.
This method is based on the observation that the signal would make better
use of the alloted bandwidth if it contained appreciable power throughout
the whole bandwidth. The modulating signal at the transmitting end is
thus passed through a network that emphasizes the higher signal frequencies,
but leaves the lower signal components unaffected. This process tends to
equalize the energy distribution throughout the frequency range of the
modulating signal (Reference 8). The premodulation filtering in the
transmitter to raise the power spectral density of the baseband signal in
its upper frequency range is called preemphasis (or predistortion). At
the output of the demodulator , the inverse process is carried out. That

is, the higher-frequency components are deemphasized in order to restore the original signal-power distribution. But in this filter process, the higher-frequency components of the noise are reduced, and thus the signal-to-noise ratio is increased. The filtering process at the receiver to undo the signal preemphasis and to suppress noise is called deemphasis.

Frequency modulation systems with no emphasis and with preemphasis-deemphasis are shown in Figures 3-2 and 3-3, respectively. Observe in Figure 3-3 that, at the transmitting end, the baseband signal m(t) is not applied directly to the FM modulator but is first passed through a filter of transfer characteristic $H_p(f)$, so that the modulating signal is $m_p(t)$. The modulated carrier is transmitted across a communication channel during which process, as usual, noise is added to the signal. The receiver is a conventional frequency demodulator except that a filter has been introduced before the baseband filter. The transfer characteristic of this filter is the reciprocal of the characteristic of the transmitter filter. The receiver filter of transfer characteristic $1/H_p(f)$ may be placed either before or after the baseband filter, since both filters are linear. Note that any distortion introduced into the baseband signal by the first filter, prior to modulation, is eliminated by the second filter which follows the demodulator. Hence, the output signal at the receiver is exactly the same as it would be if the filters had been omitted entirely. The noise, however, passes through only the receiver filter and this filter is then used to suppress the noise. The power spectral density of FM noise above threshold varies directly with the square of the frequency (quadratic in f) and is sketched in Figure 3-4. The spectrum of the rms noise voltage is directly proportional to f and so is frequently referred to as being triangular in shape. The rms noise spectrum is shown sketched in Figure 3-5. Also shown is the rms spectrum of white noise. The effect of a deemphasis network on this noise is to suppress the higher frequencies and consequently make the noise spectrum uniform in the band of the emphasized signal frequencies. Figure 3-6 illustrates the flattening effect of the deemphasis network upon the FM noise spectrums and the resultant noise which is eliminated through the use of deemphasis.

Since the original signal-power distribution has been restored, while
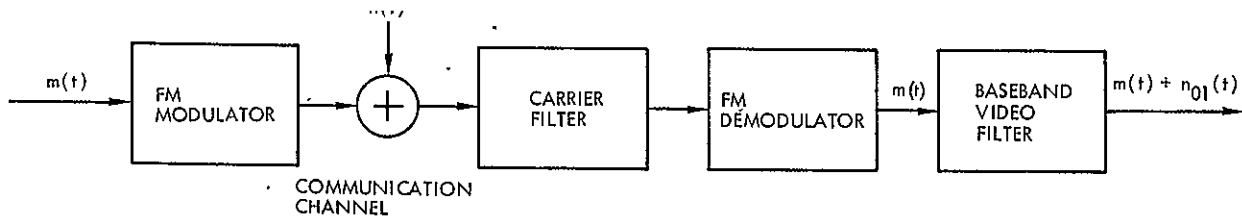
Figure 3-2. FM System Without Emphasis, Above Threshold Condition
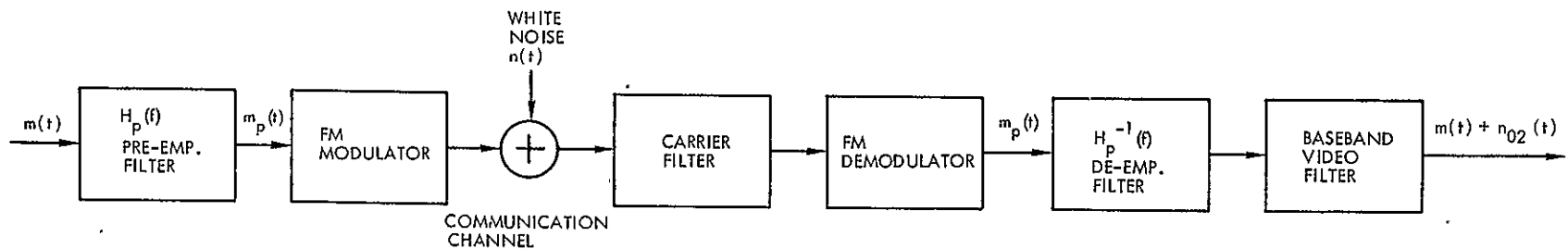
Figure 3-3. FM System With Emphasis, Above Threshold Condition
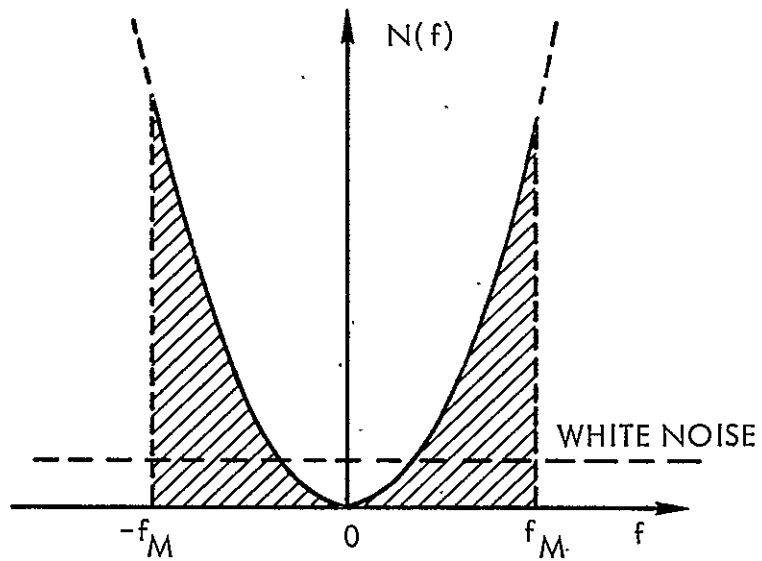
Figure 3-4. Noise Power Spectral Density at the Output of an
FM Demodulator
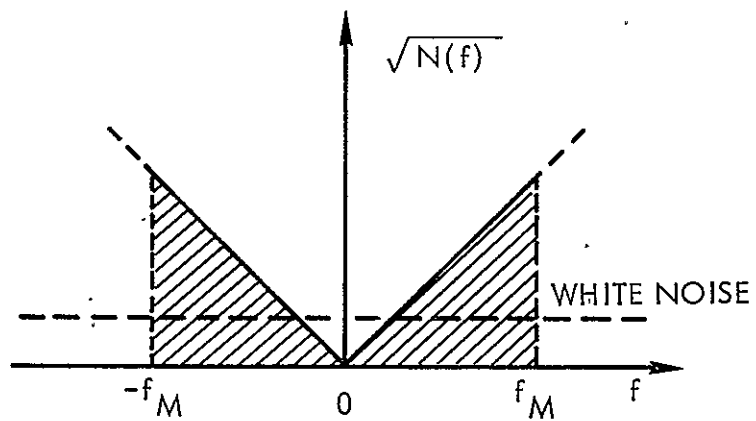
Figure 3-5. Spectrum of RMS Noise Voltage at the Output of an
FM Demodulator
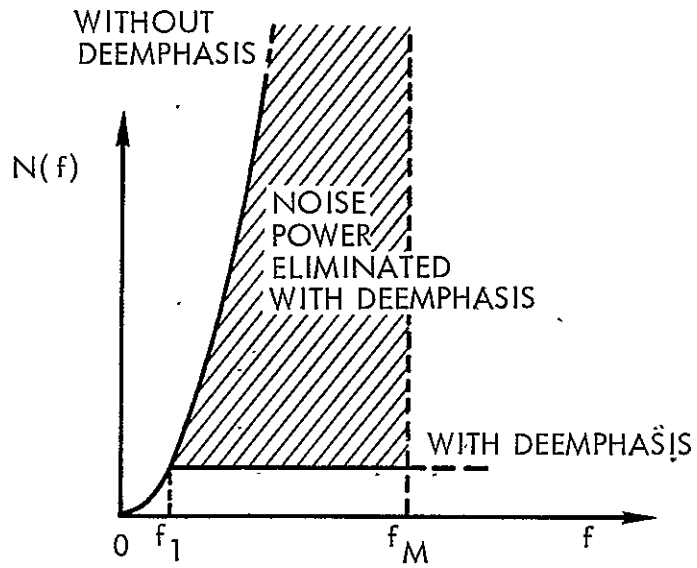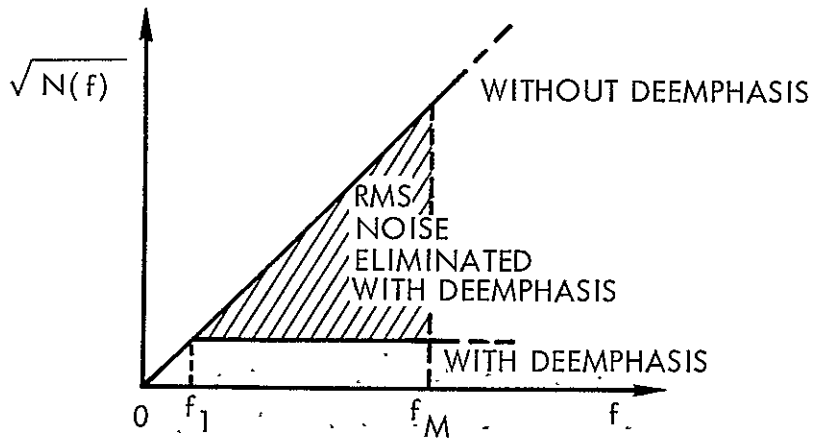
Figure 3-6. Effect of Deemphasis Upon FM Noise (a) Noise Power
Spectrum; (b) RMS Noise Spectrum

the high frequency noise components have been attenuated, there is a resultant increase in signal-to-noise ratio for high frequencies. The SNR improvement gained by deemphasis of the recovered noise is partially offset by an increase in the transmission bandwidth needed to accommodate the frequency modulated signal when the modulation is preemphasized. If the modulating signal power is lowered to maintain a constant transmission bandwidth, there still remains a net advantage due to emphasis. That is, the improvement in signal-to-noise ratio due to deemphasizing the parabolic FM noise outweighs the disadvantage due to the need to lower the level of the modulating signal (Reference 9).

3.1 SNR IMPROVEMENT USING EMPHASIS

From FM noise analysis, the two-sided noise spectral density at the output of a FM demodulator can be written (for large carrier-to-noise ratio) as

$$N(\omega) = \frac{\alpha^2 \eta \omega^2}{A^2} \tag{3-1}$$

where α is the demodulator constant, η the input noise spectral density, A the carrier amplitude, and $A^2/2$ the mean carrier power at the demodulator input. The total mean noise power at the output of an ideal low-pass filter of bandwidth f_M is given by

$$N_0 = \int_{-f_M}^{f_M} N(f)df = \left(\frac{\alpha^2 \eta}{A^2}\right) 4\pi^2 \int_{-f_M}^{f_M} f^2 df \tag{3-2}$$

$$= \frac{8\pi^2}{3} \left(\frac{\alpha^2 \eta}{A^2}\right) f_M^3 \tag{3-3}$$

In the absence of deemphasis, the noise at the output of the baseband video filter is given by N_0 in Equation (3-3). When using the deemphasis filter, the spectral distribution of the noise power is modified by $|H_p^{-1}(f)|^2$; and the output noise is,

$$N_{oD} = \left(\frac{\alpha^2 \eta}{A^2}\right) 4\pi^2 \int_{-f_M}^{f_M} \frac{f^2}{|H_p(f)|^2} \, df \qquad (3\text{-}4)$$

where N_{oD} represents the mean noise power with the deemphasis network included, as compared with the symbol N_o used previously for the noise power with no deemphasis network.

The ratio of the noise output without deemphasis to the noise output with deemphasis is

$$\frac{N_o}{N_{oD}} = \frac{\left(\dfrac{\alpha^2 \eta}{A^2}\right) 4\pi^2 \displaystyle\int_{-f_M}^{f_M} f^2 \, df}{\left(\dfrac{\alpha^2 \eta}{A^2}\right) 4\pi^2 \displaystyle\int_{-f_M}^{f_M} \dfrac{f^2}{|H_p(f)|^2} \, df} \qquad (3\text{-}5)$$

$$= \frac{f_M^3/3}{\displaystyle\int_o^{f_M} \dfrac{f^2}{|H_p(f)|^2} \, df} \qquad (3\text{-}6)$$

Since the modulating signal itself is unaffected in the overall emphasis process, the above quantity is the ratio by which preemphasis-deemphasis improves the signal-to-noise ratio of the baseband signal.

Recall from FM analysis that the bandwidth of an FM modulated carrier is fixed if the average power (or frequency deviation) of the modulating signal is kept constant (provided that the modulating signal spectra occupies the same band of frequencies). The concept of rms bandwidth (Reference 10) provides an estimate of the bandwidth required of the filters in the r-f and i-f stages of an FM receiver, and of the bandwidth that must be allocated for transmission of the modulated carrier. The rms bandwidth of the modulated carrier depends only on the average power of the modulating signal and therefore is independent of the shape of the modulating signal spectrum.

So that a constant transmission bandwidth may be maintained, the pre-emphasis network is selected so that the average power of the emphasized signal $m_p(t)$ has the same average power as the original baseband signal $m(t)$. The rms bandwidth will then be the same with or without preemphasis. If $S(f)$ is the power spectral density of $m(t)$, then the density of $m_p(t)$ is $|H_p(f)|^2 S(f)$ and it is required that

$$K = \int_{-f_M}^{f_M} S(f)\, df = \int_{-f_M}^{f_M} S(f)\, |H_p(f)|^2\, df \qquad (3-7)$$

where K is the total baseband signal power and f_M is both the bandwidth of the modulating signal and, also, the bandwidth of the baseband filter. The preemphasis network may be arbitrarily selected to attain the desired SNR improvement, as given in Equation (3-6), provided only that $H_p(f)$ satisfy the constraint imposed by Equation (3-7).

It is important to realize that the power in the FM modulated carrier is $A^2/2$ and is independent of the modulation. Thus, the channel signal-to-noise ratio remains unaffected by preemphasis [under the constraint of Equation (3-7)] as does the rms bandwidth and the output base-band signal power. Any improvement brought about by the use of preemphasis is thus measured directly by the change in output noise power; that is, comparing N_{oD} of Equation (3-4) with the original noise output power N_o of Equation (3-3). The improvement ratio $\mathscr{R}$ is defined to be the ratio of the output signal-to-noise ratios with and without emphasis. This ratio is thus from Equation (3-6)

$$\mathscr{R} = \frac{(S/N)_{o\ emp}}{(S/N)_{o\ no\ emp}} = \frac{N_o}{N_{oD}} \tag{3-8}$$

$$= \frac{f_M{}^3/3}{\displaystyle\int_o^{f_M} \frac{f^2}{|H_p(f)|^2}\,df} \tag{3-9}$$

3.2 PREEMPHASIS AND DEEMPHASIS OF TELEVISION

Previously in Section 3, it was noted that the noise spectral density at the output of an FM demodulator increases with the square of the frequency when the demodulator is operating above FM threshold. Thus, a deemphasis network located at the receiver will be most effective in suppressing the baseband noise if its response decreases with increasing frequency. For example, if the network response falls with the square of the frequency, then the output noise will be whitened, so as to have a flat spectral density in the high frequency region.

Conversely, the preemphasis network response must be the inverse of that of the deemphasis network; therefore its response will increase with the square of the frequency. Since it is assumed that the video power density spectrum decreases as the square of the frequency [see Equation (2-14)], the effect of the preemphasis network upon the video spectrum will be to whiten the modulating signal spectrum. This process causes the modulating signal to have a constant power spectral density throughout the frequency range of the modulating signal. This means that the video signal will make very efficient use of its alloted bandwidth, since it now contains appreciable power throughout the whole video signal bandwidth.

A simple RC deemphasis network that attenuates high frequencies and has been found very effective in practice is shown in Figure 3-7 (a). This network has a frequency transfer function $H_d(\omega)$ of the form

$$H_d(\omega) = \frac{1}{k_1} \frac{r + 1/j\omega C}{R + r + 1/j\omega C} = \frac{1}{k_1} \frac{1 + j\omega r C}{1 + j\omega(R + r)C} \qquad (3\text{-}10)$$

$$= \frac{1}{k_1} \frac{1 + j\dfrac{\omega}{\omega_2}}{1 + j\dfrac{\omega}{\omega_1}} \qquad \left(\frac{1}{k_1} \geq 1\right) \qquad (3\text{-}11)$$
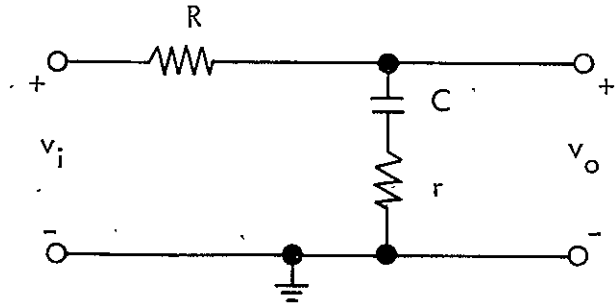
(a)
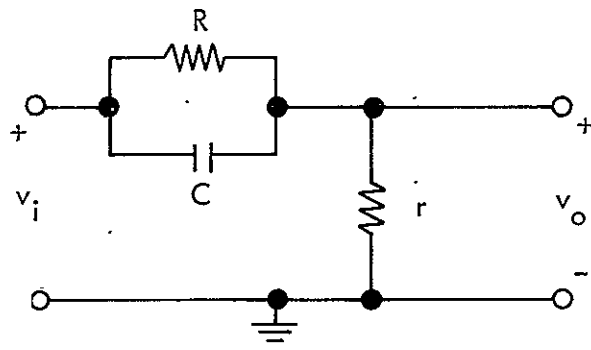
(b)

Figure 3-7. (a) Deemphasis Network and
            (b) Preemphasis Network

where $\omega_1 = 1/(R + r)C$ is the first frequency breakpoint, $\omega_2 = 1/rC$ is the second frequency breakpoint, and $1/k_1$ is the gain of an amplifier in series with the deemphasis network. A normalized logarithmic plot of $H_d(f)$ is given in Figure 3-8 (a). If it is assumed that $r << R$, then the network response can be approximated by

$$H_d(\omega) \simeq \frac{1}{k_1} \frac{1 + j\omega rC}{1 + j\omega RC} = \frac{1}{k_1} \frac{1 + j\frac{\omega}{\omega_2}}{1 + j\frac{\omega}{\omega_1}} \qquad (3\text{-}12)$$

where

$$\omega_1 \simeq \frac{1}{RC} \qquad (3\text{-}13)$$

and

$$\omega_2 = \frac{1}{rC} \qquad (3\text{-}14)$$

If the additional assumption is made that in the baseband video frequency range r is also very small in comparison with the reactance of the capacitance C, then

$$H_d(\omega) \approx \frac{1}{k_1} \frac{1}{1 + j\omega RC} = \frac{1}{k_1} \frac{1}{1 + j\frac{\omega}{\omega_1}} \qquad (3\text{-}15)$$

since $r << 1/j\omega C$ or $j\omega rC << 1$.

The deemphasis filter response then can be considered to have the form

$$H_d(f) = \frac{1}{k_1} \frac{1}{1 + j\frac{f}{f_1}} \qquad (3\text{-}16)$$

where $f_1 = 1/2\pi RC$ is the first breakpoint. The network can be easily designed so that the second breakpoint frequency lies above the highest significant video frequency to be transmitted.

At the transmitter, at the input to the modulator, a preemphasis network is used whose transfer characteristics are the inverse of those of
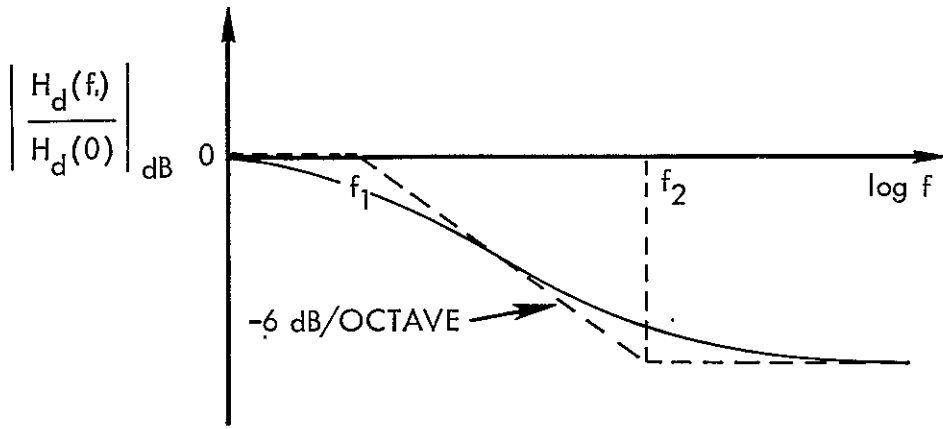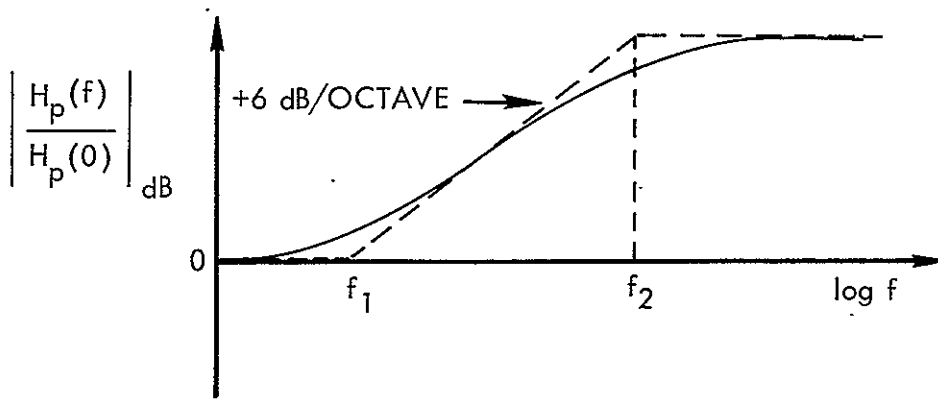
Figure 3-8.   Normalized Logarithmic Plots of the
Frequency Response of (a) the Deemphasis
Network and (b) the Preemphasis Network

the deemphasis circuit. A simple network which may be adjusted to provide the required response is shown in Figure 3-7 (b). The transfer function of this network is given by

$$H_p(\omega) = \cfrac{r}{r + \cfrac{R/j\omega C}{R + (1/j\omega C)}} = \cfrac{r}{r + \cfrac{R}{1 + j\omega RC}} \tag{3-17}$$

$$= \frac{r + j\omega r RC}{(r+R) + j\omega r RC}$$

$$= \frac{r}{R+r} \; \cfrac{1 + j\omega RC}{1 + j\,\cfrac{\omega r RC}{R+r}}$$

$$= \frac{\cdot r}{R+r} \; \cfrac{1 + j\,\cfrac{\omega}{\omega_1}}{1 + j\,\cfrac{\omega}{\omega_2}} \tag{3-18}$$

where $\omega_1 = 1/RC$ is the first breakpoint and $\omega_2 = (r + R)/rRC$ is the second breakpoint. The attenuation factor for $\omega = o$ is $r/(R + r)$. A normalized logarithmic plot of $H_p(f)$ is given in Figure 3-8 (b). If it is assumed that $r << R$, then the response can be approximated by

$$H_p(\omega) \simeq \frac{r}{R} \; \frac{1 + j\omega RC}{1 + j\omega rC} \tag{3-19}$$

where

$$\omega_1 = \frac{1}{RC} \tag{3-20}$$

and

$$\omega_2 \simeq \frac{1}{rC} \tag{3-21}$$

If, in the baseband video frequency range, r is also very small in comparison with the reactance of the capacitance C, then

$$H_p(\omega) \simeq \frac{r}{R} (1 + j\omega RC) \qquad\qquad .(3\text{-}22)$$

since $r \ll 1/j\omega C$ or $j\omega rC \ll 1$.

The simple-passive preemphasis network response can be considered to have the form

$$H_p(f) = \frac{r}{R} \left(1 + j \frac{f}{f_1} \right) \cdot \qquad\qquad (3\text{-}23)$$

where $f_1 = 1/2\pi RC$ is the first breakpoint. It can be easily arranged for the second breakpoint to lie well outside the baseband spectral range and thus be irrelevant.

The video signal to be preemphasized is transmitted through the— passive preemphasis network and also through an adjustable gain amplifier. The amplifier will compensate for the attenuation produced by the preemphasis network. The amplifier gain A is adjusted to the point where the full allowable bandwidth is occupied by the modulated carrier (Reference 9).

Thus, the baseband video signal $m(t)$ passes through a network whose transfer function is approximated by

$$H_p(f) = k_2 \left(1 + j \frac{f}{f_1} \right) \qquad\qquad (3\text{-}24)$$

where k_2 is the product of the amplifier gain A and the attenuation ratio r/R. The coefficient

$$k_2 = A \cdot \frac{r}{R} \qquad\qquad (3\text{-}25)$$

is adjusted so that the normalized power of the baseband video signal $m(t)$ is the same as the normalized power of the preemphasized signal $m_p(t)$. This constraint was introduced in Equation (3-7).

From an inspection of Equations (3-16) and (3-24), it is readily apparent that $H_p(f)$ has a frequency dependence which is inverse to that of $H_d(f)$. This is required, of course, in order that no net distortion be introduced into the video signal. Therefore,

$$H_p(f) \; H_d(f) \simeq 1 \cdot$$

(3-26)

where $k_1 = k_2 = k.$

The ratio $\mathscr{R}$ by which preemphasis-deemphasis improves the signal-to-noise ratio of an FM signal (for large carrier-to-noise ratio) was developed in Equation (3-9). That is,

$$\mathscr{R} = \frac{f_M^3 / 3}{\displaystyle\int_0^{f_M} \frac{f^2}{|H_p(f)|^2} \, df}$$

(3-27)

where the bandwidth of the video signal is given by f_M, which is also the bandwidth of the video baseband filter. From the above network analysis, it was learned that the transfer function of the preemphasis network may be approximated by

$$H_p(f) = k \left(1 + j \frac{f}{f_1} \right)$$

(3-28)

where k is the network coefficient with a value less than unity.

Inserting Equation (3-28) into the expression for the SNR improvement factor $\mathscr{R}$ yields

$$\mathscr{R} = \frac{f_M^3/3}{\displaystyle\int_0^{f_M} \frac{f^2 \, df}{k^2\left[1 + \left(\frac{f}{f_1}\right)^2\right]}} \qquad (3\text{-}29)$$

$$= \frac{k^2 \, f_M^3/3}{\displaystyle\int_0^{f_M} \frac{f^2}{1 + \left(\frac{f}{f_1}\right)^2} \, df}$$

$$\frac{k^2 f_M^3/3}{f_1^3\left(\frac{f_M}{f_1} - \tan^{-1}\frac{f_M}{f_1}\right)}$$

$$\mathscr{R} = \frac{k^2}{3}\left(\frac{f_M}{f_1}\right)^2 \frac{1}{\left(1 - \frac{f_1}{f_M} \tan^{-1}\frac{f_M}{f_1}\right)} \qquad o < k \leq 1 \qquad (3\text{-}30)$$

The numerical value for the coefficient k is determined by the power con-
straint of Equation (3-7) and accounts for the reduction in the modulation
level of the transmitter, which is required at low frequencies due to the
preemphasis process. In past analyses by other authors, this factor was
generally ignored. They assumed that the modulation level is not appre-
ciably affected by preemphasis and is the same as with no preemphasis
(k = 1). However, in order to be correct, the reduction in modulation
level (required in order to maintain a constant FM transmission bandwidth)
must be taken into consideration.

3.2.1 Solving for the Coefficient k

So that the bandwidth occupied by the FM modulated carrier may remain constant, the requirement is made that the average power of the preemphasized signal $m_p(t)$ must equal the average power of the original baseband signal $m(t)$. This condition is described by the equality [see Equation (3-7)]

$$\int_{-f_M}^{f_M} S(f)|H_p(f)|^2 \, df = \int_{-f_M}^{f_M} S(f) \, df \qquad (3\text{-}31)$$

The rms bandwidth will thus be the same with or without preemphasis.

In the discussion of Section 2.2 it was stated that for many applications the video power spectral density may be expressed as the envelope function

$$S(f) = \begin{cases} S_0 \dfrac{1}{1 + \left(\dfrac{f}{f'}\right)^2} & |f| \leq f_M \\[4mm] 0 & |f| > f_M \end{cases} \qquad (3\text{-}32)$$

where

$\qquad S_0$ = spectral density at zero frequency

$\qquad f'$ = the frequency at which $S(f)$ has fallen by 3 dB from S_0

and

$\qquad f_M$ = the bandwidth of the video signal and also the bandwidth of the baseband filter.

Substitution of the signal density function into Equation (3-31) and making use of Equation (3-28) gives

$$S_0 \, k^2 \int_{-f_M}^{f_M} \frac{1 + \left(\frac{f}{f_1}\right)^2}{1 + \left(\frac{f}{f'}\right)^2} \, df = \int_{-f_M}^{f_M} \frac{S_0}{1 + \left(\frac{f}{f'}\right)^2} \, df$$

$$(3\text{-}33)$$

The coefficient k is adjusted so that the constraint of Equation (3-33) is satisfied. Simplifying Equation (3-33) yields

$$k^2 \int_0^{f_M} \frac{df}{1 + \left(\frac{f}{f'}\right)^2} + k^2 \int_0^{f_M} \frac{\left(\frac{f}{f_1}\right)^2}{1 + \left(\frac{f}{f'}\right)^2} \, df$$

$$= \int_0^{f_M} \frac{df}{1 + \left(\frac{f}{f'}\right)^2} \qquad\qquad (3\text{-}34)$$

Evaluating the integral on the right hand side of the above equation,

$$\int_0^{f_M} \frac{df}{1 + \left(\frac{f}{f'}\right)^2} = f' \, \tan^{-1}\left(\frac{f}{f'}\right) \Big|_0^{f_M}$$

$$= f' \, \tan^{-1}\left(\frac{f_M}{f'}\right) \qquad\qquad (3\text{-}35)$$

Likewise, the first integral on the left hand side of Equation (3-34) becomes

$$\int_0^{f_M} \frac{k^2}{1 + \left(\frac{f}{f'}\right)^2} \, df \; = \; k^2 \, f' \, \tan^{-1}\left(\frac{f}{f'}\right) \Big|_0^{f_M} \, ,$$

$$= \; k^2 \, f' \, \tan^{-1}\left(\frac{f_M}{f'}\right) \tag{3-36}$$

Evaluating the second integral on the left hand side of Equation (3-34) gives the following result,

$$k^2 \int_0^{f_M} \frac{\left(\frac{f}{f_1}\right)^2}{1 + \left(\frac{f}{f'}\right)^2} \, df \; = \; k^2 \left(\frac{f'}{f_1}\right)^2 \int_0^{f_M} \frac{f^2}{f^2 + (f')^2} \, df$$

$$= \; k^2 \left(\frac{f'}{f_1}\right)^2 \left[f - f' \, \tan^{-1} \frac{f}{f'}\right] \Big|_0^{f_M}$$

$$= \; k^2 \left(\frac{f'}{f_1}\right)^2 \left[f_M - f' \, \tan^{-1} \frac{f_M}{f'}\right]$$

$$\tag{3-37}$$

Using Equations (3-35), (3-36), and (3-37), the power constraint can now be expressed as

$$k^2 \ f' \ \tan^{-1}\left(\frac{f_M}{f'}\right) \ + k^2 \left(\frac{f'}{f_1}\right)^2 \left[f_M - f' \ \tan^{-1}\left(\frac{f_M}{f'}\right)\right]$$

$$= f' \ \tan^{-1}\left(\frac{f_M}{f'}\right) \qquad (3\text{-}38)$$

or rearranging in terms of the coefficient k,

$$k^2 = \frac{f' \ \tan^{-1}\left(\frac{f_M}{f'}\right)}{f' \ \tan^{-1}\left(\frac{f_M}{f'}\right) + \left(\frac{f'}{f_1}\right)^2 \left[f_M - f' \ \tan^{-1}\left(\frac{f_M}{f'}\right)\right]} \qquad (3\text{-}39)$$

$$= \frac{1}{1 - \left(\frac{f'}{f_1}\right)^2 \left[1 - \dfrac{\dfrac{f_M}{f'}}{\tan^{-1}\left(\frac{f_M}{f'}\right)}\right]} \qquad (3\text{-}40)$$

Another way of looking at the dependence of k upon the ratio f'/f_1 is to rewrite Equation (3-39) thusly,

$$k^2 = \frac{f' \ \tan^{-1}\left(\frac{f_M}{f'}\right)}{\left[1 - \left(\frac{f'}{f_1}\right)^2\right] f' \ \tan^{-1}\left(\frac{f_M}{f'}\right) + \left(\frac{f'}{f_1}\right)^2 f_M} \qquad (3\text{-}41)$$

For the special design case where the breakpoint frequency, f_1, of the networks is located at the -3 dB point, f', of the signal density function S(f),

$$k^2 = \left(\frac{f'}{f_M}\right) \tan^{-1} \left(\frac{f_M}{f'}\right) \qquad f_1 = f' \qquad (3\text{-}42)$$

This same result was obtained in Appendix B, where the expression for k^2 was derived assuming the smoothed version (see Section 2.1) of the continuous part of the video power spectral density for the case of sequential scanning,

$$S(f) = S_0 \left[\frac{1}{1 + \left(\frac{f}{f'}\right)^2} \right] \left[\frac{\cosh \lambda T_e - 1}{\cosh \lambda T_e - \cos 2\pi Tf} \right] \cdot \qquad (3\text{-}43)$$

The fact that the identical expression for k^2 was obtained for both derivations means that k^2 is independent of the periodic fine structure of the video signal, but is dependent on the signal density envelope function. This envelope function represents the horizontal picture correlation [Equation (2-20)].

Intuitively, one would think that, in order to satisfy the equal power constraint, a larger value of k would be allowable when $f_1 > f'$ than when $f_1 = f'$. Conversely, a smaller value of k would be required when $f_1 < f'$ than when $f_1 = f'$. This fact is clearly brought out by the sketches in Figure 3-9.

The figure depicts three possible conditions: (a) $f_1 > f'$, (b) $f_1 = f'$, and (c) $f_1 < f'$. For the first case, sketched in Figure 3-9 (a), the preemphasis network breakpoint, f_1, occurs when the signal density has fallen considerably from its low frequency value, S_0. This condition results in little preemphasis to the input signal spectra. Thus, the coefficient k must be decreased only slightly from its unity value (without preemphasis) in order to satisfy the equal modulating signal power constraint. In the second case $f_1 = f'$, shown in Figure 3-9 (b), preemphasis of the input signal spectra causes the preemphasized signal spectra to be
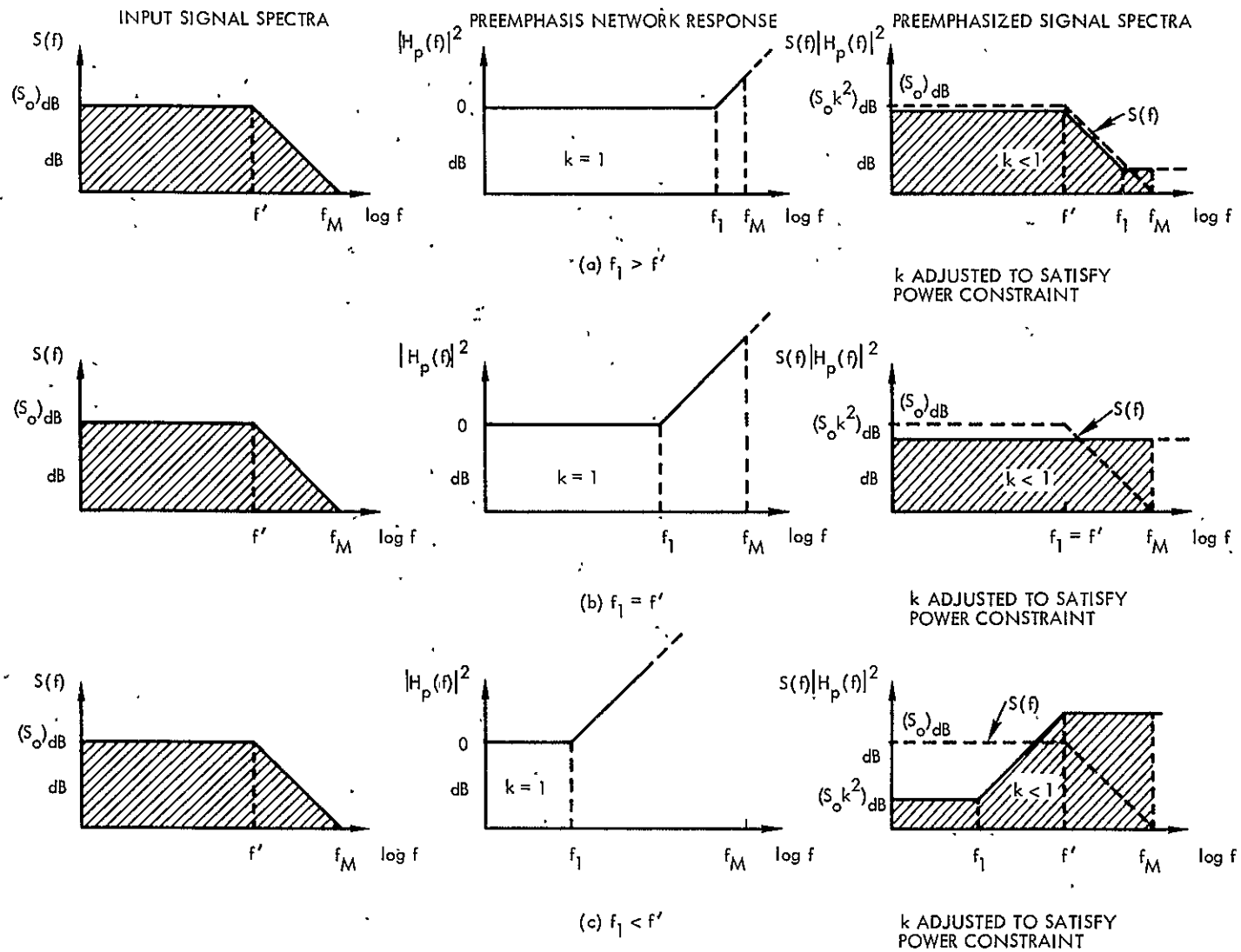
Figure 3-9. Effect of Preemphasis Network on Input Signal Spectra for Various Configurations of f' and f_1 (Assuming Power Constraint)

uniform over the whole video bandwidth. This condition presents the optimum case in terms of effectively maximizing the video signal-to-noise ratio improvement with no resultant signal distortion. The third case is sketched in Figure 3-9 (c) for the condition, $f_1 < f'$. Here, the network has begun to preemphasize the input signal spectra before the function has begun to roll-off. This causes video spectral components, below the -3 dB frequency f', to be preemphasized as well as those above f'. In order to satisfy the power constraint, the coefficient k must be drastically reduced from its unity value for no preemphasis.

Now that the expression for the value of k^2 has been derived, the improvement ratio can be further developed by substituting Equation (3-41) into Equation (3-30). Having done this, the signal-to-noise ratio improvement is given by

$$\mathcal{R} = \cfrac{f' \, \tan^{-1}\left(\cfrac{f_M}{f'}\right)}{\left[1 - \left(\cfrac{f'}{f_1}\right)^2\right] f' \, \tan^{-1}\left(\cfrac{f_M}{f'}\right) + \left(\cfrac{f'}{f_1}\right)^2 f_M}$$

$$\cfrac{\dfrac{1}{3}\left(\dfrac{f_M}{f_1}\right)^2}{1 - \dfrac{f_1}{f_M}\,\tan^{-1}\left(\dfrac{f_M}{f_1}\right)} \tag{3-44}$$

When the breakpoint frequency, f_1, of the networks is located at the -3 dB point, f', of the envelope signal density function ($f_1 = f'$), the improvement resulting from preemphasis and subsequent deemphasis becomes

$$\mathcal{R} = \frac{\tan^{-1}\left(\frac{f_M}{f_1}\right)}{3\left(\frac{f_1}{f_M}\right) \cdot \left[1 - \frac{f_1}{f_M} \tan^{-1}\left(\frac{f_M}{f_1}\right)\right]} \qquad f_1 = f' \quad \text{(3-45)}$$

This same result may be obtained by inserting Equation (3-42) into Equation (3-30). Figure 3-10 is a plot of the SNR improvement in decibels versus the ratio f_M/f_1 according to Equation (3-45).

If the power in the baseband signal is concentrated at low frequencies, so that $f_M/f_1 \gg 1$, then $\mathcal{R}$ will be considerably greater than one. For very large values of f_M/f_1

$$1 - \frac{f_1}{f_M} \tan^{-1}\left(\frac{f_M}{f_1}\right) \approx 1 \qquad \text{(3-46)}$$

and

$$\tan^{-1}\left(\frac{f_M}{f_1}\right) \approx \frac{\pi}{2} \qquad \text{(3-47)}$$

and the improvement ratio in Equation (3-45) is approximately

$$\mathcal{R} \approx \frac{\pi}{6} \frac{f_M}{f_1} \quad , \qquad \frac{f_M}{f_1} \gg 1 \qquad \text{(3-48)}$$

Plots of the exact [Equation (3-45)] and the approximate [Equation (3-48)] SNR improvement factor versus the ratio f_M/f_1 are shown in Figure 3-11.

From inspection of·Figure 3-11, it ·is seen that the improvement factor $\mathcal{R}$, as expressed in Equation (3-45), is greater than or equal to 1 in value. This is because the deemphasis network reduces the output noise.
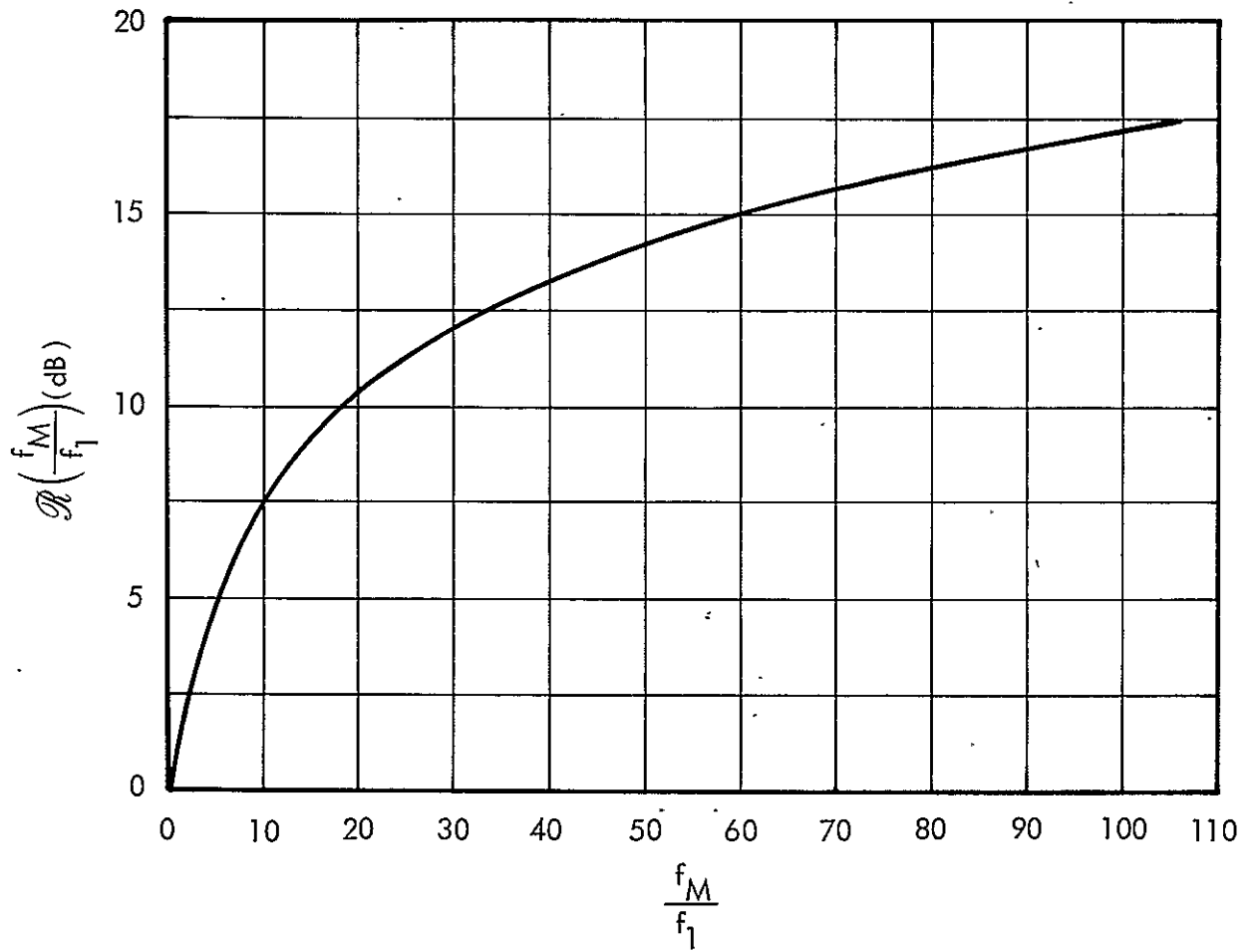
Figure 3-10. Signal-to-Noise Ratio Improvement in Decibels versus f_M/f_1
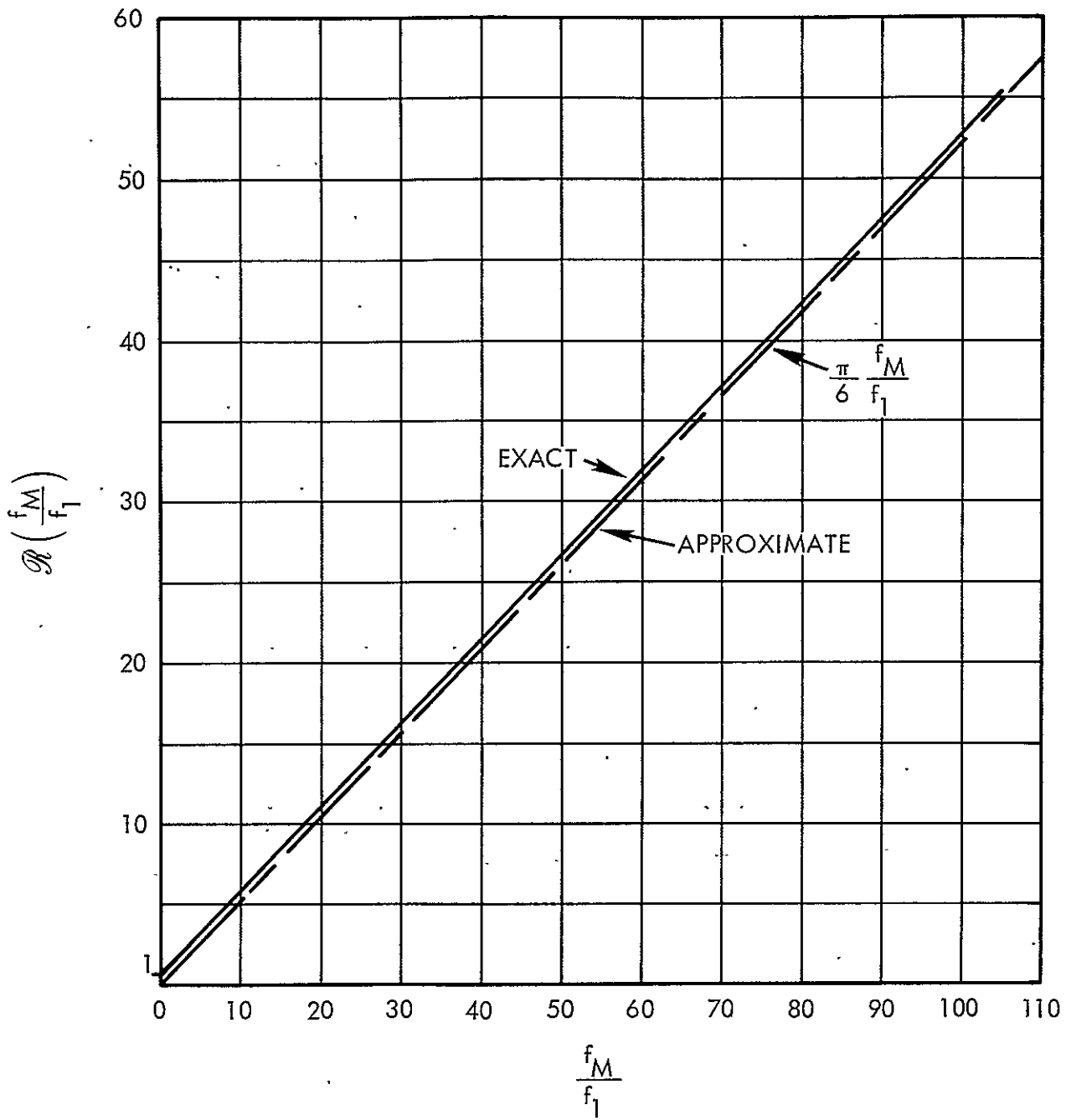
Figure 3-11. Exact and Approximate ($f_M/f_1 \gg 1$) SNR
Improvement Factor versus f_M/f_1

For $f_M \ll f_1$ (the deemphasis effect is then introduced beyond the range of the baseband filter)

$$\mathscr{R} \to 1, \qquad \frac{f_M}{f_1} \ll 1 \qquad\qquad\qquad (3\text{-}49)$$

as is to be expected. For $f_M \gg f_1$, as was shown in Equation (3-48)

$$\mathscr{R} \to \frac{\pi}{6} \frac{f_M}{f_1}, \quad \frac{f_M}{f_1} \gg 1 \qquad\qquad\qquad (3\text{-}50)$$

The SNR improvement increases linearly with increasing f_M.

Increasing f_M indefinitely provides no <u>absolute</u> improvement in the output signal-to-noise ratio, however, for the output noise N_{oD} increases linearly with increasing f_M, while the signal density $S(f)$ decreases as the square of the frequency. <u>The output filter bandwidth f_M should thus be restricted to just the bandwidth required to pass the highest significant video frequency and no more.</u> Figure 3-12 serves to illustrate this point. While the theoretical SNR improvement increases as f_M is increased to f_M', actually, more noise power may be allowed in the filter bandwidth than signal power, and thus the <u>absolute</u> signal-to-noise ratio in the output filter bandwidth decreases.

WITHOUT EMPHASIS
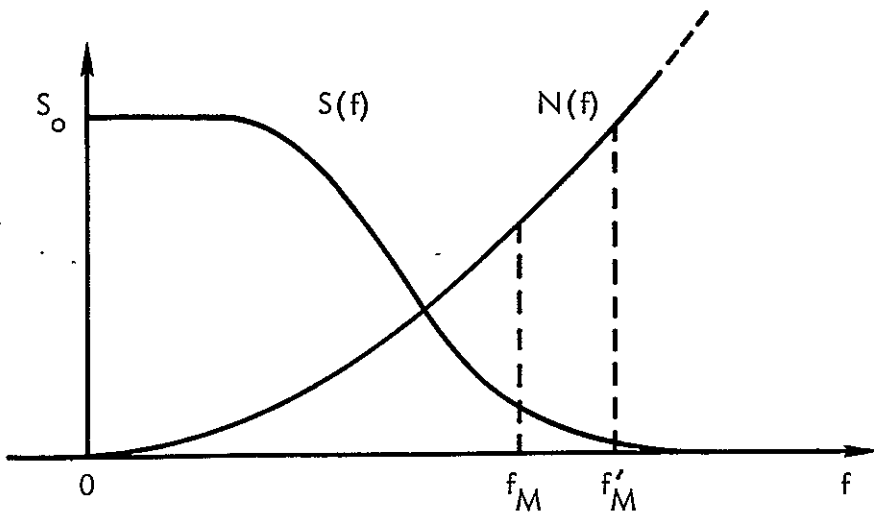
(a)

WITH EMPHASIS
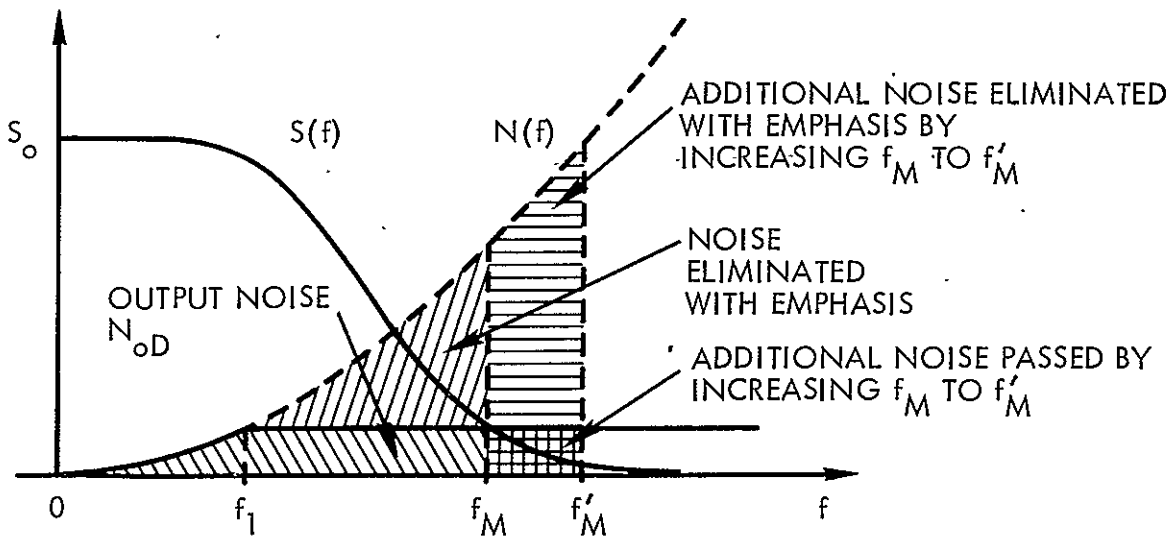
(b)

Figure 3-12. Output of Video Baseband Filter

3.3 CONSIDERATION OF VARIOUS VIDEO PICTURE CORRELATIONS

The purpose of this section is to present the results of theoretical calculations for the SNR improvement $\mathcal{R}$, above threshold, for various video picture correlations. Comments are made on the design of a preemphasis/ deemphasis network pair for a practical television system where the scene images have a varying degree of correlation.

Before the effects of picture correlation are discussed, it is advantageous to review the shaping of the input video spectrum by the preemphasis-deemphasis filtering process for the special case where $f_1 = f'$. Figure 3-13 shows the sequence of events that make up the emphasis process. The input signal spectrum at the transmitter is sketched in (a) with a -3 dB breakpoint at f'. The highest significant video frequency is shown as f_M, which is also the output filter bandwidth. The preemphasis network response is depicted in (b) with a network coefficient k of value less than one and a breakpoint at f_1. During preemphasis, the signal spectrum is flattened because the upward slope of the preemphasis network exactly compensates for the downward slope of the video spectrum. Notice that the k of the preemphasis network has been adjusted so that the preemphasized signal power in (c) is equal to the original signal power in (a). This guarantees that the modulated carrier bandwidth will remain the same in the FM transmission channel. At the receiver in sketch (d), the inverse of the preemphasis network response is shown - which is the deemphasis network response. As a result of the deemphasis process, the preemphasized signal spectrum is post-distorted to recover the original input signal spectrum. Figure 3-13 is an accurate representation of the effect of the emphasis process on a signal spectrum that corresponds to a video picture whose horizontal correlation is such that f' equals f_1.

The logical question is, What happens when the horizontal picture correlation changes and f' is no longer equal to f_1?   Figure 3-14 is a graphical attempt to answer this question. Since the networks are static, the values for f_1 and k are <u>fixed</u>. Assume, for example, that the networks
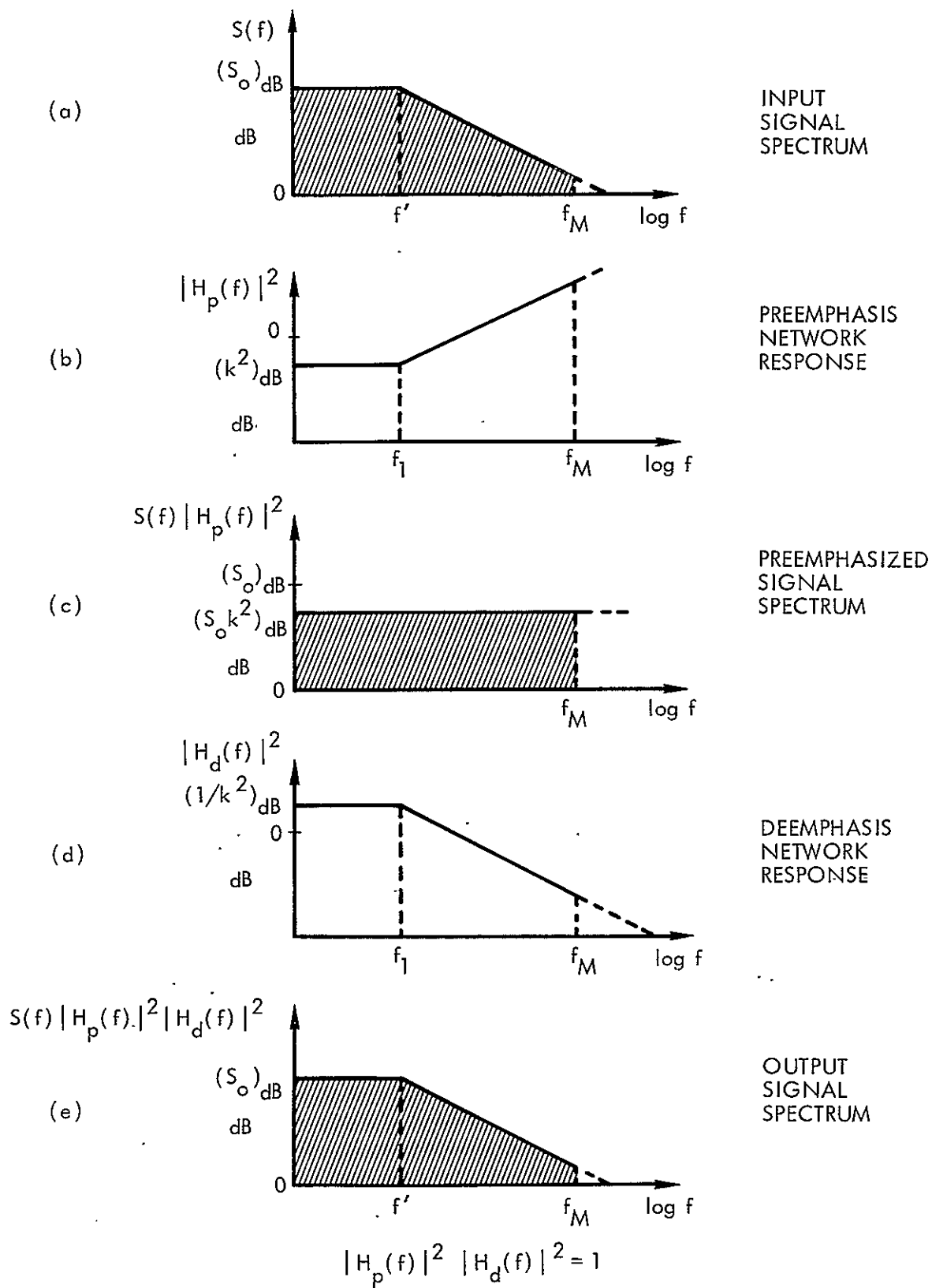
Figure 3-13. Emphasis Process Sequence ($f_1 = f'$)

are designed for a horizontal video picture correlation, ρ_h, equal to 0.95, which later will be shown corresponds to f' equal to 100 kHz. As long as ρ_h equals 0.95, the conditions portrayed in Figure 3-13 remain true. However, when the correlation increases to a value greater than 0.95, a new condition exists, as shown at the top of Figure 3-14. The preemphasized signal spectra no longer occupies the total signal spectral space. The total modulating signal power on the channel is less (channel SNR is decreased) and, consequently, the FM modulated carrier no longer makes full use of its alloted IF bandwidth. Since k and f_1 are fixed, the SNR improvement $\mathscr{R}$ will theoretically remain the same [see Equation (3-30)], even though it is clear that the absolute signal-to-noise ratio at the output of the deemphasis network is going to be less. The actual SNR improvement, therefore, must be less than that calculated using Equation (3-30), which has the inherent assumption that f' = f_1.

Now consider the opposite situation where the horizontal picture correlation decreases to a value less than 0.95. This condition is depicted at the bottom of Figure 3-14. The preemphasized signal spectra now exceeds the originally designed signal spectral space. The result, of course, is an increased amount of modulating signal power and therefore a transmission bandwidth which exceeds the designed IF bandwidth. This causes nonlinear distortion in the demodulated signal. In addition, if the horizontal picture correlation becomes too low, significant baseband signal spectral components will be lost outside of the baseband filter bandwidth - causing a decrease in video picture resolution. Again, Equation (3-30) cannot be used indiscriminately. The conclusion arrived at is that the SNR improvement given by Equation (3-30) or Equation (3-45) is for the optimum situation, only, and must be considered to be an upper limit to the actual SNR improvement realized experimentally. While Equation (3-44), at first glance, might seem to be applicable, it must be remembered that this equation was also derived under the assumption that the equal power constraint is satisfied.

INPUT SIGNAL SPECTRA

PREEMPHASIS NETWORK RESPONSE

PREEMPHASIZED SIGNAL SPECTRA

$\rho_h > .95$

$\rho_h = .95$

$\rho_h < .95$

$\rho_h > .95$

$\rho_h = .95$

$\rho_h < .95$
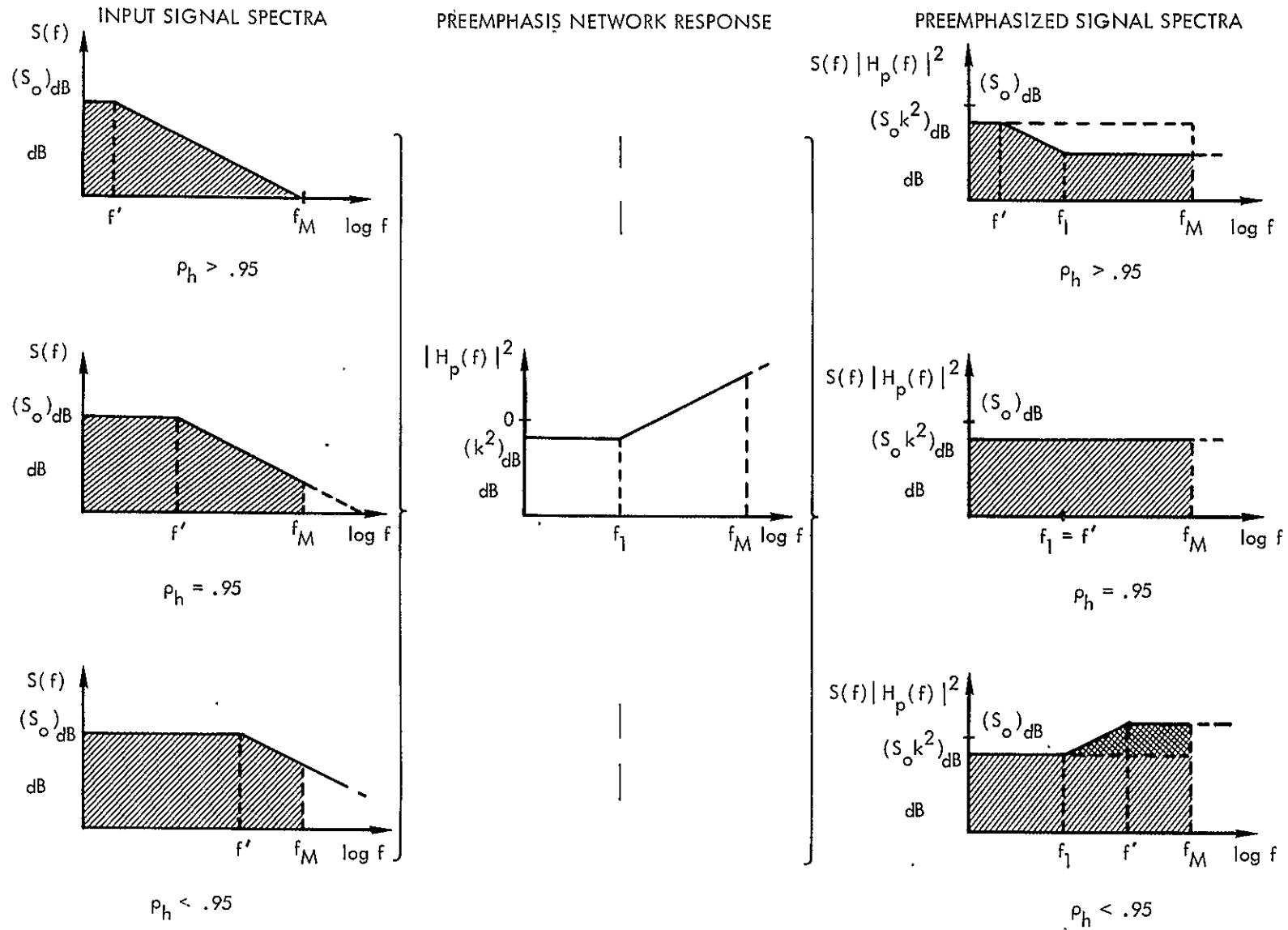
Figure 3-14.   Effect of Preemphasis Network on Input Signal Spectra for
Various Picture Correlations (No Power Constraint)

From Section 2.2, it was learned that the relationship between the video signal density -3 dB frequency, f', and the horizontal picture correlation, ρ_h is

$$f' = \frac{|\ln \rho_h|}{2\pi T_e} = \frac{\lambda_h T_e}{2\pi T_e} = \frac{\lambda_h}{2\pi} \qquad (3\text{-}51)$$

where T_e is the picture element scan interval and λ_h is the Poisson rate parameter describing the luminance process in the horizontal direction. For broadcast television, $T_e/T = 0.00128$. The quantity T_e/T is a fundamental parameter of the raster design depending on the number of lines per frame, the aspect ratio of the visible portion of the picture, and the relative size of the blank portions of the horizontal and vertical scans. Table 3-1 shows the calculated signal density -3 dB frequencies for various values of ρ_h and $\lambda_h T_e$. The relationship used for the calculations is

$$f' = \frac{|\ln \rho_h|}{.51(10)^{-6}} = \frac{\lambda_h T_e}{.51(10)^{-6}} \qquad (3\text{-}52)$$

An interesting measure of the signal power transmitted through the baseband filter is given by the ratio P_t/P_T where

P_t = signal power transmitted through the baseband filter

and

P_T = total signal power.

Table 3-1. Values of f' For Various Values of ρ_h

ρ_h	$\lambda_h T_e = -\ln \rho_h$	f' (kHz)
0.80	0.223	437.3
0.85	0.163	319.6
0.88	0.128	250.0
0.90	0.105	205.9
0.95	0.051	100.0
0.96	0.041	80.4
0.97	0.030	58.8
0.98	0.020	39.2
0.99	0.010	19.6

The signal power passed by the video baseband filter is

$$P_t = 2 \int_0^{f_M} \frac{S_0}{1 + \left(\frac{f}{f'}\right)^2} \, df \tag{3-53}$$

$$= 2 \, f' \, S_0 \, \tan^{-1} \left(\frac{f}{f'}\right) \Big|_0^{f_M}$$

$$= 2 \, S_0 \, f' \, \tan^{-1} \left(\frac{f_M}{f'}\right) \tag{3-54}$$

The total power contained in the video signal is

$$P_T = 2 \int_0^{\infty} \frac{S_0}{1 + \left(\frac{f}{f'}\right)^2} \, df \tag{3-55}$$

$$= 2 \, f' \, S_0 \, \tan^{-1} \left(\frac{f}{f'}\right) \Big|_0^{\infty}$$

$$= \pi \, f' \, S_0 \tag{3-56}$$

The ratio of power transmitted through the output filter to the total spectral power is

$$\frac{P_t}{P_T} = \frac{2 \, f' \, S_0 \, \tan^{-1} \left(\frac{f_M}{f'}\right)}{\pi \, f' \, S_0}$$

$$= \frac{2}{\pi} \tan^{-1}\left(\frac{f_M}{f'}\right) \cdot \qquad (3\text{-}57)$$

In Figure 3-15 the ratio P_t/P_T, as given by Equation (3-57), has been plotted versus the ratio f_M/f' for an ideal low pass filter given a signal power density of the form

$$S(f) = \frac{S_o}{1 + \left(\frac{f}{f'}\right)^2}$$

Using the equation below, derived for the special case where $f_1 = f'$, the SNR improvement

$$\mathcal{R} = \frac{\tan^{-1}\left(\frac{f_M}{f'}\right)}{3\left(\frac{f'}{f_M}\right)\left[1 - \frac{f'}{f_M} \tan^{-1}\left(\frac{f_M}{f'}\right)\right]} \qquad (3\text{-}58)$$

is plotted in Figure 3-16 versus ρ_h assuming a 2 MHz baseband filter bandwidth. As expected, the greater the ρ_h for a specifically designed system, the larger the improvement in signal-to-noise ratio. For a fixed f_M, the larger the ρ_h, the larger the ratio f_M/f' will be. This is true because f' decreases for increasing horizontal picture correlation.

From Figure 3-16, it is seen that for an emphasis network pair designed with breakpoints at 100 kHz, the optimum $\mathcal{R}$ will be 10.4 dB for video pictures with a horizontal correlation coefficient of 0.95. For a network pair with breakpoints at 250 kHz, the optimum $\mathcal{R}$ will be 6.7 dB for video pictures with a horizontal correlation coefficient of 0.88.

Equation (3-44) is used to plot the relationship of SNR improvement through emphasis versus horizontal picture correlation when $f_1 \neq f'$, and
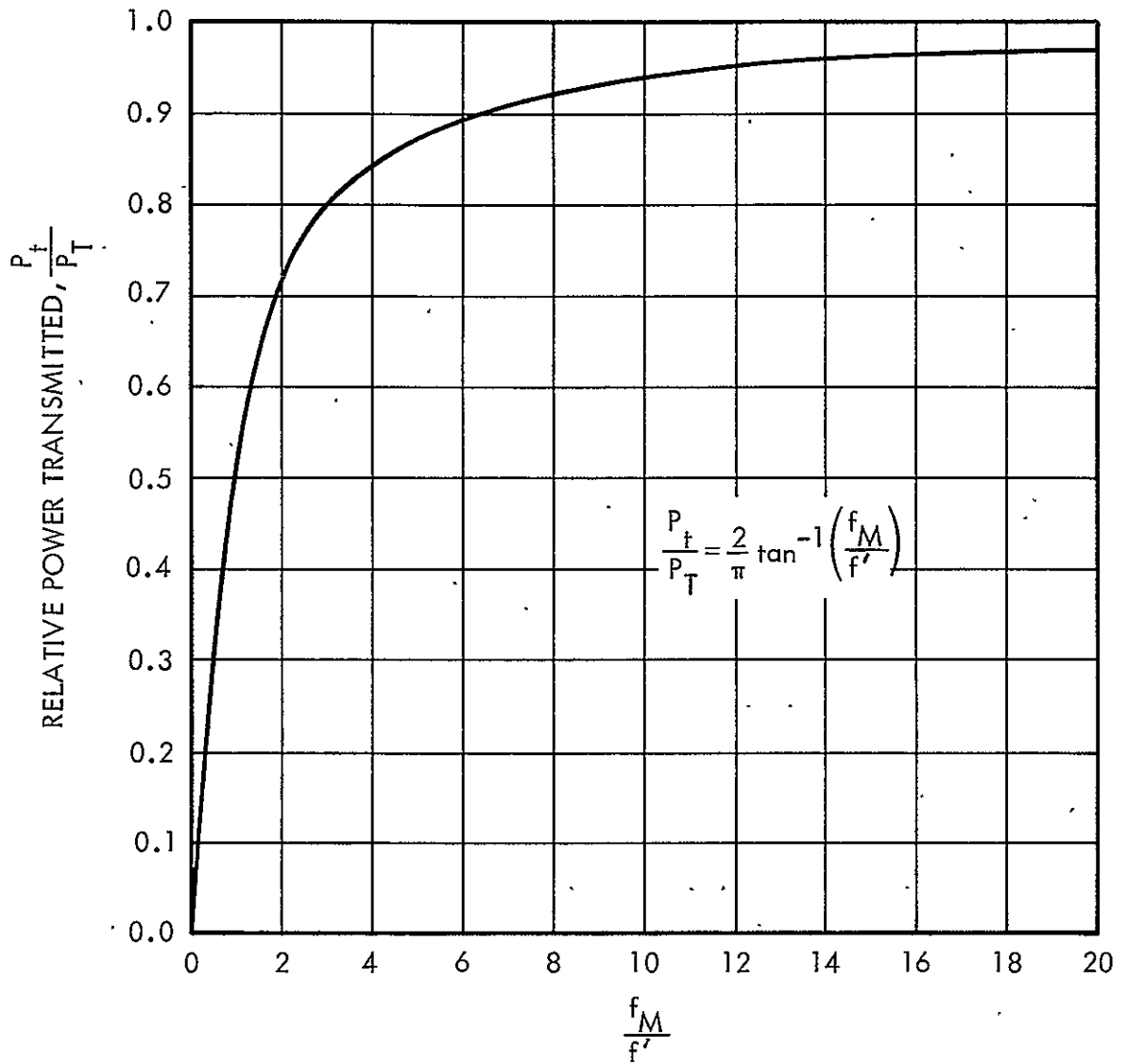
Figure 3-15. Relative Power Transmitted for Video Signal versus f_M/f', Rectangular Baseband Filter
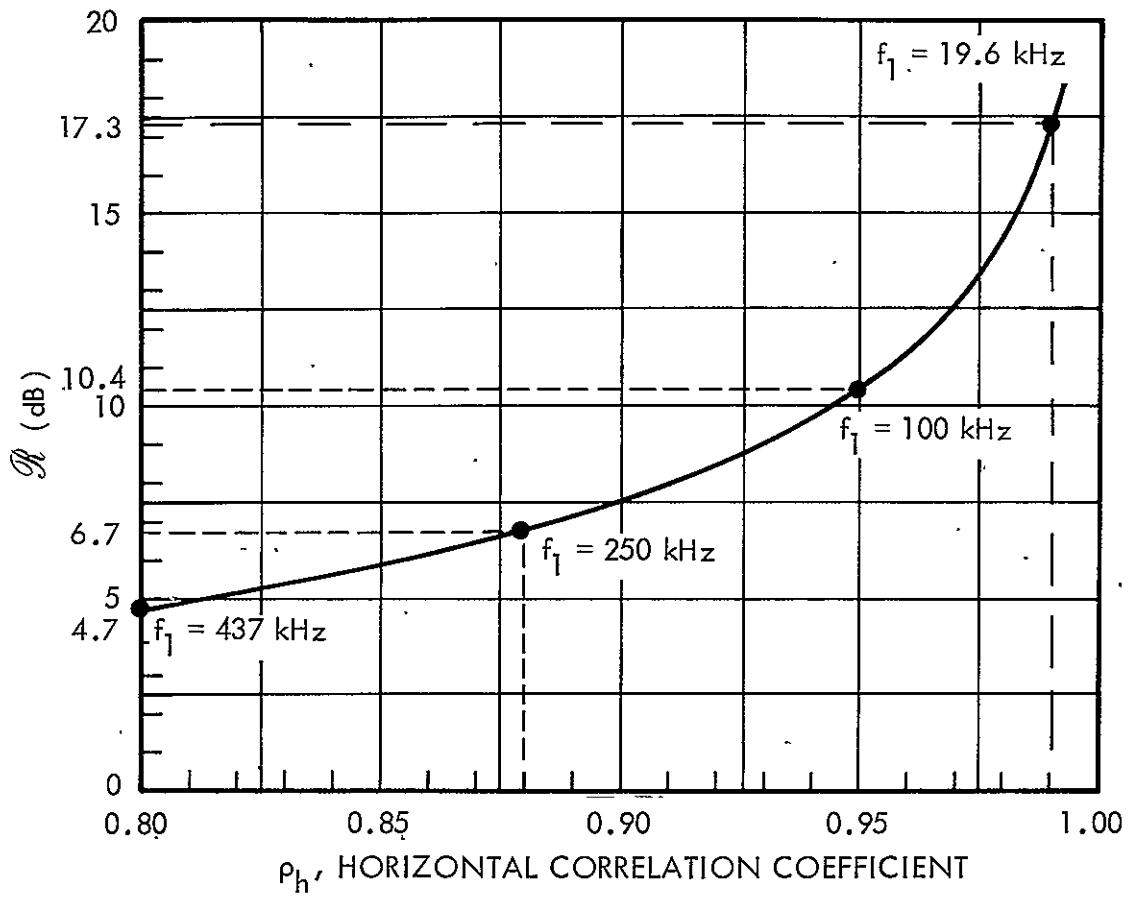
Figure 3-16.   Optimum Non-Weighted SNR Improvement
                versus Horizontal Correlation Coefficient,
                Assuming Power Constraint and Special
                Case $f_1 = f'$ (f_M = 2 MHz)

the average power constraint of Equation (3-31) is satisfied. This plot
is shown in Figure 3-17. A network pair design responsive to the average
power of the preemphasized video input signal is required to achieve the
distortionless results indicated in Figure 3-17. Two responsive systems
are considered. Both networks automatically vary their network coefficients
k to maintain the equal power constraint. One network pair has breakpoints
at 100 kHz .and the other network pair has breakpoints at 250 kHz.
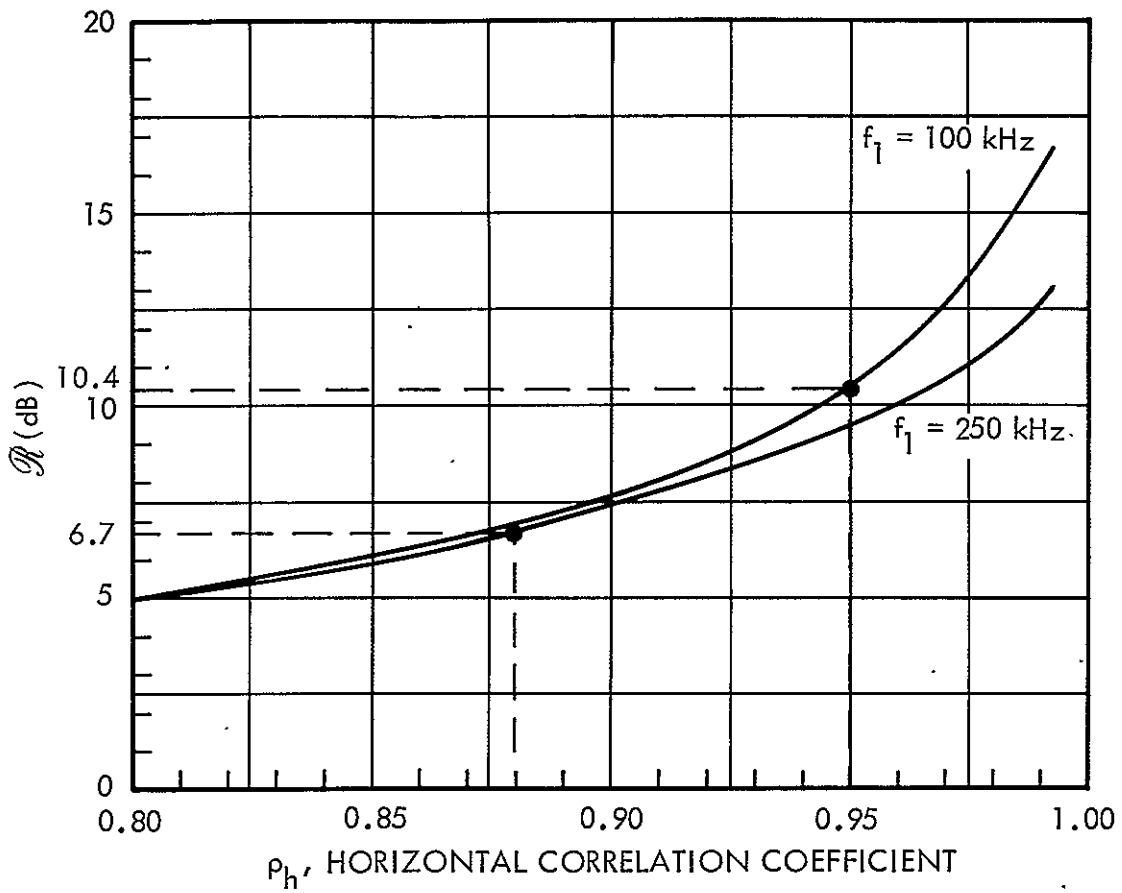
Figure 3-17. Optimum Non-Weighted SNR Improvement versus
Horizontal Correlation Coefficient, Assuming
Adaptive System to Satisfy Power Constraint
$(f_M = 2 \text{ MHz})$

3.4 WEIGHTING OF RANDOM VIDEO NOISE

Random interference or noise (often referred to in television as snow) is a type of interference corresponding to thermal noise, which, at its source of origin, has a frequency composition in which the power density is constant from near zero frequency to well above any frequencies used in the transmission of television signals. However, because of the characteristics of transmission circuits, the frequency composition of random interference at the receiving end of television circuits departs widely from a constant power spectrum. From this situation there stems a need to find a method by which random interference to television pictures could be measured so that equal measured magnitudes of interference would mean equal interfering effects, essentially regardless of the frequency composition of the random noise.

3.4.1 History

The subjective effect of noise in monochrome and color still television pictures has been studied by several researchers at the Bell System Labs [see Mertz (Reference 11); Barstow and Christopher (Reference 12)]. They proposed that the objectionableness of independent additive Gaussian noise is proportional to its weighted power

$$P = \int_0^\infty w(f)\ n(f)\ df \qquad (3\text{-}59)$$

where $n(f)$ is the one-sided power density spectrum of the noise and the weighting function $w(f)$ represents the relative sensitivity of the eye to the various noise frequency components. Mertz derived the form of $w(f)$ from considering the analogy of television random noise to photographic granularity, while the other researchers determined $w(f)$ from subjective tests. The

weighting functions they obtained show a low-pass characteristic. Because the results depend on test equipment and viewing conditions, it is difficult to compare studies conducted by different people except for the general trends. Note that Equation (3-59) assumes tacitly that the subjective effect of noise is additive. Barstow and Christopher checked this assumption by applying Equation (3-59) to wide band-pass noises and found the results roughly consistent.

3.4.2 Monochrome Weighting

A paper by Barstow and Christopher (Reference 12) reports on the results of two studies, one on random interference as it appears to affect pictures seen on black-and-white picture tubes, and the other on random interference as it affects pictures seen on the shadow-mask type of color picture tube. "Still" pictures, derived from slides approved for National Television Systems Committee (NTSC) color testing, were used throughout for both the monochrome and color tests. Barstow and Christopher have obtained estimates of the sensitivity of the average observer to noise as a function of noise frequency. These results apply to low noise levels on commercial television pictures and specify noise sensitivity at frequencies above the line rate.

The frequency weighting functions derived from these studies are shown in Figure 3-18. Numerical values of the weightings are given also in Table 3-2. Since noise weighting characteristics are normalized to 0-dB at zero frequency, the weighted noise level is lower than the unweighted level. It is apparent from the random noise weighting curves for monochrome and color transmissions that low-frequency interference is judged to be more interfering than high-frequency interference of equal power. The noise
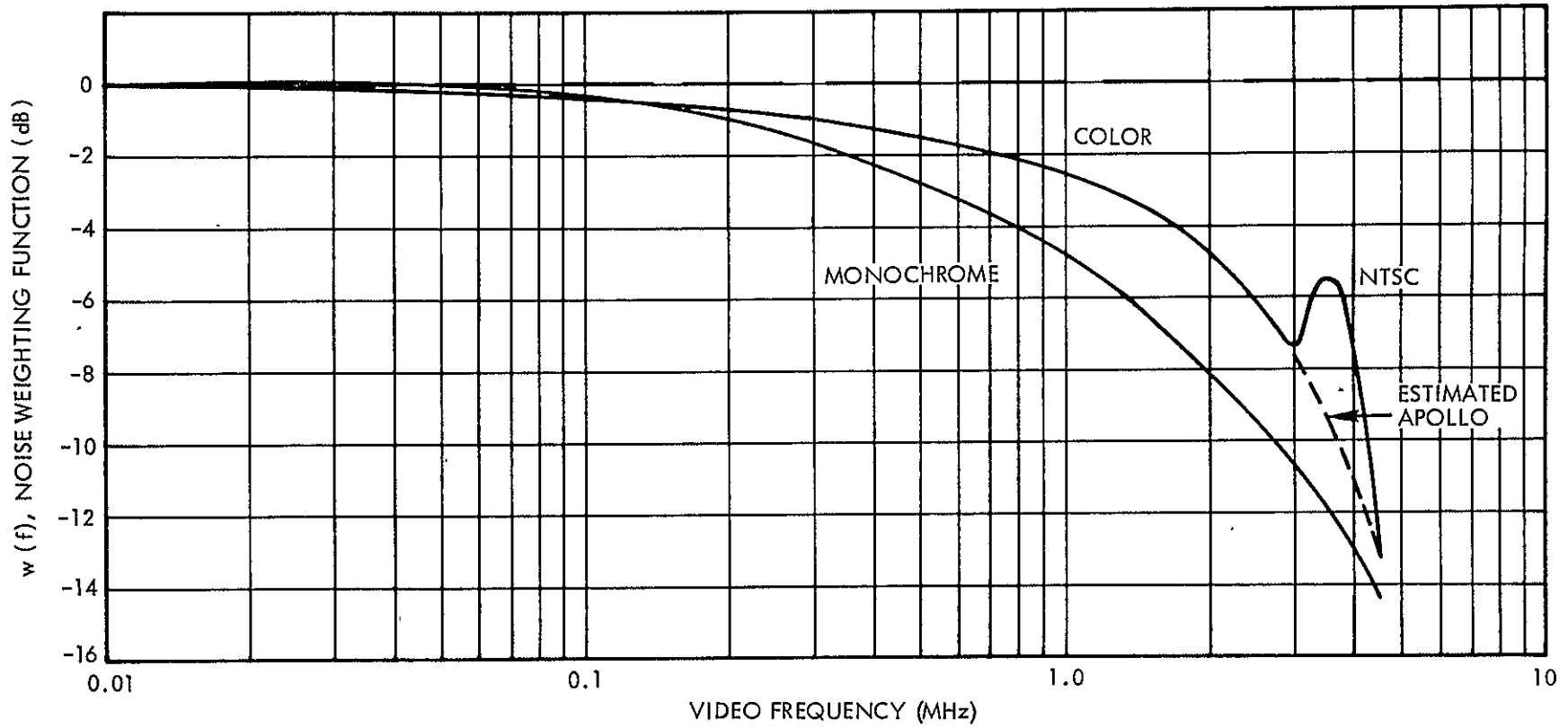
Figure 3-18.   Random Noise Weighting for American 525-Line Television

Table 3-2. Monochrome and Color Weightings

Frequency MHz	Monochrome dB	Color dB
0.1	-0.3	-0.4
0.3	-1.7	-1.0
0.5	-2.8	-1.4
0.7	-3.6	-1.9
0.9	-4.4	-2.3
1.0	-4.7	-2.5
1.1	-5.1	-2.7
1.3	-5.8	-3.1
1.5	-6.5	-3.5
1.7	-7.1	-3.8
1.9	-7.8	-4.4
2.0	-8.1	-4.7
2.1	-8.4	-5.0
2.3	-8.9	-5.5
2.5	-9.5	-6.1
2.7	-10.0	-6.6
2.9	-10.5	-7.3
3.0	-10.8	-7.4
3.1	-11.0	-7.2
3.3	-11.5	-6.0
3.5	-11.9	-5.5
3.7	-12.4	-5.6
3.9	-12.8	-6.5
4.0	-13.0	-7.5
4.1	-13.2	-8.5
4.3	-13.7	-10.7
4.5	-14.3	-13.2

sensitivity function for monochrome TV is flat out to 100 kHz and then falls off some 8 dB from 100 kHz to 2 MHz.

The subjective noise-weighting function is the transfer function of the system consisting of the television kinescope and the human visual system, specified as a function of the electrical video-signal frequencies. The input is an electrical signal; the output is the response of the viewer.

The subjective noise-weighting function is most valuable in determining a figure of merit for the comparison of television communication channels. However, when considering the results of calculations on only one frame of a television sequence, one can be lead to erroneous results regarding visibility of noise. This is due to the significant difference in visibility between stationary and moving patterns in a TV presentation. The noise sensitivity function for live pictures is generally flatter than the noise sensitivity function for still pictures.

3.4.3 Color Weighting

With regard to the color weighting curve shown in Figure 3-18, equal magnitudes of random video noise in the region 0 to 100 kHz are about equally interfering to color and monochrome pictures. However, above 100 kHz, the color weighting curve is flatter (noise is more objectionable) than that of the monochrome weighting curve and at 2 MHz has fallen about 4.3 dB from its value at 100 kHz (compared to 7.8 dB for monochrome). In addition, equal magnitudes of similar bandwidths of noise in the region of 3.6 MHz - region of color subcarrier - are noticeably more interfering to color pictures than to monochrome pictures. In this frequency range, according to Barstow and Christopher, substantial variations in results are obtainable, depending upon the brightness and hues of the colors in the pictures being observed.

For pictures having bright colors such as yellow, dark blue, or light gray (more like black and white), the hump in the weighting curve is several dB lower than its magnitude for deeply saturated reds and blues. The noise weighting shown in Figure 3-18 in the region of the color subcarrier is correct for pictures having important areas covered with moderately heavy saturations of blues and reds, but not for maximum saturations of these hues.

Since the Apollo color television camera generates a field-sequential color signal without a color subcarrier, unlike the parallel NTSC color TV format, the color weighting curve for Apollo applications may be assumed to have the dotted response shown in Figure 3-18.

3.5 VIDEO PICTURE QUALITY

The quality of television pictures is a subjective concept because it is a measure of the degree to which deficiencies in the received video signals are experienced by the individual viewers. The relationship between this subjective picture quality and the measurable signal deficiencies is a difficult one to determine.

The discussion presented in this section is largely extracted from a TRW study by J. Jansen and others (Reference 13).

The impairment in picture quality by noise is a direct function of the relative level and spectral distribution of the video noise at the picture tube. A commonly used parameter of picture quality is the picture signal-to-noise ratio, defined by

$$\left(\frac{S}{N}\right)_p = \left(\frac{\text{blank-to-white video voltage}}{\text{rms voltage of video noise}}\right)^2 \tag{3-60}$$

The name, picture-SNR, refers to the fact that it compares the noise voltage with the voltage range of the picture signal (see Figure 3-19). In the definition of a similar signal-to-noise ratio, used by AT&T, the signal is considered to be the entire video voltage range, including the sync pulse as well. This leads to an approximately 3-dB higher figure.
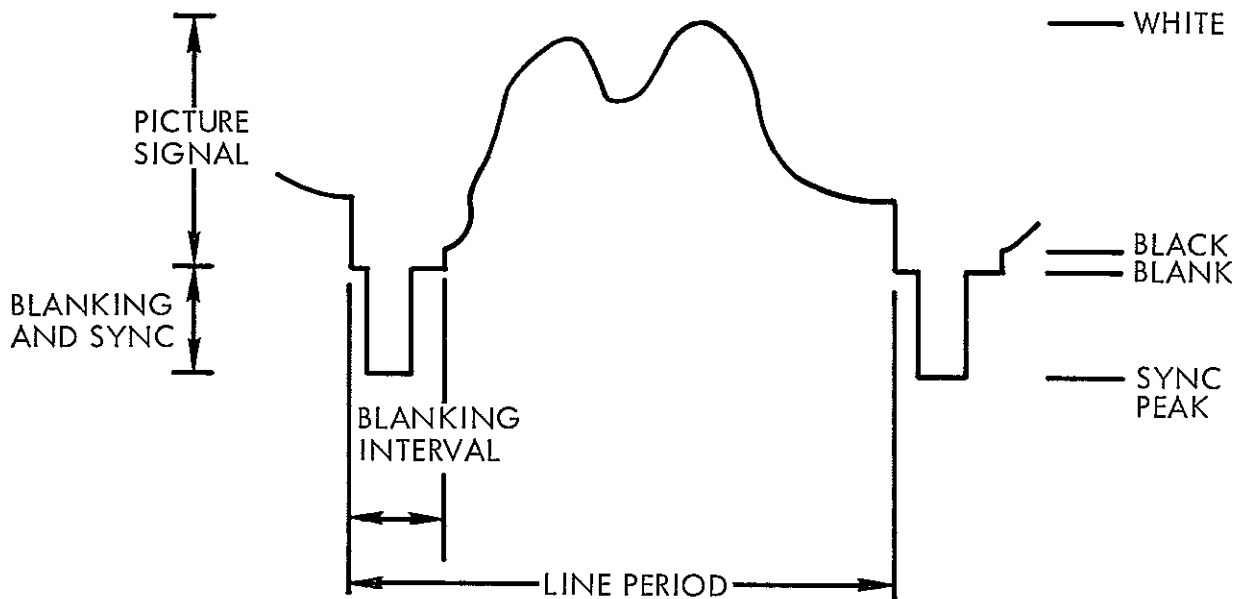
Figure 3-19. Luminance Signal

Neither of these definitions is a meaningful measure of the effect of noise on the picture quality, as subjectively experienced by viewers, unless qualified by an indication of the video noise spectrum. This is because noise at the upper end of the video frequency band is less objectionable than equal noise power at the lower end. This ambiguity in the picture-SNR is to a large extent eliminated by the concept of weighted noise, defined as video noise measured with a weighting network which represents the spectral perception of noise by an average observer. The power transfer characteristic of such a filter was shown in Figure 3-18.

The definition of picture-SNR based on weighted noise becomes

$$\left(\frac{S}{N}\right)_{p,w} = \left(\frac{\text{blank-to-white video voltage}}{\text{weighted rms voltage of video noise}}\right)^2 \quad (3-61)$$

where the subscript w refers to the weighting. The correlation of this quantity with subjectively graded picture quality is in essence independent of the video noise spectra.

The weighting factor, i.e., the ratio by which random noise weighting increases the picture-SNR, is defined as

$$W_{dB} = 10 \log \frac{\int_0^{f_M} n(f)\, df}{\int_0^{f_M} n(f)\, w(f)\, df} \quad (3-62)$$

where

f_M = the upper frequency limit of the video band

f = video frequency

$n(f)$ = one-sided power spectral density of video noise

$w(f)$ = power transfer characteristic of the noise weighting network.

While the video noise spectrum is essentially flat for AM transmission of television, the power spectral density of video noise in a FM system is proportional to the square of the frequency. Compared with AM, FM shows a shift of noise power distribution to higher video frequencies, where the attenuation in the weighting network is larger. Therefore, the weighting factor for FM transmission of video is larger than for AM transmission.

Table 3-3 shows values for noise weighting factors taken from CCIR (International Radio Consultative Committee) Recommendations and Reports and from EIA (Electronic Industries Association) Standard 250-A. The

Table 3-3. Random Video Noise

Number of Lines Per Frame		525	
Nominal Video Bandwidth		4.2 MHz	
Noise Weighting Factors, dB	AM	Monochrome	6.1
		Color, Composite Video	4.0
	FM	Monochrome	10.2
		Color, Composite Video	7.0

values apply to the American NTSC Standard television broadcast system with 525-line, 4.2 MHz transmission.

As a result of subjective quality tests by Barstow and Christopher (Reference 12), it is known that equal magnitudes of noise near the color subcarrier frequency are noticeably more interfering in color pictures than in monochrome pictures. This observation is manifested by a "hump" in the noise weighting curve at the color subcarrier frequency, leading to a lower weighting factor for color pictures than for monochrome pictures. The effect is extremely dependent upon the degree of picture color saturation. The results of Barstow and Christopher's tests with a flat noise spectrum indicate noise weighting factors of 6.5 dB and 4.3 dB for monochrome and color pictures, respectively.

Unfortunately, adequate data on the correlation between subjectively experienced picture quality and signal-to-noise ratio are not available for FM transmission. Therefore, it must be assumed that FM transmission with a given weighted picture-SNR would rate the same subjective grade in a viewer panel test as AM transmission with the same weighted picture-SNR. In other

words, it is assumed that the weighting network accounts exactly for the effect of spectral distribution of random video noise on the subjectively experienced interference.

3.6 WEIGHTED SNR IMPROVEMENT USING EMPHASIS

For FM transmission of television above threshold (for large carrier-to-noise ratio), the weighted picture-SNR [as defined in Equation (3-61)] is

$$\left(\frac{S}{N}\right)_{p,w} = \frac{3}{2} \; \beta^2 \; \left(\frac{B_{IF}}{B_o}\right) \; CNR \cdot W \qquad (3-63)$$

where

W = weighting factor

$\beta = \dfrac{\Delta f}{B_o}$ = modulation index

Δf = peak carrier frequency deviation

B_{IF} = rectangular IF bandwidth

B_o = rectangular output bandwidth of the postdetection low pass video baseband filter

CNR = input carrier-to-noise ratio.

When <u>preemphasis-deemphasis</u> is used in the FM transmission of television, above threshold, the weighted picture-SNR is increased by the <u>weighted SNR improvement factor</u> $\mathscr{R}_w$ so that

$$\left(\frac{S}{N}\right)_{p,w} = \frac{3}{2} \; \beta^2 \left(\frac{B_{IF}}{B_o}\right) \; CNR \cdot W \cdot \mathscr{R}_w \qquad (3-64)$$

where

$$\mathscr{R}_w = \frac{\displaystyle\int_0^{B_o} f^2 \, w(f) \, df}{\displaystyle\int_0^{B_o} \frac{f^2 \, w(f)}{|H_p(f)|^2} \, df} \qquad (3-65)$$

= weighted SNR improvement through emphasis

$$W = \frac{\int_{0}^{B_0} f^2 \, df}{\int_{0}^{B_0} f^2 \, w(f) \, df} \qquad \qquad (3\text{-}66)$$

$\qquad \qquad$ = weighting factor

$w(f)$ = frequency weighting function of subjective random noise

$H_p(f)$ = preemphasis network frequency response

B_0 = video bandwidth.

Substitution of Equations (3-65) and (3-66) into the expression for the weighted picture-SNR [Equation (3-64)] yields

$$\left(\frac{S}{N}\right)_{p,w} = \frac{3}{2} \, \beta^2 \left(\frac{B_{IF}}{B_0}\right) \frac{\int_{0}^{B_0} f^2 \, df}{\int_{0}^{B_0} \dfrac{f^2 w(f)}{|H_p(f)|^2} \, df} \, CNR \qquad (3\text{-}67)$$

$$= \frac{1}{2} \, (\Delta f)^2 \, B_{IF} \, \frac{1}{\int_{0}^{B_0} \dfrac{f^2 w(f)}{|H_p(f)|^2} \, df} \, CNR \qquad (3\text{-}68)$$

for large carrier-to-noise ratio (for example, values of CNR greater than 10 dB, typically). The above equation gives the weighted picture-SNR at the output of a baseband FM television channel when preemphasis - deemphasis is utilized. Without emphasis, $|H_p(f)|$ becomes unity, and Equation (3-67) reduces to the expression given in Equation (3-63), which represents only the effect of random noise weighting on video picture-SNR.

The weighted SNR improvement $\mathcal{R}_w$ obtained with emphasis, is always less than the non-weighted SNR improvement $\mathcal{R}$. This is due to the decreasing objectionableness of random noise for increasing video frequencies, where

preemphasis - deemphasis is intended to be most effective. Since random noise is more objectionable to color TV than monochrome TV for a given video frequency range, [see Figure 3-18], the weighted SNR improvement with emphasis is subsequently greater for color TV than for monochrome TV.

The RF bandwidth occupied by frequency modulation transmission is by Carson's rule (Reference 13),

$$B_{rf} = 2B_o + \mu\epsilon D , \qquad (3-69)$$

where

$$\mu = \frac{\text{sync peak-to-white video voltage}}{\text{blank-to-white video voltage}} ,$$

ϵ = ratio of change in peak-to-peak frequency deviation of composite video modulation due to preemphasis

D = blank-to-white frequency deviation, measured with preemphasis removed, i.e., with $|H_p(f)| \equiv 1$.

3.7 THEORETICAL RESULTS

The calculated results for the non-weighted SNR improvement $\mathscr{R}$ due to video emphasis, above FM threshold, are summarized in Table 3-4. Equation (3-45) was used to generate the data. Assumptions made in the calculations are that $f_1 = f'$, the transmission bandwidth is kept constant, and that there is a 2 MHz video baseband filter ($f_M = 2$ MHz). When no attempt is made to keep the preemphasized video transmission bandwidth equal to the original no emphasis bandwidth ($k = 1$), the calculated optimum values for $\mathscr{R}$ will be greater than the figures presented in Table 3-4. Equation (3-30) with $k = 1$ is then the appropriate equation to use. The <u>additional</u> SNR improvement due to the increased modulation level for a 250 kHz/2000 kHz network pair is +7.42 dB, for a 100 kHz/2000 kHz network pair the additional SNR improvement is +11.2 dB. For a particular network pair, where $f_1 = f'$, the additional improvement in $\mathscr{R}$, above that recorded in Table 3-4, due to the increased modulation level of the modulating signal is given by the factor

$$\frac{1}{k^2} = \frac{f_M/f_1}{\tan^{-1}(f_M/f_1)} \tag{3-70}$$

As explained in Section 3.3, the values for $\mathscr{R}$ are optimum and may not be actually realized in practice, depending on the variation in picture correlation. If the horizontal video picture correlation is lower than the network design picture correlation, then nonlinear distortion may be experienced in the received signal, as well as degraded resolution. The preemphasis-deemphasis networks should have breakpoints sufficiently high in frequency, so that picture correlations having spectra with -3 dB rolloff points greater than f_1 will occur rarely, and only for short periods of time. In this way, any possible distortion will be minimized.

Table 3-4. Non-Weighted SNR Improvement ($f_1 = f!$; $f_M = 2$ MHz)

ρ_h	$\lambda_h T_e = -\ln \rho_h$	f' (kHz)	f_M/f'	P_t/P_T (%)	$\mathscr{R}$ (dB)
0.80	0.223	437.3	4.6	86.4	4.7
0.85	0.163	319.6	6.3	90.0	5.8
0.88	0.128	250.0	8.0	92.1	6.7
0.90	0.105	205.9	9.7	93.5	7.5
0.95	0.051	100.0	20.0	96.9	10.4
0.96	0.041	80.4	24.9	97.5	11.4
0.97	0.030	58.8	34.0	95.0	12.6
0.98	0.020	39.2	51.0	98.8	14.3
0.99	0.010	19.6	102.0	99.4	17.3

If the noise density is weighted as shown in Figure 3-18, the weighted SNR improvement $\mathscr{R}_w$ may be calculated according to the definition given in Equation (3-65). The weighted SNR improvement $\mathscr{R}_w$ obtained with emphasis is always less than the non-weighted SNR improvement $\mathscr{R}$. The weighted SNR improvement with emphasis is greater for color TV than for monochrome TV.

4. DESIGN OF PREEMPHASIS AND DEEMPHASIS NETWORKS

As discussed in the previous sections, significant improvement in video signal-to-noise ratio can be realized with the use of signal preemphasis-deemphasis networks in a FM channel system. Simple passive networks can be designed which will furnish improved television performance at minimal cost in terms of circuitry and implementation. Excellent results have been obtained with preemphasis and deemphasis networks each composed of only three passive elements (2 resistors and 1 capacitor).

This section describes the experimental preemphasis and deemphasis networks utilized in the search for and evaluation of the best possible pair of networks for eventual implementation in the lunar communications relay unit color television system. The experimental networks were designed so that frequency breakpoints could be easily changed in a matter of minutes. This furnished the experimenters with complete flexibility in the amount of signal preemphasis and deemphasis desired and the particular network configuration to be tested.

4.1 CONSIDERATION OF VIDEO INTERFERENCE WITH VOICE

In the early stages of evaluating the preemphasis-deemphasis technique, as applied to the LCRU television system, it was felt that any preemphasis of the video signal, with respect to the 1.25 MHz voice subcarrier, would cause excessive interference with the FM voice baseband signal. The 1.25 MHz subcarrier is a FM/FM signal modulated by baseband signals consisting of analog biomedical information and voice. Any significant increase in video interference to the 1.25 MHz subcarrier data - due to TV preemphasis - would create an intolerable situation. The reason for the video interference with the FM voice data is immediately obvious from observing the downlink baseband spectrum for the TV/voice mode (FM/FM) in Figure 4-1. The approximate 2.5 megahertz spectrum of the baseband color TV extends out over the voice and biomedical signal-frequency region. Figure 4-2 is a simplified block diagram of the FM/FM communication system with the video preemphasis-deemphasis networks installed.

BASEBAND
COLOR TV

1.25 MHz
ANALOG
VOICE

0   0.5   1.0 1.25 1.5   2.0   2.5
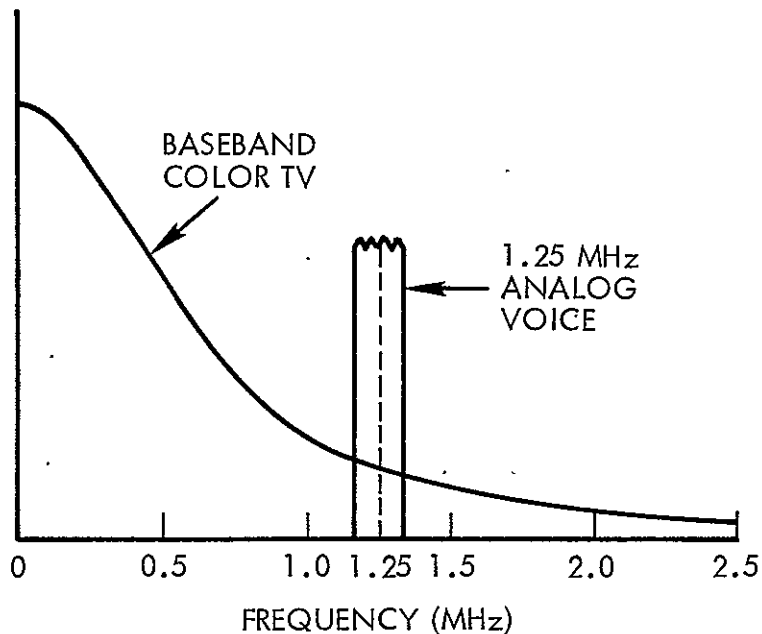
FREQUENCY (MHz)

Figure 4-1. Baseband Spectrum for LCRU
TV/Voice Mode (FM/FM)

A clever way of circumventing the potential problem of preemphasized
video information interfering significantly with FM voice is suggested by
the emphasis network responses sketched in Figure 4-3. As seen from the
preemphasis network response, all video frequencies are preemphasized as
required except for those frequencies in the region of the 1.25 MHz FM
modulated subcarrier. While the network boosts the high frequencies
relative to the low frequencies, the frequencies about the 1.25 MHz sub-
carrier remain relatively unchanged. This means that the use of preemphasis
will not contribute to or worsen the effect of video interference with FM
voice. Furthermore, since the networks are near inverses of each other,
the effect of the preemphasis-notch on the video signal will be canceled
out by the equal but opposite effect of the deemphasis-peak. Thus, the
video signal is completely unaffected by the preemphasis-deemphasis process.
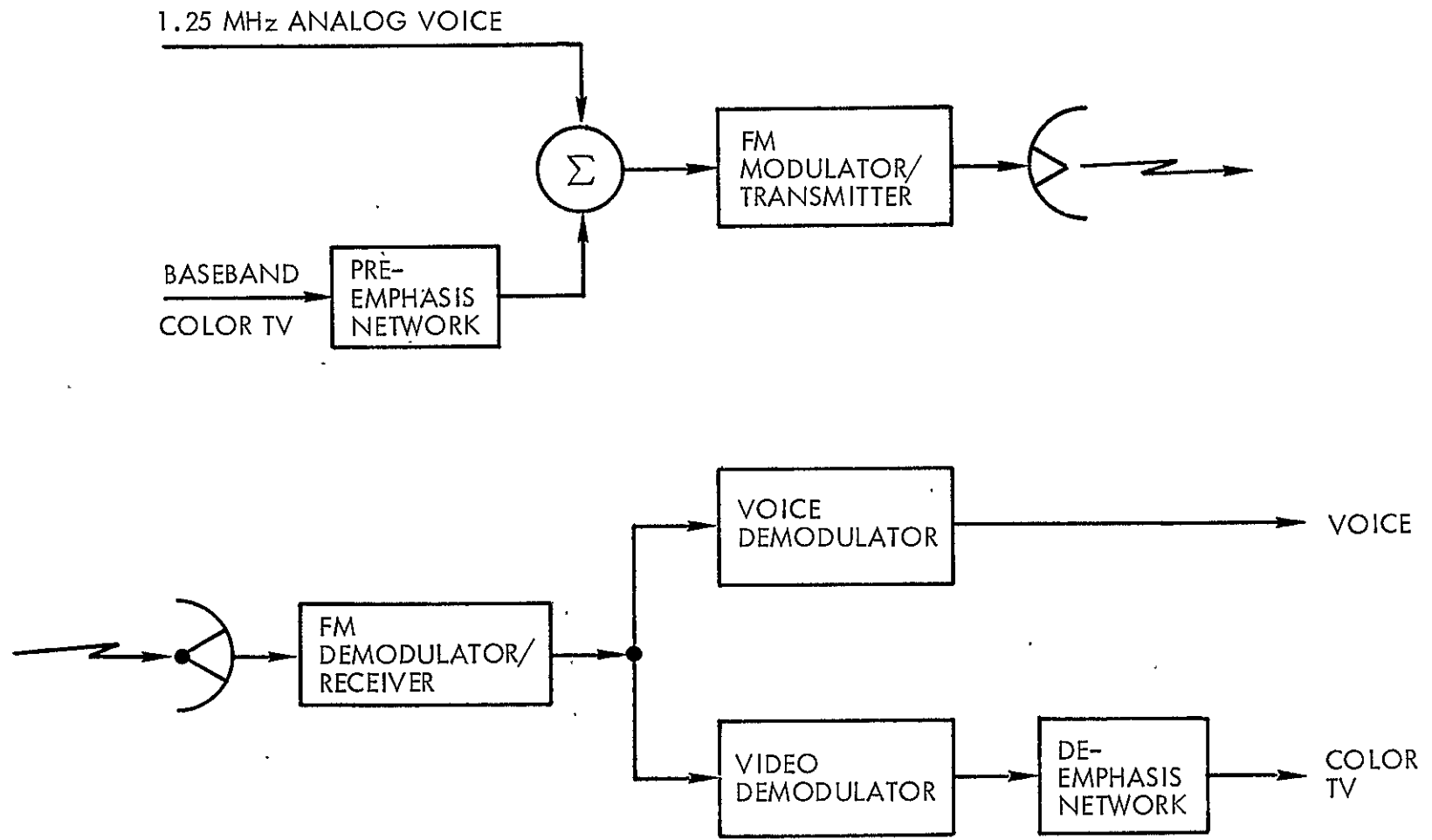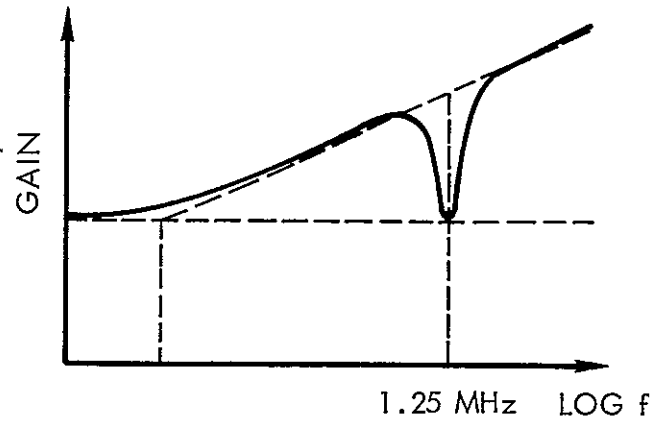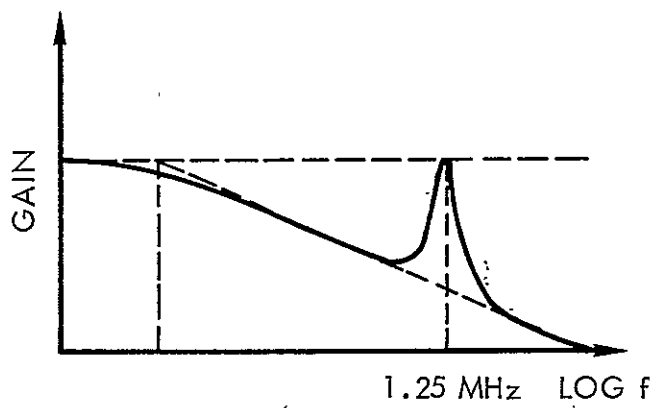Unfortunately, there is a disadvantage to adding the peak response to the

4-2

Figure 4-2. Simplified Diagram of FM/FM Communication
System With Video Signal Emphasis

(a) PREEMPHASIS NETWORK WITH NOTCH

(b) DEEMPHASIS NETWORK WITH PEAK

Figure 4-3. Video Emphasis Networks

basic low pass response of the deemphasis circuit. Because of the peak response, the noise components around the 1.25 MHz region are not attenuated as the rest of the noise frequencies in the video spectral bandwidth. This means that there is no video signal-to-noise ratio improvement obtained in the 1.25 MHz frequency region, when using the notch-peak combination. This is the small price that may have to be paid in order to guarantee that the video emphasis technique does not contribute to video interference with voice.
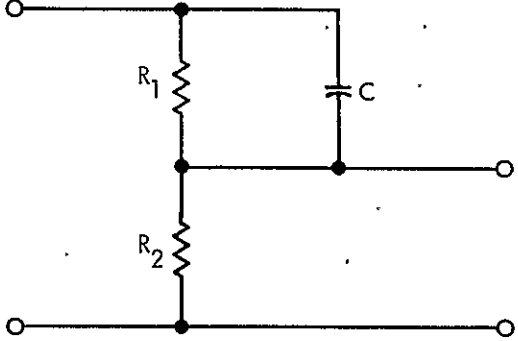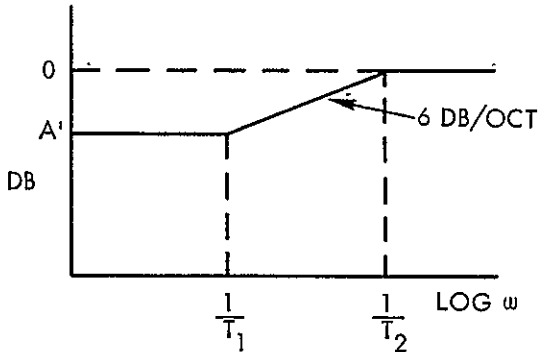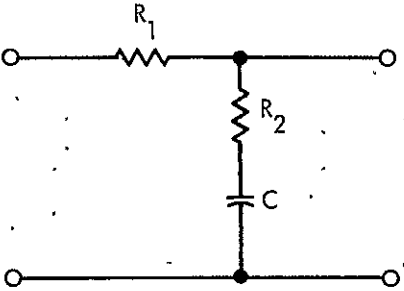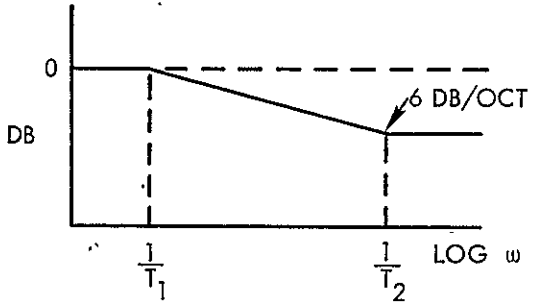
4.2 NETWORK DESCRIPTION AND RESPONSE

The following pages describe the experimentally designed preemphasis and deemphasis networks which were used to evaluate a number of network configurations, each with a different set of frequency breakpoints. Two of the most extensively tested and successful of the preemphasis/deemphasis networks evaluated had frequency breakpoints at 100 kHz/2000 kHz and 250 kHz/2500 kHz. The first frequency value refers to the first breakpoint f_1 while the second frequency value refers to the second breakpoint f_2. Numerous other simple passive network pairs (without 1.25 MHz notch/peaks) were tested with breakpoint combinations of 100 kHz/400 kHz, 100 kHz/800 kHz, and 250 kHz/2000 kHz. All of the networks tested were designed to have ± 6 dB/octave slopes.

It was found that the lower the frequency value of the first breakpoint, the better the noise suppression characteristic (better SNR improvement) of the network pair at low RF total received power levels. This is in agreement with theory since the first breakpoint of the deemphasis filter determines the frequency at which the FM parabolic noise density function is flattened. Since the noise power density is flat above the first frequency breakpoint f_1 (rather than parabolic), significantly less noise power is transmitted over the baseband video bandwidth.

Table 4-1 presents the RC circuit, transfer function, and approximate amplitude response for the preemphasis and deemphasis networks tested most extensively. The frequency breakpoints are expressed in terms of the circuit

Table 4-1. RC Emphasis Circuits

Circuit	Transfer Function	Approximate Amplitude Response
PREEMPHASIS	$$\dfrac{s + \dfrac{1}{T_1}}{s + \dfrac{1}{T_2}}$$ where $T_1 = R_1 C$ $T_2 = \dfrac{R_1 R_2 C}{R_1 + R_2}$ $A'(dB) = 20 \log_{10} \dfrac{R_2}{R_1 + R_2}$	
DEEMPHASIS	$$\dfrac{R_2 \left(s + \dfrac{1}{T_2} \right)}{(R_1 + R_2) \left(s + \dfrac{1}{T_1} \right)}$$ where $T_1 = (R_1 + R_2)C$ $T_2 = R_2 C$	

parameters where the first breakpoint $f_1 = 1/2\pi T_1$ and the second breakpoint $f_2 = 1/2\pi T_2$.

4.2.1 Preemphasis Network

The network is comprised basically of a passive three element preemphasis filter and an active single-transistor-stage 1.25 MHz notch generation circuit. Emitter-follower circuits were added for isolation purposes, while a voltage gain stage was added to compensate for the attenuation of the preemphasis filter. The network will accept a 1 volt peak maximum input signal before encountering distortion, and provides a 180 degree phase reversal.

The video signal preemphasis network, diagramed in Figure 4-4, consists of the following six electronic circuits:

a) Isolation amplifier
b) Preemphasis circuit
c) Voltage amplifier
d) Low pass filter
e) Notch generation circuit
f) Isolation amplifiers.

A brief discussion is given of each circuit explaining its purpose and operation.

Isolation Amplifier

The purpose of this circuit is to isolate the preemphasis filter from the video channel system source. The circuit is called a single-stage emitter-follower (also called common-collector) and has a high input impedance and a low output impedance.

Preemphasis Circuit

This particular RC network is commonly used in commercial FM voice transmission as a preemphasis circuit to emphasize high frequencies. Actually the higher-frequency components are passed unaltered, and the
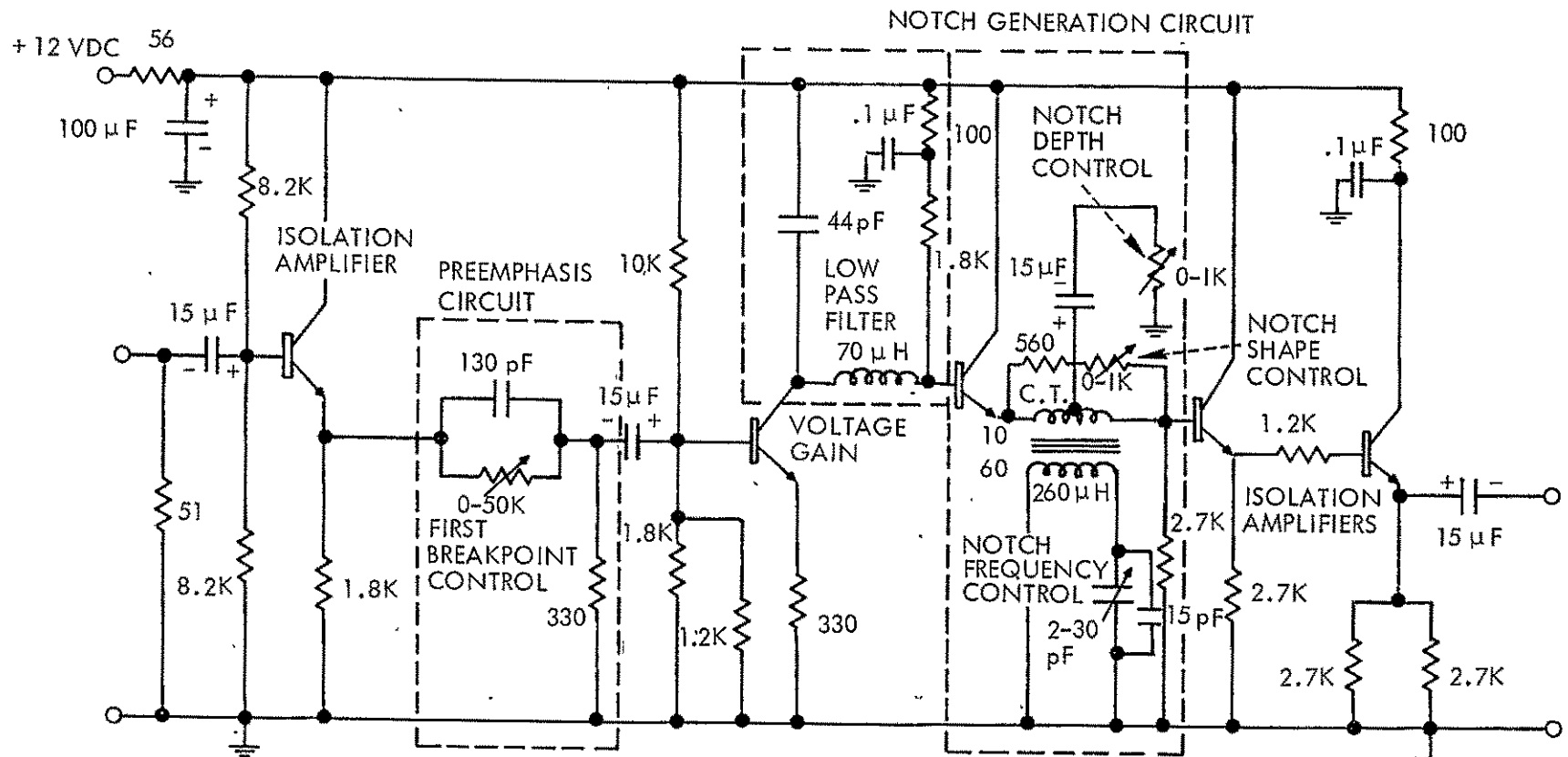
Figure 4-4. Video Signal Preemphasis Network

lower-frequency components are attenuated. The attenuation is made up by subsequent amplification.

An example of a magnitude frequency response curve for the video signal preemphasis network (with the 1.25 MHz notch) is given in Figure 4-5. The particular preemphasis circuit used had frequency breakpoints at 100 kHz and 2500 kHz. The first breakpoint is determined by the component values of the parallel resistor-capacitor combination (see Table 4-1). Variation of this breakpoint is achieved by varying the resistance value of the 50 KΩ pot. The second breakpoint is determined by the parameter values of all three components. However, if the resistance value of the 50 KΩ pot is much greater than 330 Ω (as is usually the case), then the second breakpoint is approximately determined by the 130 pF capacitor and the 330 Ω resistor.

Voltage Amplifier

A single-stage common-emitter voltage amplifier with current feedback follows the preemphasis circuit to compensate for the attenuation loss through the RC filter.

Low Pass Filter

A low pass filter was added to terminate the preemphasis effect at 3 MHz in order to preclude the possibility of excessive frequency modulation due to preemphasized high frequencies. Since the video baseband filter bandwidth is around 2 MHz, preemphasis is not required much beyond this frequency. The 2 element filter has a Butterworth response with a cutoff frequency of 3 MHz and an attenuation rolloff of 12 dB/octave.

Notch Generation Circuit

The purpose of the T-notch circuit is to selectively attenuate the video signal in a narrow band of frequencies centered at 1.25 MHz, and thus prevent any possible further interference to voice information caused by video preemphasis. The 3-dB bandwidth of the notch response (referenced
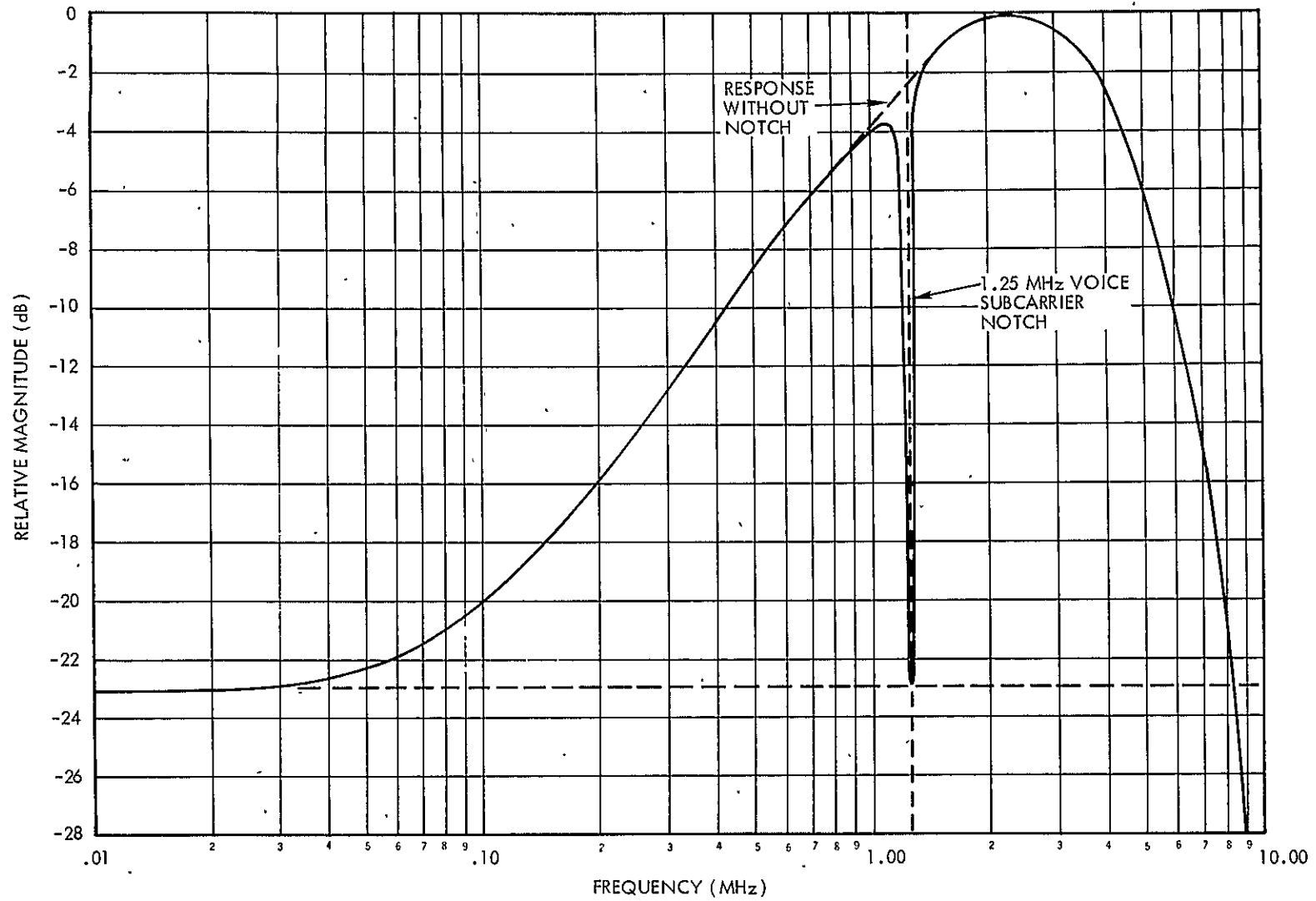
Figure 4-5. Relative Magnitude Frequency Response Curve for the Video Signal
Preemphasis Network (100 kHz/2500 kHz) With 1.25 MHz Notch

to the notch minimum) is approximately 40 kHz. A relative magnitude
frequency response curve for the 1.25 MHz voice subcarrier notch is shown
in Figure 4-6.

The depth of the notch is easily varied through the use of the 1 KΩ
variable resistor as shown in Figure 4-4. The notch center frequency can
be manually adjusted by varying the 2-30 picofarad capacitor in the reso-
nant frequency section of the notch circuit. In order to accurately match
the magnitude frequency response of the preemphasis-notch with the response
of the deemphasis-peak, it is sometimes necessary to adjust the shape of
the notch response. This is accomplished by controlling the Q factor
of the circuit with the aid of the notch shape control. Varying the
resistance of the 1 KΩ pot will change the Q and therefore the shape of
the notch.

If it is so desired, the effect of the notch generation circuit can
be removed entirely from the preemphasis network response. This is easily
done by placing a shorting wire between the emitter of the third transistor
stage and the base of the fourth transistor stage (isolation amplifier).

Isolation Amplifier

The cascade connection of two single-stage emitter-followers affords
a high degree of isolation between the notch generation circuit and the
rest of the video channel system.

4.2.2 Deemphasis Network

This network is comprised basically of a passive three element deempha-
sis filter and an active single-transistor-stage 1.25 MHz peak generation
circuit. Emitter-follower circuits were added to isolate the network from
the rest of the video channel system. The network has a 180 degree phase
reversal and will accept input voltage signals no greater than 1 volt peak
before distortion occurs.

The video signal deemphasis network, diagramed in Figure 4-7, consists
of the following five electronic circuits:
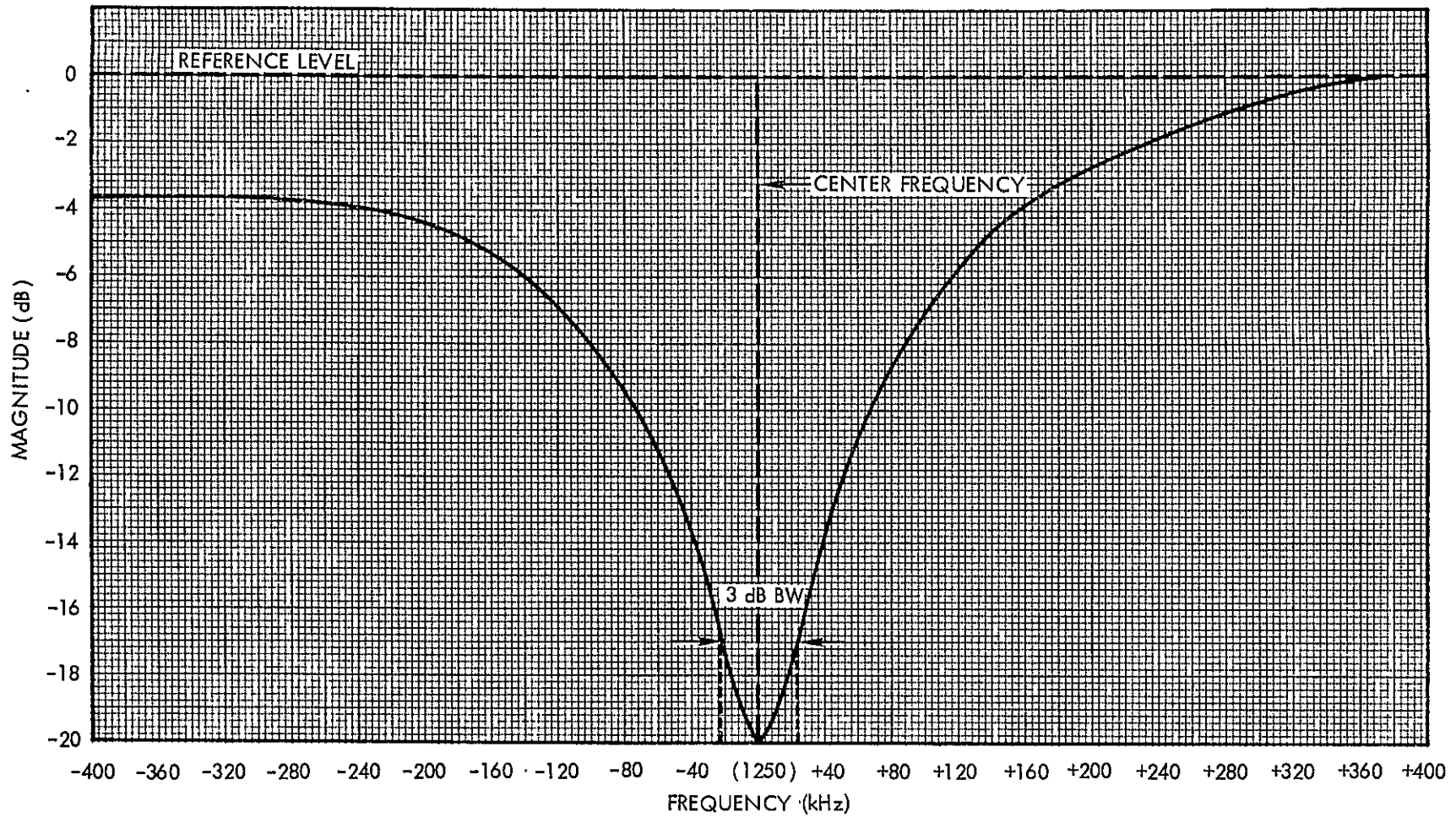
Figure 4-6. Relative Magnitude Frequency Response Curve for the
Video-Signal-Preemphasis Network 1.25 MHz Notch
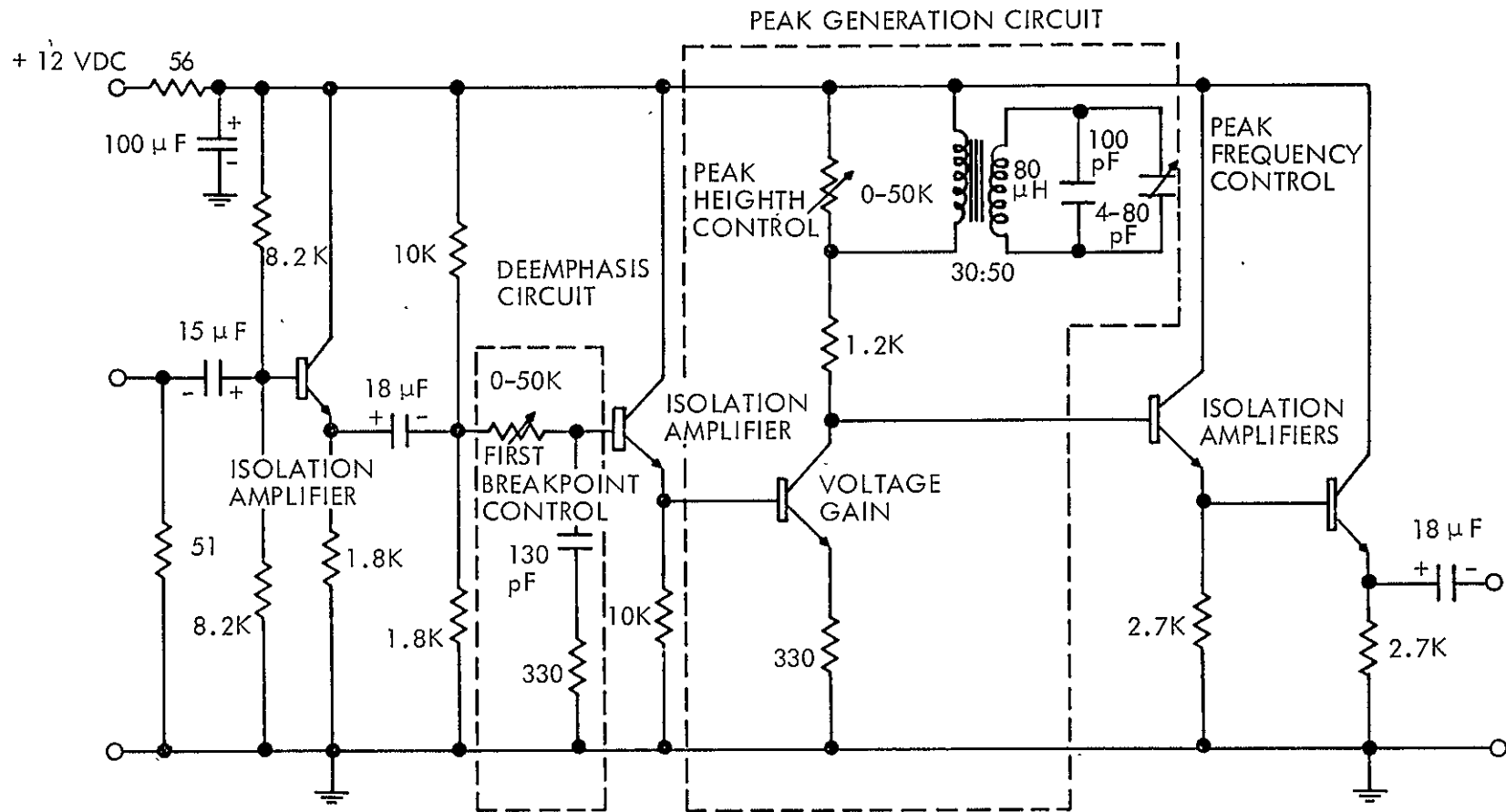
Figure 4-7. Video Signal Deemphasis Network

a) Isolation amplifier

b) Deemphasis circuit

c) Isolation amplifier

d) Peak generation circuit

e) Isolation amplifiers.

Each circuit will be discussed, outlining its purpose and operation.

Isolation Amplifier

The purpose of this circuit is to isolate the deemphasis filter from the preceding networks. The circuit is a high impedance emitter-follower stage with near unity voltage gain.

Deemphasis Circuit

The deemphasis circuit has a frequency dependence inverse to that of the preemphasis circuit, as required in order that no net distortion be introduced into the video signal. This serves to restore all the signal frequencies to their original relative values. Since the noise spectral density at the output of an FM demodulator increases with the square of the frequency, the deemphasis network is very effective in suppressing noise because of its low pass response (response falls with increasing frequency).

A typical magnitude frequency response curve for the video signal deemphasis network (with the 1.25 MHz peak) is shown in Figure 4-8. The particular deemphasis circuit used had frequency breakpoints at 100 kHz/2500 kHz. The first frequency breakpoint is determined exactly by the parameter values of all three components (see Table 4-1). However, if the variable resistance is much greater than 330 Ω, then the approximate breakpoint-frequency is determined by the variable resistor and fixed capacitor only. The second breakpoint is determined by the component values of the series resistor-capacitor combination. It is easily arranged that this second breakpoint lie well outside the video baseband spectral range and hence is not relevant.
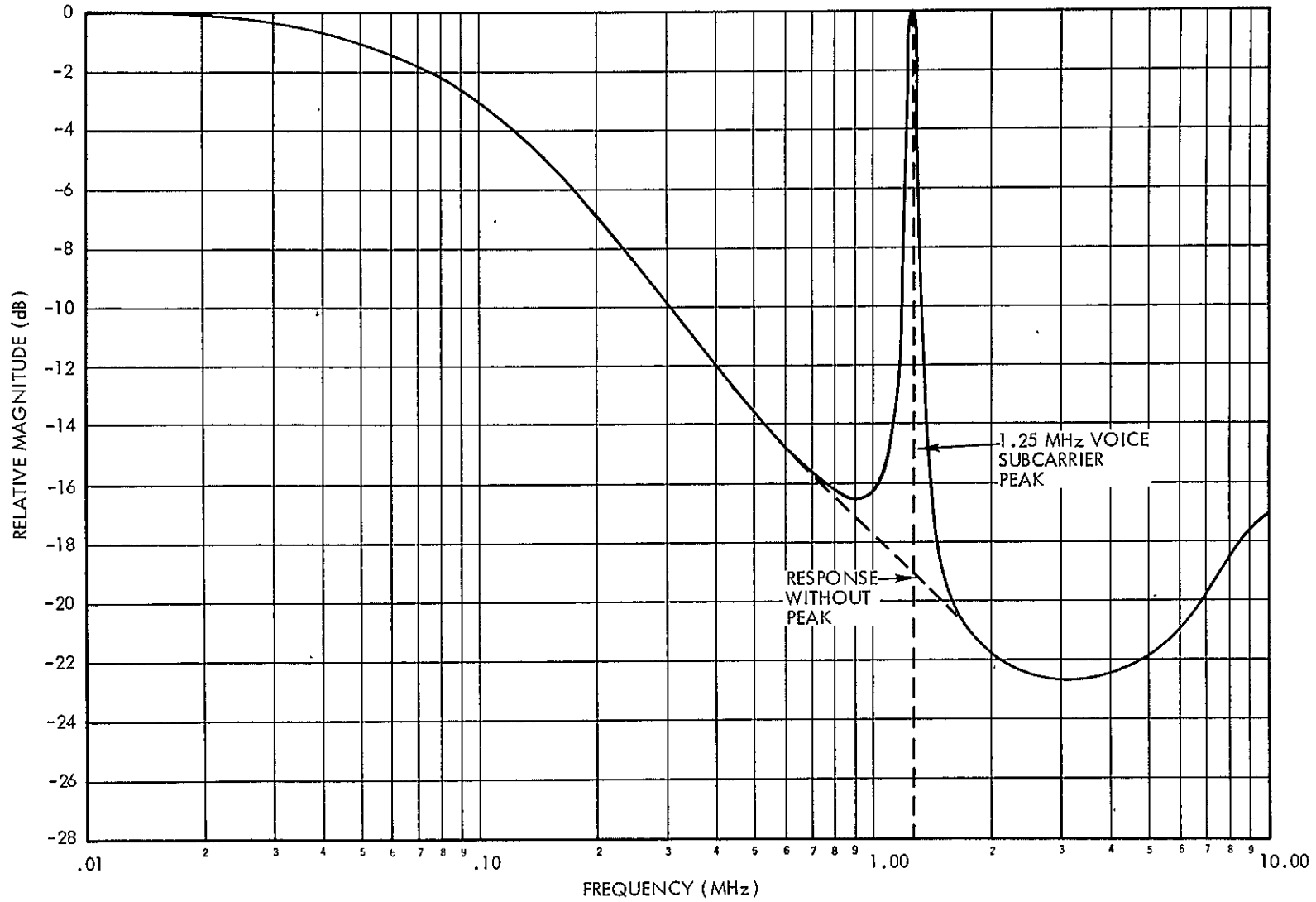
Figure 4-8.   Relative Magnitude Frequency Response Curve for the Video Signal
Deemphasis Network (100 kHz/2500 kHz) With 1.25 MHz Peak

Isolation Amplifier

A single-stage emitter-follower provides needed isolation between the passive deemphasis circuit and the active peak generation circuit.

Peak Generation Circuit

The addition of a peak generating circuit to the deemphasis filter is required in order to maintain the integrity of the inverse relationship between the preemphasis-deemphasis network responses. The narrow peak centered at 1.25 MHz corrects for the video signal distortion caused by the preemphasis-notch. Without the compensating effect of the deemphasis-peak to preserve the fidelity of the video signal, a portion of the video spectrum would remain distorted, yielding the all too familiar result of a ringing effect (vertical or horizontal line patterns) in the video picture. With proper adjustment of the notch and peak circuits, however, there is no observance of ringing in the video picture due to video emphasis.

A relative magnitude frequency response curve for the 1.25 MHz voice subcarrier peak is given in Figure 4-9. The 3-dB bandwidth of the peak response is approximately 40 kHz - the same as the notch 3-dB bandwidth.

As can be seen in Figure 4-7, the height of the peak is regulated by the 50 KΩ variable resistor in the circuit. The peak center frequency can be changed by varying the 4-80 picofarad capacitor in the resonant frequency section of the peak generation circuit.

If desired, the effect of the peak generation circuit can be eliminated from the deemphasis network response. This may be done easily by placing a shorting wire across the peak heighth control pot.

Isolation Amplifiers

The purpose of the cascade connection of emitter-followers is to provide isolation between the peak generation circuit and the rest of the video channel system.
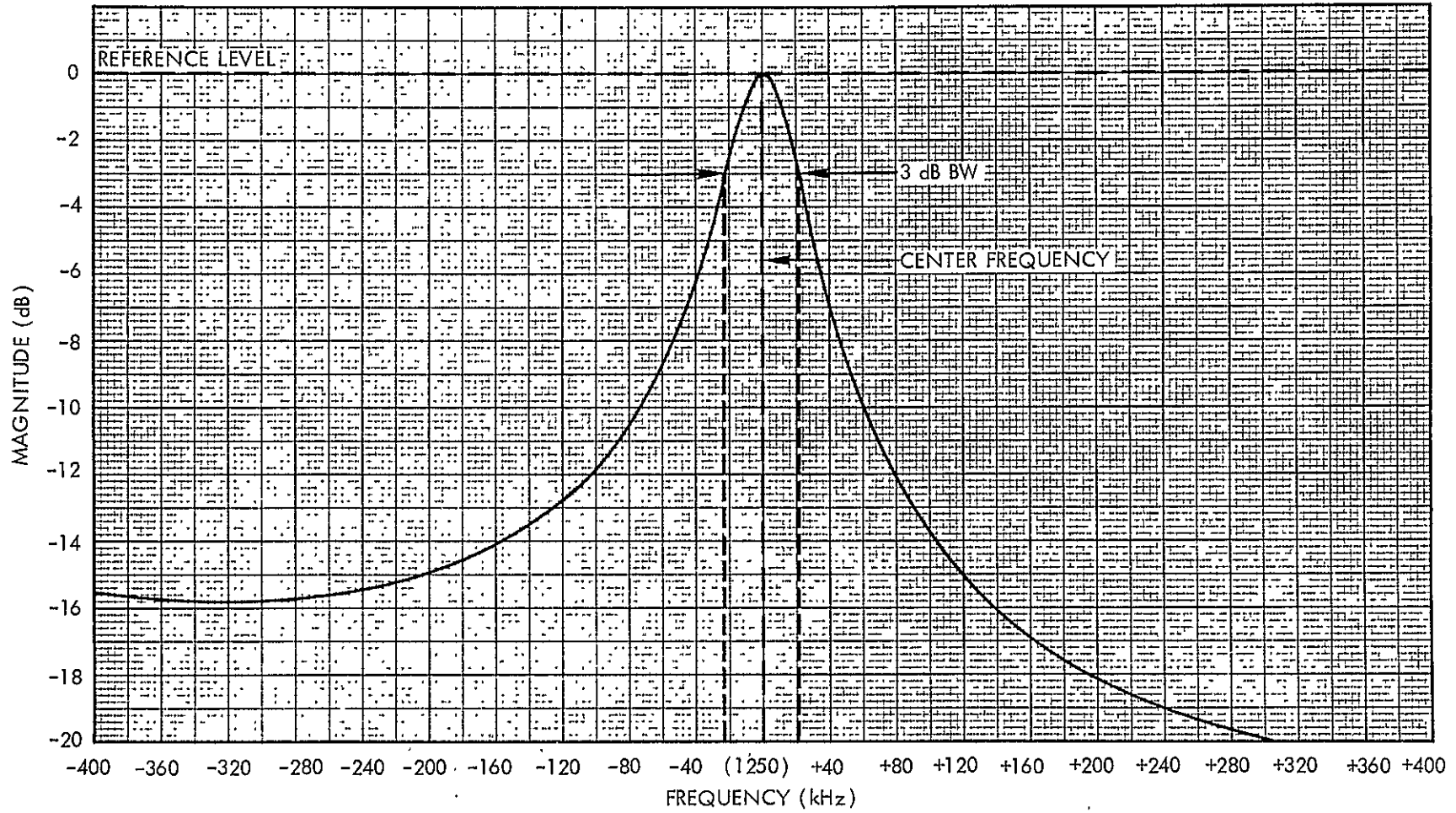
Figure 4-9. Relative Magnitude Frequency Response Curve for the
Video-Signal-Deemphasis Network 1.25 MHz Peak

4.3 PREEMPHASIS/DEEMPHASIS SYSTEM RESPONSE

As noted previously, the relative magnitude responses of the preemphasis and deemphasis networks exhibit an inverse relationship. Ideally, the overall relative magnitude response of both networks in series should be perfectly flat. Figure 4-10 (a) shows the relative magnitude frequency response curve for the two networks in cascade. The response is relatively flat to within ±1.5 dB from 0 to 4.5 MHz with a +1.5 dB hump around 1 MHz. The figure shows the net effect of the networks upon the video spectrum. From Figure 4-10 (b) it is seen that the series network combination has a very linear phase frequency response curve, indicating a constant time delay over all frequencies.

In order to insure that the inverse relationship criterion is preserved in the frequency region around the 1.25 MHz voice subcarrier (and eliminate potential pattern interference), it is sometimes necessary to adjust the shape of the preemphasis network notch to match that of the preemphasis network peak. Usually this becomes necessary when the breakpoints of the networks have been manually shifted in frequency. Figure 4-10 (c) shows the resulting appearance of the relative magnitude frequency response curve in the voice subcarrier region after a typical adjustment. The magnitude response is flat to approximately ±.5 dB from .75 MHz to 1.75 MHz, which is quite satisfactory.

The series preemphasis/deemphasis network system test set-up used to generate the overall magnitude and phase responses sketched in Figure 4-10 is given in Figure 4-11.
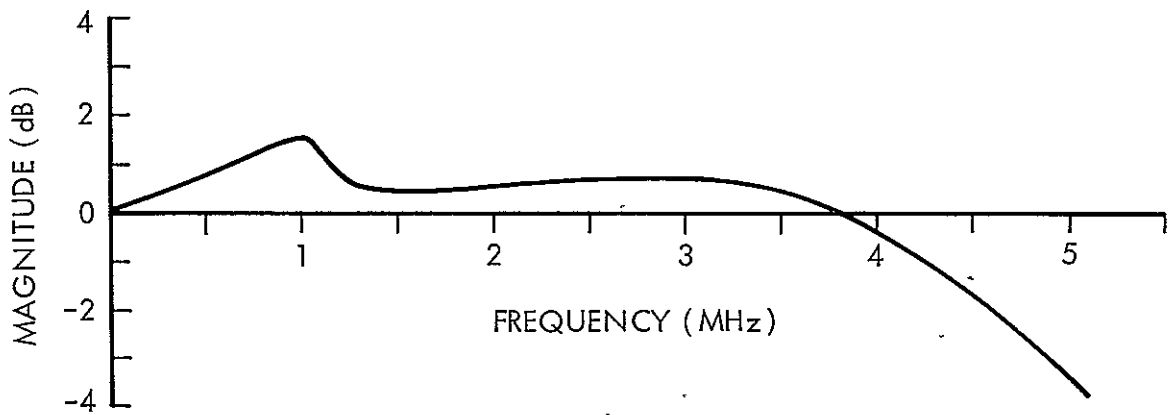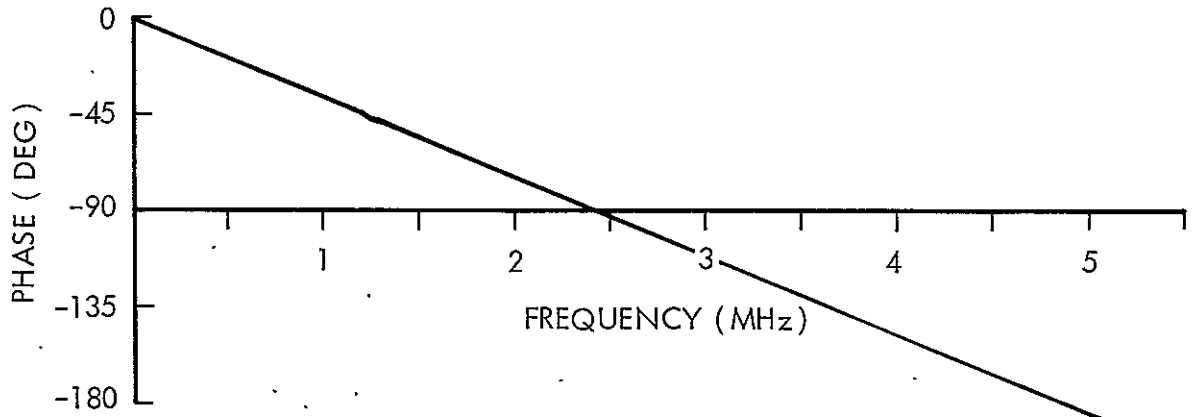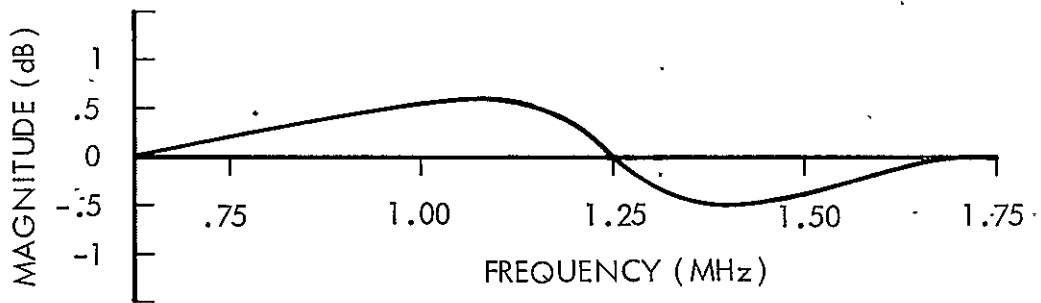
Figure 4-10. Preemphasis/Deemphasis Network System Relative
Magnitude and Phase Frequency Response Curves
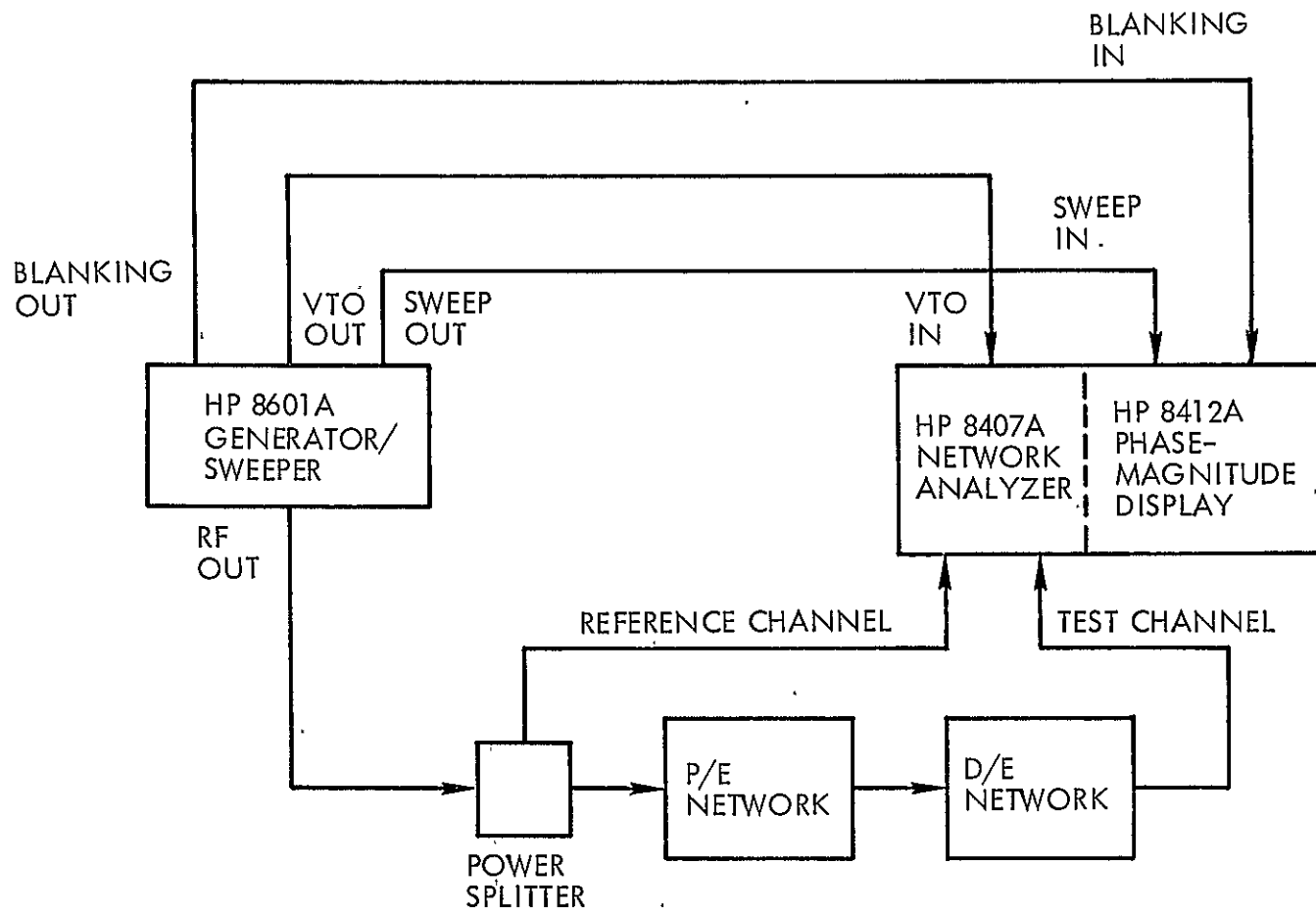
Figure 4-11. Preemphasis/Deemphasis Network System Test Set-up

5. EXPERIMENTAL RESULTS

This section presents photographs and experimental data obtained as a result of total system tests conducted at the Manned Spacecraft Center (MSC) Electronic Systems Test Laboratory (ESTL). The tests were performed to evaluate the effectiveness of the preemphasis/deemphasis networks, cited in Section 4, in improving the video picture quality of the LCRU color television system. Production LM spacecraft equipment together with an MSFN ground-station receiver and associated demodulation equipment was used in the tests. The LCRU-to-ground link was simulated with a calibrated rf attenuator.

A number of preemphasis and deemphasis networks were experimentally tested. It was determined that the preemphasized video did not appreciably degrade (less than 1 dB) the 1.25 MHz voice subcarrier, thereby eliminating the need for the 1.25 MHz notch-peak combination in the networks. A preemphasis/deemphasis circuit pair with frequency breakpoints at 250 kHz and 2000 kHz has good noise suppression characteristics, while minimizing picture "tearing" at low received RF power levels. The total system tests in the ESTL with the colorplexer were conducted with the 250 kHz/2000 kHz network pair. A network pair with frequency breakpoints at 100 kHz and 2000 kHz, which theoretically has a noise suppression performance superior to that of the 250 kHz/2000 kHz network pair, was also tested. The resultant picture quality was slightly improved (less random noise), but unfortunately, this advantage was offset to a degree by an equally slight increase in "tearing", at the -93 dBm RF level.

The "tearing" in the video picture at low RF levels is partially caused by the high amplitude spikes in the preemphasized video signal. These spikes are created by the preemphasis circuit which acts as a differentiator, thereby causing spikes to appear in the preemphasized video signal whenever there is a rapid change in voltage level (i.e., due to an edge in the picture). In order to eliminate the large voltage spikes which would result from partial differentiation of the sync pulses, only the non-composite video signal (video signal without synchronization pulses) is preemphasized. After the preemphasis process, the sync pulses are added to the preemphasized non-composite video signal.

5.1 PICTURE QUALITY IMPROVEMENT

In an effort to subjectively evaluate the improvement in color TV picture quality, due to emphasis of the video signal, one particular landscape scene was studied with and without emphasis, for three different total-received RF power levels. The video scene chosen is supposed to represent a typical lunar scene - such as one that might be transmitted back to earth via the LCRU. The three LCRU-to-MSFN total-received RF power levels of interest are:

-82 dBm	Worst-case RF power level received from lunar distance, using the LCRU dish and the MSFN 210-foot dish
-90 dBm	Worst-case RF power level received from lunar distance, using the LCRU dish and the MSFN 85-foot dish
-93 dBm	3 dB below worst-case RF power level received from lunar distance, using the LCRU dish and the MSFN 85-foot dish.

Figures 5-1 through 5-6 are photographs taken from the sequential color TV monitor in the MSC ESTL. They indicate the received television signal picture quality which is expected as a result of the LCRU-to-MSFN transmission link. All pictures were taken under exactly the same testing conditions, except for the presence or absence of video emphasis and the value of total-received RF power level. During the television picture quality evaluation test, the 1.25 MHz voice subcarrier, with voice modulation, was FM modulated on the downlink S-band carrier. A passive 1.25 MHz voice notch filter with a 3 dB bandwidth of 80 kHz was inserted in the output video channel to eliminate the 1.25 MHz spectrum from the baseband video spectrum. When the preemphasis and deemphasis networks were not utilized in the communication system link, a dual section Krohn-hite filter with a maximally flat amplitude response and a 2 MHz cut-off was used as the video baseband filter. All testing was carried out with a video 1.7 MHz ($\pm$10%) peak frequency deviation, set by a 25 kHz sine wave, and a 1.25 MHz voice subcarrier peak frequency deviation of 440 kHz.

As compared with no preemphasis, in practice, preemphasis may require that the peak frequency deviation of the modulator be reduced at low frequencies. However, in the system testing, this factor was ignored. The signal used for comparison purposes was a 25 kHz sinusoidal modulating wave, which is at a low enough frequency not to be appreciably affected by preemphasis. At this frequency of 25 kHz, it may be assumed that the modulation level is the same as with no preemphasis.

Figures 5-1 and 5-2 show the LCRU television picture quality without emphasis and with emphasis, respectively, for an RF level of -93 dBm. The suppression of the Gaussian white noise through the use of deemphasis is dramatically evident from an inspection of these figures. Figure 5-2 has considerably less snow than Figure 5-1, as evidenced by the bluer sky background, and thus has a great deal more definition and contrast. With emphasis, there is a better color quality present in the received television picture with better highlights. Note the more distinct shadows in the rock area. The presence of horizontal or vertical bar patterns should be ignored when inspecting the various photographs, because they are a function of the ESTL modulation/demodulation equipment and are not caused by the preemphasis-deemphasis technique.

Just as for the previous photographs, Figures 5-3 and 5-4 illustrate the marked reduction in snow due to deemphasis of the output video noise power. Figure 5-3, taken without video emphasis, shows the definite graininess of the television image due to the presence of the individual random noise grains (random white dots). Figure 5-4, taken with video emphasis, shows little of this granular appearance. The presence of the random noise does indeed mask and distort the original TV image. Both Figures 5-3 and 5-4 were taken at an RF level of -90 dBm, which is the worst-case RF power level received from lunar distance using the LCRU parabolic dish and the MSFN 85-foot antenna. This means that Figure 5-4 is the worst-case LCRU television image expected when using the emphasis technique.

Figure 5-1. TV Picture Quality Evaluation Photograph
Without Video Emphasis, RF Level = -93 dBm

Figure 5-2. TV Picture Quality Evaluation Photograph
With Video Emphasis, RF Level = -93 dBm

TPET050770-1
PHOTO 15

TPET050770-1
PHOTO 18

Figure 5-3.   TV Picture Quality Evaluation Photograph
               Without Video Emphasis, RF Level = -90 dBm

Figure 5-4.   TV Picture Quality Evaluation Photograph
               With Video Emphasis, RF Level = -90 dBm

TPET050770-1
PHOTO 14

TPET050770-1
PHOTO 17

Figure 5-5.   TV Picture Quality Evaluation Photograph
Without Video Emphasis, RF Level = -82 dBm

Figure 5-6.   TV Picture Quality Evaluation Photograph
With Video Emphasis, RF Level = -82 dBm

TPETQ50770-1
PHOTO 13

TPETQ50770-1
PHOTO 16

The worst-case RF level for the LCRU-to-210-foot MSFN station link is -82 dBm and is the condition portrayed in Figures 5-5 and 5-6. Although there is less random noise present at -82 dBm (corresponds to an input CNR of 16.5 dB), because the MSFN FM demodulator is operating above threshold, there is still a definite picture quality improvement obtained through the use of emphasis. Note the better detail and definition displayed in Figure 5-6 over that found in Figure 5-5. The television picture obtained with emphasis is certainly much sharper and clearer than the picture obtained without emphasis, even for high input CNR's.

The television emphasis test configurations used in simulating the LCRU color television communication system are presented in Figures 5-7, 5-8, and 5-9.

5.2 RF LEVEL IMPROVEMENT

As explained in Section 5.1, a comparison of Figure 5-1 (picture without emphasis) and Figure 5-2 (picture with emphasis) clearly shows the significant reduction in white noise accomplished by the deemphasis process. There is no doubt that the quality of the picture in Figure 5-2 is improved over that found in Figure 5-1. The question certain to be asked is, How much picture quality improvement is there between Figures 5-1 and 5-2? A way of answering is to compare the television photographs in Figures 5-2 (picture with emphasis) and 5-3 (picture without emphasis). Careful inspection of these two photographs reveals that the quality of Figure 5-2 is better than that displayed in Figure 5-3, even though the latter television picture is for an RF level 3 dB above that for Figure 5-2! A very approximate and conservative way of qualitatively expressing the improvement in Figure 5-2 over Figure 5-1 is to state that there is at least a 3 dB improvement in RF power level through the use of video emphasis at these low RF levels. A comparison of Figures 5-2, 5-3, and 5-5 indicates that the RF power level improvement obtained with emphasis is greater than 3 dB and less than 11 dB. The upper bound is valid assuming that Figure 5-5 (RF level = -82 dBm) has less random noise or snow than Figure 5-2 (RF level = -93 dBm).

ABBREVIATIONS

EKG   – ELECTROCARDIOGRAM
PAM   – PULSE AMPLITUDE MODULATION
VDA   – VIDEO DISTRIBUTION
             AMPLIFIER
AMP   – AMPLIFIER
ATTEN – ATTENUATOR
ESTL   – ELECTRONIC SYSTEMS
             TEST LABORATORY
RCVR – RECEIVER
RCDR – RECORDER
SDDS – SIGNAL DATA DEMODULATOR
             SYSTEM
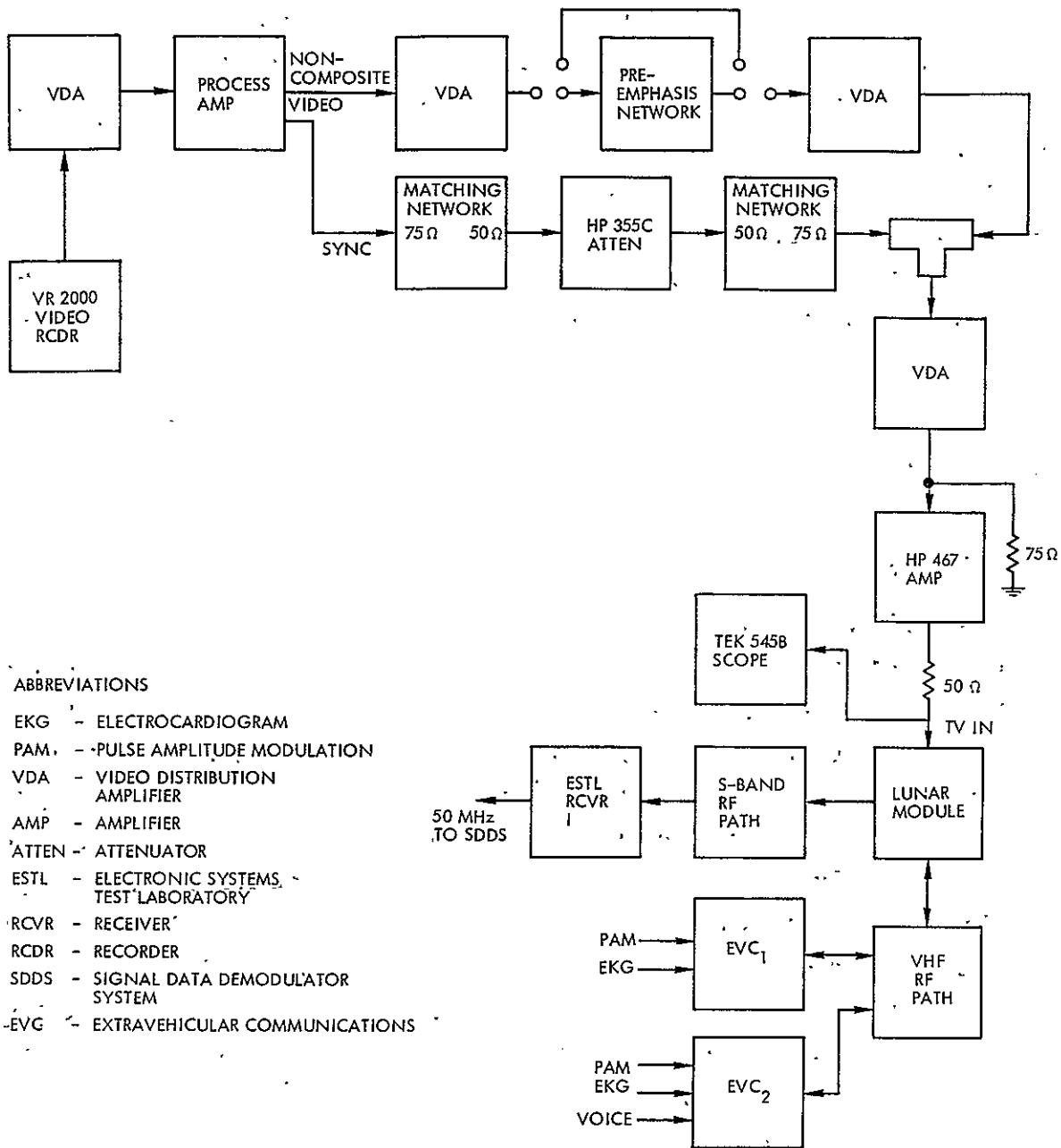EVG   – EXTRAVEHICULAR COMMUNICATIONS

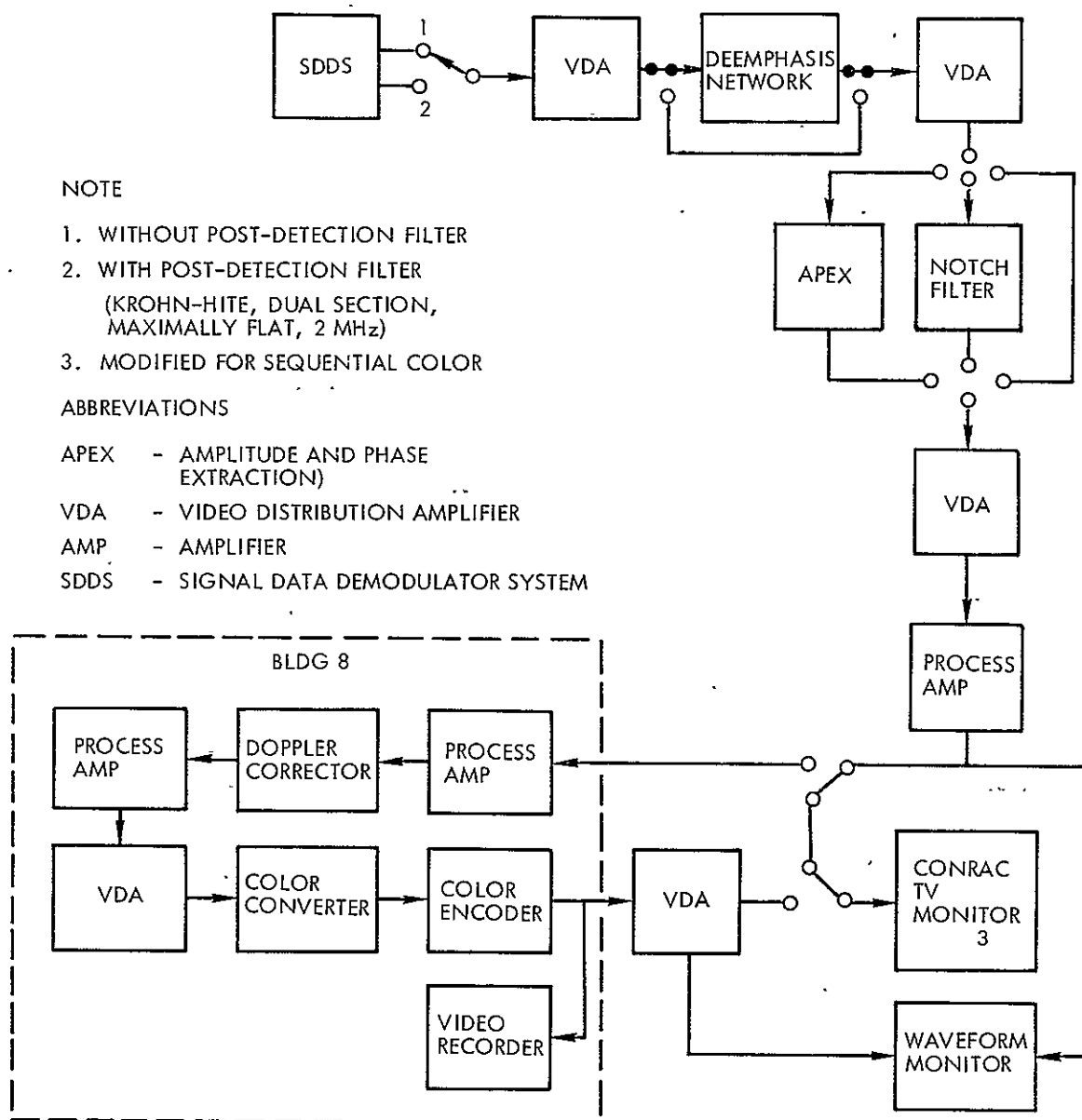Figure 5-7.   Television Emphasis Test Configuration

5-12

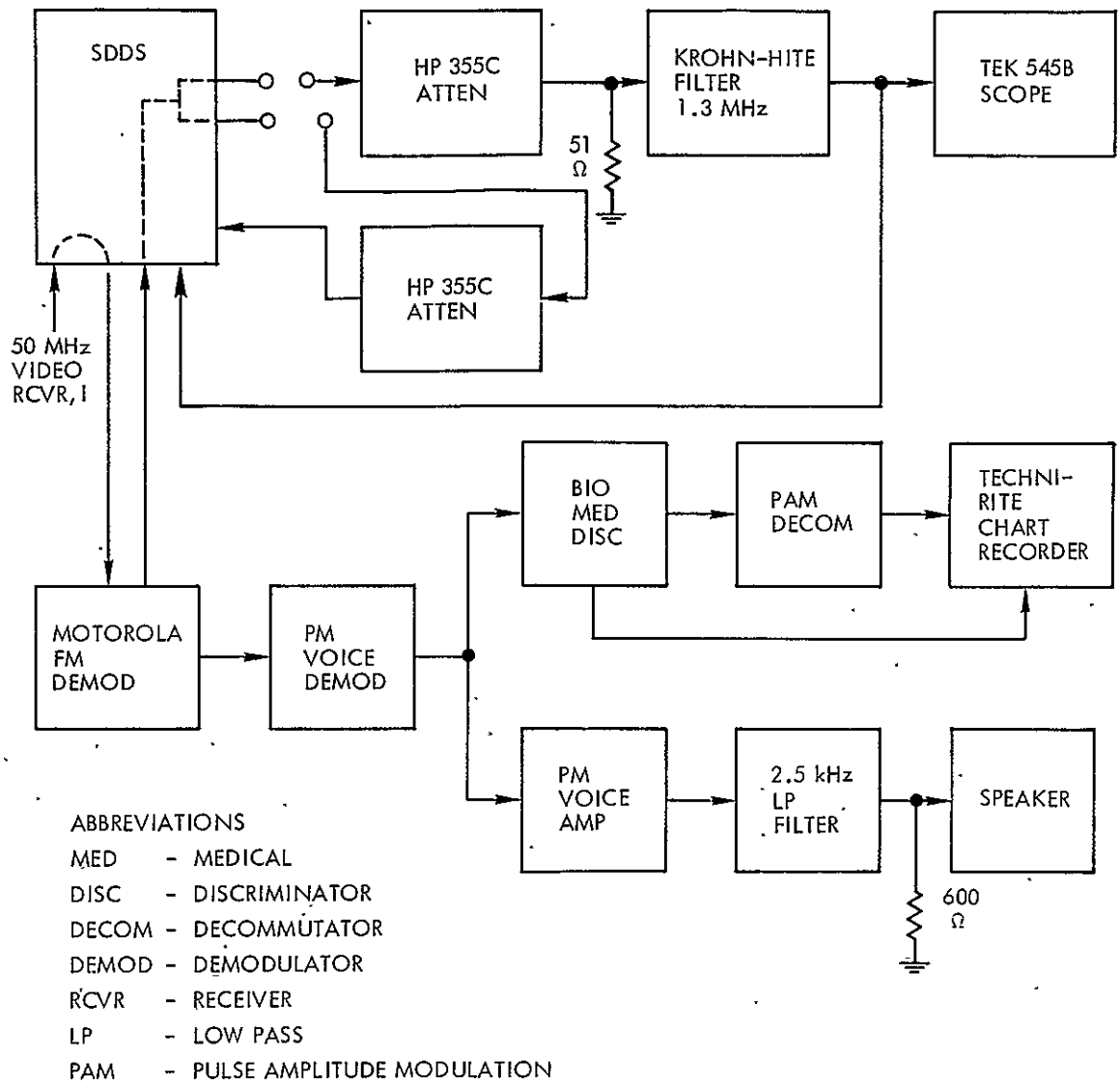Figure 5-8. Television Emphasis Test Configuration

Figure 5-9. Television Emphasis Test Configuration

5.3 SNR IMPROVEMENT

The concept of signal-to-noise ratio improvement or noise power reduc-
tion is the prime criterion by which one can judge the effectiveness of the
video emphasis technique. This section will describe an approximate method
of determining an experimental SNR improvement based on the observation of
RF level improvement cited in Section 5.2.

The advantages of using frequency modulation are well known, one of the
primary being the SNR improvement at the receiving end. This advantage holds,
however, only at relatively high values of the input CNR. If the input CNR
falls below a certain critical value, the output SNR drops rapidly resulting
in a great deterioration and eventual loss of the demodulated signal. It is
conventional to describe this situation by plotting the output SNR as a func-
tion of the input carrier-to-noise ratio for an unmodulated carrier. A typical
plot is shown in Figure 5-10 for the MSFN FM demodulator used in the tele-
vision emphasis testing. The point of departure from linearity is defined
as threshold. One accepted definition of FM threshold is the specific input
CNR value whose corresponding output SNR occurs exactly 1 dB below the linear
extension of the transfer characteristic. This method of defining FM thresh-
old is illustrated in Figure 5-10. For proper operation of the FM demodu-
lator, it is normally required that the CNR be maintained sufficiently high
to avoid the threshold region. Notice in Figure 5-10 that the RF power level
of -93 dBm (3 dB below worst-case for the MSFN 85-foot station) is only
slightly above FM threshold.

The relationship used in describing the demodulator performance in
and above the threshold region (Reference 14), as shown in Figure 5-10,
is given in Equation (5-1) for an unmodulated carrier

$$SNR = \left[\frac{\frac{3}{2} \beta^2 \left(\frac{B_{IF}}{B_0} \right)}{1 + \sqrt{3} \left(\frac{B_{IF}}{B_0} \right)^2 CNR \ (1-erf \ \sqrt{CNR})} \right] CNR \qquad (5-1)$$
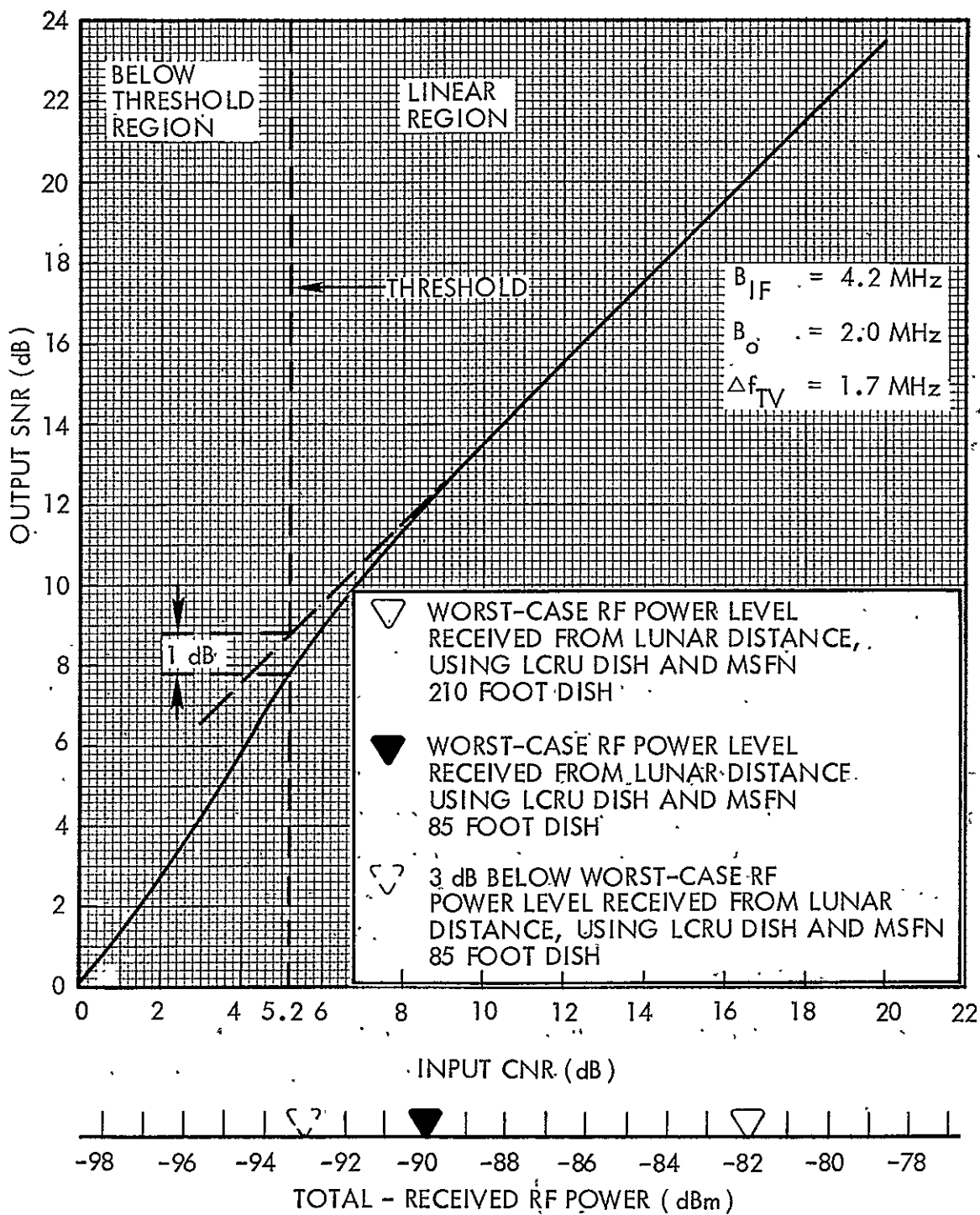
Figure 5-10. SNR Characteristic of MSFN FM Demodulator
Used in Television Emphasis Testing

where

B_{IF} = rectangular IF bandwidth

B_o = rectangular output bandwidth of the postdetection low pass video baseband filter

$\beta = \dfrac{\Delta f}{B_o}$ = modulation index

Δf = peak carrier frequency deviation.

For the purpose of obtaining a conservative estimate of the SNR improvement experimentally obtained through emphasis, a 3 dB improvement in RF level will be assumed. This figure was the minimum estimate cited in Section 5.2. In other words, it is being assumed (a conservative assumption, really) that Figure 5-2 (with emphasis) and Figure 5-3 (without emphasis) have equal noise suppression characteristics or equal output signal-to-noise ratios. The difference in output SNR's, corresponding to the RF power levels of Figures 5-2 and 5-3, will be the estimated improvement in picture SNR due to emphasis. To make things easier, the SNR characteristic of Figure 5-10 is replotted versus total-received RF power and is given in Figure 5-11. As can be seen from the graph, the output SNR for -90 dBm is 12 dB and the output SNR for -93 dBm is 8.3 dB. The difference between the two SNR's which is 3.7 dB, is the experimental estimate of the video signal-to-noise ratio improvement obtained as a result of preemphasis-deemphasis. Remember that this estimate is based on the assumption that Figures 5-2 and 5-3 have equal picture quality. Actually, Figure 5-2 appears to have better picture quality than Figure 5-3 and, therefore, the SNR improvement is higher than the conservative estimate of 3.7 dB.

In Appendix C, the signal-to-noise ratio improvement through emphasis at CNR's in the non-linear region of the demodulator SNR characteristic is considered. As a result of this theoretical analysis, a plot was made of the non-weighted SNR improvement factor through emphasis versus input CNR (see Figure C-4). This plot was used to generate the non-weighted theoretical curves of output SNR versus input CNR, when utilizing emphasis, shown
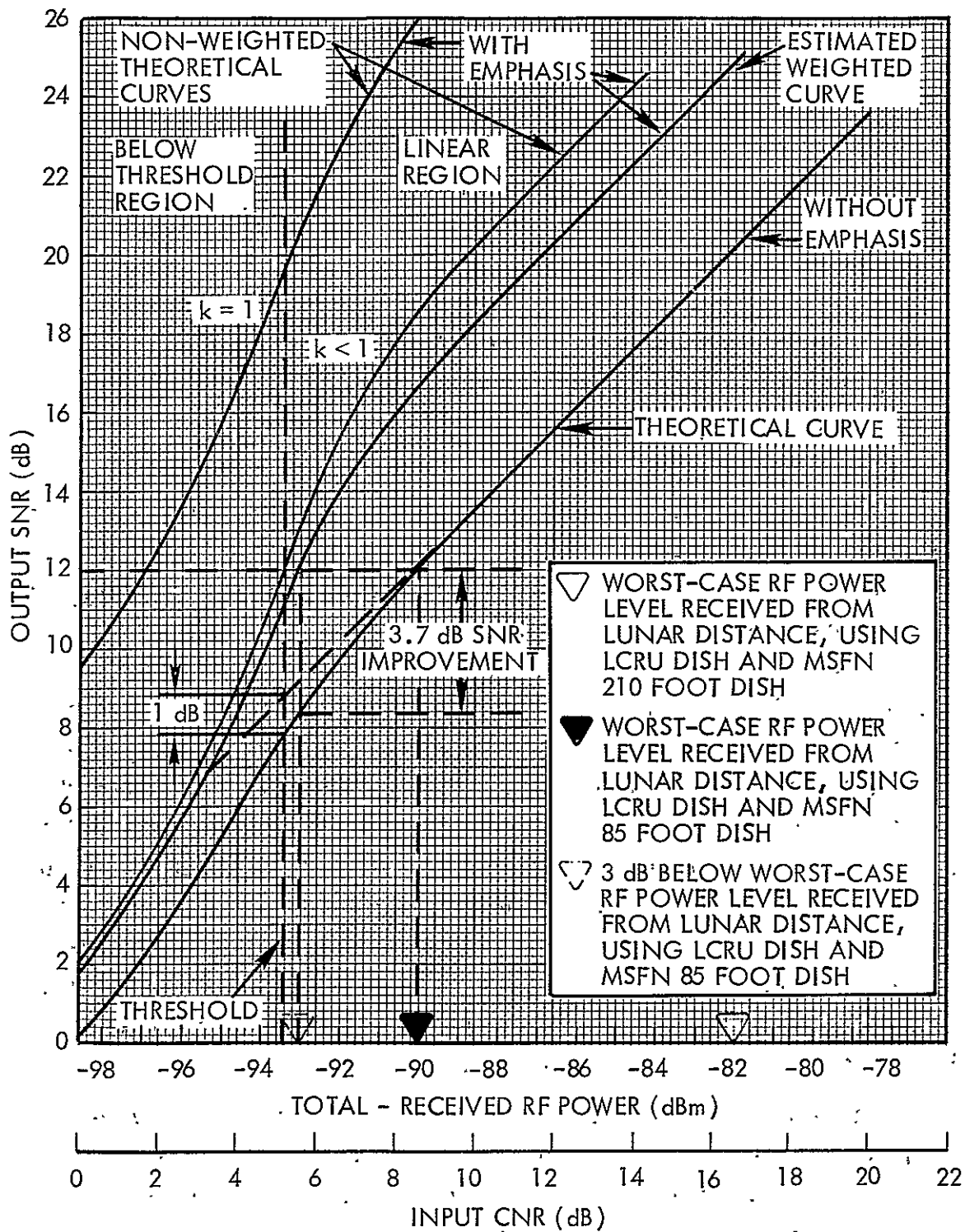
Figure 5-11. SNR Characteristic at TV Monitor With and Without Emphasis for Weighted and Non-Weighted Random Noise (f_1 = 0.25 MHz, f_M = 2.0 MHz)

in Figure 5-11. The top non-weighted theoretical curve (k = 1) is for the case where no effort is made to reduce the average power of the preemphasized modulating signal. This is essentially the condition under which the system testing was conducted (see Section 5.1). Section 3.7 shows that the additional SNR improvement due to the increased modulation level (case when k = 1) for a 250 kHz/2000 kHz network pair is +7.42 dB. The bottom curve (k < 1) depicts the non-weighted theoretical SNR when the equal modulating power constraint is satisfied. Notice that at -93 dBm (CNR = 5.7 dB) the top theoretical non-weighted curve (k = 1) with emphasis predicts a 12.3 dB improvement in signal-to-noise ratio. This value compares reasonably well with the minimum estimate of 3.7 dB SNR improvement determined experimentally when it is realized that:

(a) The theoretical curves are based on the optimum condition $f_1 = f'$, which is not generally the case due to the variation in video picture correlation. This means that the actual SNR improvement should be significantly less than the optimally predicted value.

(b) The theoretical curves assume non-weighted random noise. If the frequency weighting function of subjective random noise for color television were to be taken into account, the theoretically calculated SNR improvement would be weighted and thus would be significantly less than the non-weighted value.

(c) The experimentally observed estimate of a 3 dB RF power level improvement, corresponding to a 3.7 dB SNR improvement, is a minimum estimate only. The actual SNR improvement is greater than this value. No attempt was made to precisely determine the actual subjective SNR improvement in video picture quality.

For CNR's high above threshold, the SNR improvement becomes constant, as would be expected, since the noise density is now essentially parabolic.

From Section 3.6, it was learned that the weighted SNR improvement $\mathscr{R}_w$ obtained with emphasis is always less than the non-weighted SNR improvement $\mathscr{R}$. Thus, if an estimated weighted theoretical curve with emphasis were to be plotted in Figure 5-11, it would lie below the non-weighted theoretical curves. This is just what is done in Figure 5-11. It is an estimate only, since time did not allow for a computed curve to be drawn. Since the noise sensitivity weighting function (see Figure 3-18) was determined experimentally, there is no equation which represents it. Either the integration would have to be done numerically, or an approximating function for $w(f)$ would have to be found. The reason that the estimated weighted curve tends toward the non-weighted theoretical curves for low CNR's, in Figure 5-11, is because of the changing characteristic of the noise power density at the output of an FM demodulator for CNR's in and below threshold. As stated in Section 3.5, the weighting factor for FM transmission of video is larger than for AM transmission. Similarly, the weighting factor for parabolic noise is larger than for click noise. Since this is so, the weighted SNR improvement factor through emphasis, $\mathscr{R}_w$, will decrease for decreasing CNR's near threshold. The general form for $\mathscr{R}_w$ is

$$\mathscr{R}_w = \frac{\int_0^{B_0} N(f)\ w(f)\ df}{\int_0^{B_0} \frac{N(f)\ w(f)\ df}{|H_p(f)|^2}} \tag{5-2}$$

where $N(f)$ is the total noise spectrum at the output of an FM demodulator given by Equation (C-1).

6. CONCLUSIONS

The results of this study show that significant improvement in LCRU television performance can be achieved when using the preemphasis/deemphasis technique. This fact was demonstrated by total system tests, conducted at the MSC Electronic Systems Test Laboratory, involving subjective visual assessment of video color picture quality. Experimental results indicate that a minimum 3 dB RF level improvement can be obtained when using video signal preemphasis-deemphasis. This approximately corresponds to a minimum 3.7 dB video SNR improvement at an RF level 3 dB below the worst-case LCRU RF level. The experimentally estimated video SNR improvement was at the -93 dBm total-received RF power level for the LCRU-to-85-foot MSFN station link. The worst-case RF received power level from lunar distance, using the LCRU dish and MSFN 85-foot dish antennas, is -90 dBm. The RF level, -93 dBm, is then 3 dB <u>below</u> the expected worst-case RF level.

The subjectively observed SNR improvement was estimated to be a minimum of 3.7 dB at the -93 dBm RF power level (see Section 5.3). It is extremely difficult to compare this minimum estimate with a theoretically calculated figure because of the inherent difficulties associated with subjectively evaluating television picture quality and the very approximate manner in which the video picture quality improvement was estimated. The latter was primarily due to a time limitation and other factors. The experimental estimate obtained is just that, an estimate, and should be viewed as such. In addition, there are certain important facts which must be fully realized when comparing the estimated data with the theoretical data. They are:

- (a) The theoretical data is based upon the optimum condition $f_i = f'$, which is not generally the case due to the possible large variation in video picture correlation. This means that the actual SNR improvement should be <u>significantly</u> less than the optimally predicted value.

(b) The theoretical data assumes non-weighted random noise. If the frequency weighting function of subjective random noise for color television were to be taken into account, the theoretically calculated SNR improvement would be weighted and thus would be significantly less than the non-weighted value (perhaps by as much as 2 dB or more).

(c) The experimentally observed estimate of a 3 dB RF power level improvement, corresponding to a 3.7 dB SNR improvement, is a minimum estimate only. The actual SNR improvement is significantly greater than this value (see Section 5.2). No attempt was made to precisely determine the actual subjective SNR improvement in video picture quality.

A theoretical non-weighted SNR improvement of 12.3 dB for the -93 dBm RF power level (corresponds to CNR = 5.7 dB) was calculated (see Section 3.7 and Appendix C) for the case where no attempt is made to reduce the pre-emphasized signal modulation level (k = 1). This was the condition under which the system testing was conducted. With the above outlined pertinent facts well in mind, the theoretically calculated SNR improvement of 12.3 dB can be considered to compare reasonably well with the minimum estimate of 3.7 dB SNR improvement. According to the theoretical analysis contained in Appendix C, video SNR improvement increases with input carrier-to-noise ratio until the MSFN FM demodulator is operating far above threshold (RF levels above -90 dBm), at which point the SNR improvement becomes constant.

· A number of preemphasis and deemphasis networks were experimentally tested. It was determined that the preemphasized video did not appreciably degrade (less than 1 dB) the 1.25 MHz voice subcarrier, thereby eliminating the need for the 1.25 MHz notch-peak combination in the networks. Two examples of successfully tested preemphasis/deemphasis networks were those with 3 dB breakpoints at 100 kHz/2000 kHz and 250 kHz/2000 kHz, all with 6 dB/octave slopes.

In summary, good television picture quality is now obtainable at -90 dBm, the worst-case RF total-received power level for the LCRU-to-85-foot MSFN station link, when using video emphasis. Thus, simple preemphasis and deemphasis networks can provide improved LCRU television performance at a modest cost in terms of circuitry. It is recommended, therefore, that video signal preemphasis and deemphasis networks be implemented in the LCRU television system.

APPENDIX A

FRANKS' MODEL FOR A RANDOM VIDEO SIGNAL

A video signal was modeled and analyzed by L. E. Franks (Reference 2) in 1965 and earlier, in 1934, by Pierre Mertz and Frank Gray. Franks proposed a model, involving only a few essential parameters, which characterized the power spectral density of the random video signal. The continuous part of the power spectral density has been expressed as a product of three factors, which show separately the influence of point-to-point, line-to-line, and frame-to-frame correlation. Using parameters representative of typical picture material, Franks observed that the video spectral components were concentrated near multiples of the line scan and frame scan rates. This conclusion was in agreement with the results obtained earlier by Mertz and Gray.

It is common practice to interrupt the video signal after each line scan and frame scan in order to insert control signals such as synchronizing and blanking pulses. The resulting signal is called the composite video signal, $z(t)$, which is expressed as a random video process interrupted every T seconds for a time duration of αT seconds by an arbitrary periodic pattern, $w(t)$, inserted in the blank interval. The composite video signal, $z(t)$, is given by

$$z(t) = p(t)v(t) + w(t) \tag{A-1}$$

where $p(t)$ is periodic with period T, equal to one in the video interval and equal to zero in the blank interval; $w(t)$ is periodic with period T and equal to zero in the video interval; and $v(t)$ is a zero-mean random video process. The constant $1 - \alpha$ is the relative amount of time devoted to the video signal, since α is the relative amount of time devoted to the synchronization signal.

Franks found that the properties of typical picture material enabled him to make certain approximations which led to especially simple, closed-form expressions for the video power spectral density. The power spectral

density for the composite video signal as determined by Franks is

$$S(f) = (1 - \alpha)G_h(f)G_v(f)G_t(f)$$

$$+ \sum_{\ell=-\infty}^{\infty} |w_\ell|^2 \, \delta(f - \frac{\ell}{NT}) + \overline{d}^2\delta(f) \qquad (A-2)$$

where

$$G_h(f) = (\overline{d^2} - \overline{d}^2) \, \frac{2\lambda_h}{(2\pi f)^2 + \lambda_h^2} \qquad (A-3)$$

= an envelope function representing
horizontal picture correlation

$$G_v(f) = \frac{\sinh \lambda_v T_e}{\cosh \lambda_v T_e - \cos 2\pi Tf} \qquad (A-4)$$

= a function, periodic 1/T, representing
vertical picture correlation

$$G_t(f) = \frac{\sinh N\lambda_t T}{\cosh N\lambda_t T - \cos 2\pi NTf} \qquad (A-5)$$

= a function, periodic 1/NT, representing
frame-to-frame correlation

and

α = relative amount of time occupied by non-
video (synchronizing and blanking) portion
of the signal

$\overline{d}$ = mean value of the picture luminance

$\overline{d^2} - \overline{d}^2$ = variance of the picture luminance

λ_h, λ_v = average number of statistically independent luminance levels in a unit distance along the horizontal and vertical directions, respectively; Poisson rate parameter describing luminance process in horizontal and vertical directions, respectively

T_e = time interval equivalent to distance between adjacent lines at scanner velocity; time dimension of picture element

T = line scan interval in seconds

λ_t = Poisson rate parameter describing the luminance of a point at successive frames

N = number of lines per frame

w_ℓ = ℓth Fourier coefficient of the periodic signal $w(t)$ added to $\overline{d}$ in the blank interval.

As indicated in Figure A-1, the factors $G_v(f)$ and $G_t(f)$ impose a "fine structure" on the video power spectral density.
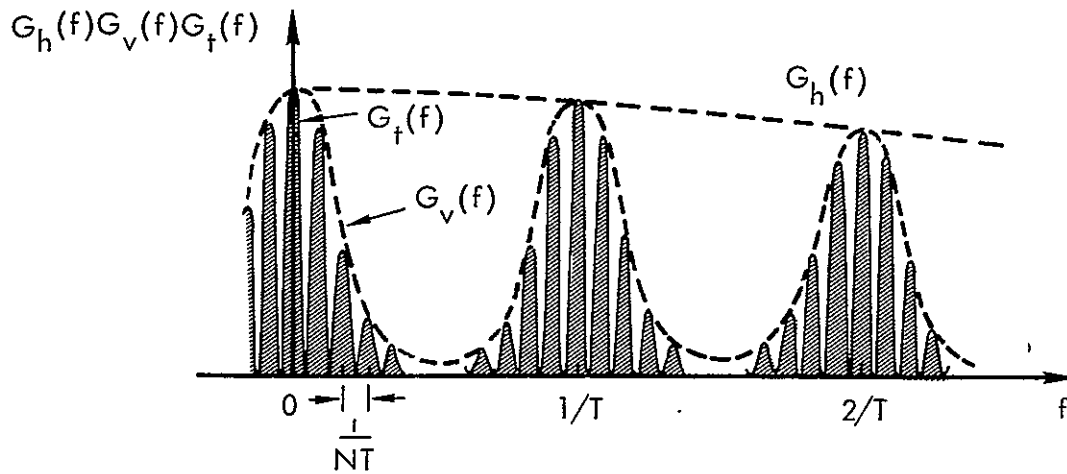
Figure A-1. Power Spectral Density of Video Signal With
Frame-to-Frame Correlation

In applications where the structure of $G_t(f)$ is too fine to resolve,
the smoothed version, $(1 - \alpha)G_h(f)G_v(f)$, of the continuous part of the
power spectral density is of interest. This quantity is shown in
Figure A-2 and is expressed as

$$S(f) = (1 - \alpha)G_h(f)G_v(f) \qquad (A-6)$$

$$= (1 - \alpha)(\overline{d^2} - \overline{d}^2)\left[\frac{2\lambda_h}{(2\pi f)^2 + \lambda_h^2}\right]\left[\frac{\sinh \lambda_v T_e}{\cosh \lambda_v T_e - \cos 2\pi Tf}\right] \qquad (A-7)$$

$$= K\left[\frac{2\lambda_h}{(2\pi f)^2 + \lambda_h^2}\right]\left[\frac{\sinh \lambda_v T_e}{\cosh \lambda_v T_e - \cos 2\pi Tf}\right] \qquad (A-8)$$

A-4

where

$\qquad$ K $\;=\;$ average video signal power

$$= \int_{-\infty}^{\infty} S(f)df \qquad\qquad\qquad\text{(A-9)}$$

$$= (1 - \alpha)(\overline{d^2} - \overline{d}^2). \qquad\qquad\qquad\text{(A-10)}$$
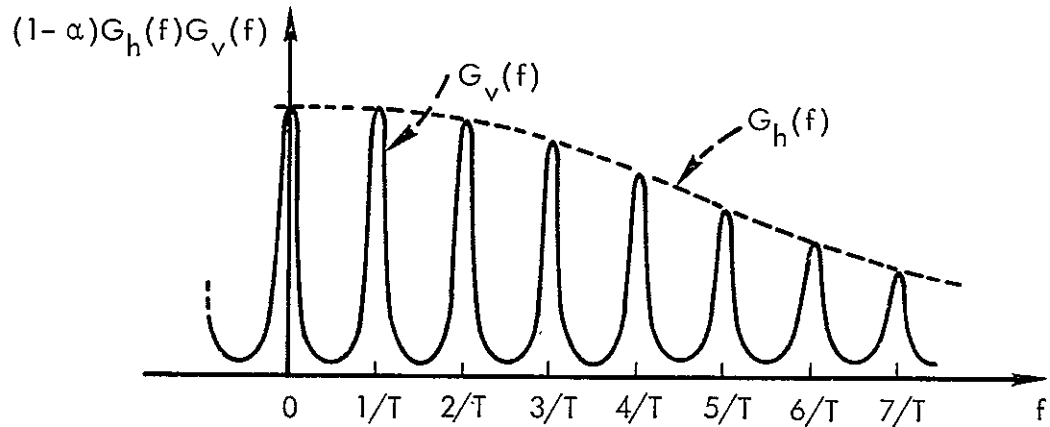
Figure A-2. Continuous Part of Power Spectral Density for Typical
Video Signal With Frame Rate Structure Smoothed Out

In addition, if it is assumed that the video picture has the same correlation between picture elements of dimension T_e in both the horizontal and vertical directions $(\lambda_h = \lambda_v = \lambda)$, then the continuous part of the video signal power spectral density for the case of sequential scanning becomes

$$S(f) = K \left[\frac{2\lambda}{(2\pi f)^2 + \lambda^2} \right] \left[\frac{\sinh \lambda T_e}{\cosh \lambda T_e - \cos 2\pi T f} \right]. \qquad\text{(A-11)}$$

The power spectral density for the case of 2:1 interlace scanning can be obtained from Equation (A-11) by replacing T_e by $2\ T_e$.

According to Franks (Reference 2), the random video picture may be characterized by an autocovariance which depends only on the variance, $\overline{d^2}$, (assuming the mean value of the picture luminance is zero) of the luminance and the two parameters λ_h and λ_v, which specify the average number of statistically independent luminance levels in a unit distance along the horizontal and vertical directions, respectively. Alternatively, the correlation is characterized by the parameters

$$\rho_h = e^{-\lambda_h T_e} \tag{A-12}$$

and

$$\rho_v = e^{-\lambda_v T_e} \tag{A-13}$$

which are the horizontal and vertical correlation coefficients between luminance values in adjacent picture elements when the picture area is quantized into small squares of dimension T_e. Similarly,

$$\rho_t = e^{-\lambda_t NT} \tag{A-14}$$

is defined as the frame-to-frame correlation coefficient between luminance values of a point (picture element) at successive picture frames.

APPENDIX B

SOLVING FOR THE COEFFICIENT k ASSUMING
FRANKS' MODEL FOR A RANDOM VIDEO SIGNAL

The ratio $\mathcal{R}$ by which preemphasis-deemphasis improves the signal-to-noise ratio of a FM signal has been shown previously to be

$$\mathcal{R} = \frac{f_M^3/3}{\displaystyle\int_0^{f_M} \frac{f^2}{|H_p(f)|^2}\,df} \, . \tag{B-1}$$

A suitable transfer function for the preemphasis network is

$$H_p(f) = k \left(1 + j\,\frac{f}{f_1}\right) \tag{B-2}$$

where f_1 is the frequency break point and k is the product of an amplifier gain A and the passive network attenuation ratio $\frac{r}{R}$. The bandwidth of the modulating video signal is given by f_M, which is also the bandwidth of the video baseband filter.

So that the bandwidth occupied by the output of the FM modulator may remain fixed, the requirement is made that the normalized power of the baseband signal m(t) must equal the normalized power of the preemphasized signal $m_p(t)$. This condition is described by the equality

$$\int_{-f_M}^{f_M} S(f)\,df = \int_{-f_M}^{f_M} S(f)\ |H_p(f)|^2\,df. \tag{B-3}$$

The power spectral density, S(f), of the video signal is assumed to have the form (Appendix A)

$$S(f) = S_0 \left[\frac{1}{1 + \left(\frac{f}{f_1}\right)^2}\right] \left[\frac{\cosh \lambda T_e - 1}{\cosh \lambda T_e - \cos 2\pi T f}\right]. \tag{B-4}$$

Substitution of Equation (B-4) into Equation (B-3) yields

$$\int_{-f_M}^{f_M} \frac{S_0}{1 + \left(\frac{f}{f'}\right)^2} \frac{\left(\cosh \lambda T_e - 1\right) df}{\cosh \lambda T_e - \cos 2\pi Tf}$$

$$\int_{-f_M}^{f_M} S_0 k^2 \frac{\left(\cosh \lambda T_e - 1\right) df}{\cosh \lambda T_e - \cos 2\pi Tf} \quad , \qquad (f_1 = f') \qquad (B-5)$$

when assuming that the preemphasis network has been designed so that its break point frequency, f_1, equals the -3 dB frequency, f', of the video spectral density envelope

$$S_e(f) = \frac{S_0}{1 + \left(\frac{f}{f'}\right)^2} . \qquad (B-6)$$

The coefficient k is then suitably adjusted so that the power constraint of Equation (B-5) is satisfied.

The integral on the left hand side of Equation (B-5) will now be evaluated. Integrals of this type, having an integrand A(f)B(f) where B(f) is periodic 1/T and A(f) is a slowly changing envelope function, can be closely approximated by (Reference 2)

$$\int_{-f_M}^{f_M} A(f)B(f) df \cong \sum_{m=-f_M T}^{f_M T} A\left(\frac{m}{T}\right) \int_{1/T} B(f) df$$

$$\cong T \int_{-f_M}^{f_M} A(f) df \int_{1/T} B(f) df . \qquad (B-7)$$

Accordingly, the first integral is evaluated,

$$\int_{-f_M}^{f_M} \frac{S_o}{1 + \left(\frac{f}{f'}\right)^2} \, df = \int_{-f_M/f'}^{f_M/f'} \frac{f'S_o}{1 + x^2} \, dx$$

$$= S_o f' 2 \tan^{-1} \frac{f_M}{f'} \tag{B-8}$$

The second integral is

$$\int_{1/T} \frac{\left(\cosh \lambda T_e - 1\right) df}{\cosh \lambda T_e - \cos 2\pi T f} \quad , \tag{B-9}$$

which after using the suitable change of variable $x = 2\pi T f$ becomes

$$\frac{(\cosh \lambda T_e - 1)}{2\pi T} \int_{1/T} \frac{dx}{\cosh \lambda T_e - \cos x} \tag{B-10}$$

$$= \frac{\cosh \lambda T_e - 1}{2\pi T} \frac{2}{\sqrt{\cosh^2 \lambda T_e - 1}} \tan^{-1} \frac{(\cosh \lambda T_e + 1) \tan(x/2)}{\sqrt{\cosh^2 \lambda T_e - 1}} \Bigg|_{1/T}$$

$$\left[\cosh^2 \lambda T_e > 1\right]$$

$$= \frac{\cosh \lambda T_e - 1}{\pi T \sqrt{\cosh^2 \lambda T_e - 1}} \quad \left[\frac{3\pi}{2} - \frac{\pi}{2}\right]$$

$$= \frac{\cosh \lambda T_e - 1}{T \sqrt{\cosh^2 \lambda T_e - 1}}$$

$$= \frac{\cosh \lambda T_e - 1}{T \sinh \lambda T_e} \quad , \tag{B-11}$$

since

$$\sinh \lambda T_e = \sqrt{\cosh^2 \lambda T_e - 1} \tag{B-12}$$

The integral on the left hand side of Equation (B-5) may now be easily solved by applying Equation (B-7),

$$
\int_{-f_M}^{f_M} \frac{S_0}{1 + \left(\frac{f}{f'}\right)^2} \; \frac{(\cosh \lambda T_e - 1)}{\cosh \lambda T_e - \cos 2\pi T f} \; df
$$

$$
= T \cdot S_0 f' \; 2 \tan^{-1} \frac{f_M}{f'} \cdot \frac{\cosh \lambda T_e - 1}{T \sinh \lambda T_e}
$$

$$
= 2 f' S_0 \frac{(\cosh \lambda T_e - 1)}{\sinh \lambda T_e} \; \tan^{-1} \frac{f_M}{f'} \tag{B-13}
$$

The integral on the right hand side of Equation (B-5) is evaluated in he following straightforward manner

$$
S_0 k^2 \int_{-f_M}^{f_M} \frac{\left(\cosh \lambda T_e - 1\right)}{\cosh \lambda T_e - \cos 2\pi T f} \; df = \frac{2 S_0 k^2 (\cosh \lambda T_e - 1)}{2\pi T} \int_0^{2\pi T f_M} \frac{dx}{\cosh \lambda T_e - \cos x}
$$

$$
= \frac{S_0 k^2 (\cosh \lambda T_e - 1)}{\pi T} \cdot \frac{2}{\sqrt{\cosh^2 \lambda T_e - 1}} \; \tan^{-1} \left. \frac{(\cosh \lambda T_e + 1) \tan x/2}{\sqrt{\cosh^2 \lambda T_e - 1}} \right|_0^{2\pi T f_M}
$$

$$
\left[\cosh^2 \lambda T_e > 1 \right]
$$

$$= \frac{2S_0 k^2 (\cosh \lambda T_e - 1)}{\pi T \sinh \lambda T_e} \cdot \frac{2 \, f_M}{f_1}$$

$$\tan^{-1} \left. \frac{(\cosh \lambda T_e + 1) \, \tan x/2}{\sqrt{\cosh^2 \lambda T_e - 1}} \right|_0^{\frac{2\pi T f_1}{2}}$$

$$= \frac{2S_0 k^2 (\cosh \lambda T_e - 1)}{\pi T \sinh \lambda T_e} \cdot \frac{2f_M}{f_1} \cdot \frac{\pi}{2}$$

$$= \frac{2 \, f_M \, S_0 k^2 (\cosh \lambda T_e - 1)}{\sinh \lambda T_e} \qquad \text{(B-14)}$$

where f_1 is the video signal line frequency $\left(\frac{1}{T}\right)$ and $2f_M/f_1$ is an integer.

After integrating the expressions according to Equation (B-5), k is determined by the condition that

$$2f' \, S_0 \, \frac{(\cosh \lambda T_e - 1)}{\sinh \lambda T_e} \, \tan^{-1} \frac{f_M}{f'}$$

$$= 2f_M \, S_0 k^2 \, \frac{(\cosh \lambda T_e - 1)}{\sinh \cdot \lambda T_e} \quad , \qquad \text{(B-15)}$$

which follows from the results of Equations (B-13) and (B-14). Finally solving for k^2, it is found that

$$k^2 = \frac{f'}{f_M} \tan^{-1} \frac{f_M}{f'} \qquad (B-16)$$

Using this expression for k, the transfer function of the preemphasis network becomes

$$H_p(f) = \sqrt{\frac{f'}{f_M}} \left[\tan^{-1} \frac{f_M}{f'} \right]^{\frac{1}{2}} \left(1 + j \frac{f}{f'} \right) \qquad (B-17)$$

$$= \sqrt{\frac{f_1}{f_M}} \left[\tan^{-1} \frac{f_M}{f_1} \right]^{\frac{1}{2}} \left(1 + j \frac{f}{f_1} \right) \qquad (B-18)$$

APPENDIX C
SNR IMPROVEMENT THROUGH EMPHASIS IN THE FM
THRESHOLD REGION

In the previous appendix and in the main body of the report, the signal-to-noise ratio improvement possible when using preemphasis/deemphasis on a FM channel was considered. At the time, the discussion was limited to high-input carrier-to-noise ratios, namely, where the carrier is above the threshold level and the FM demodulator is operating over the linear region of the output SNR - input CNR characteristic curve. By making this restriction, it was possible to considerably simplify the results.

In this appendix, the signal-to-noise ratio improvement through emphasis at CNR's in the nonlinear region of the FM detection process is considered. The calculation of noise effects in FM detection is usually quite tedious and difficult mathematically. Physical insight into the phenomena taking place, particularly in the case of the first FM threshold in which the noise begins to increase precipitously, tends to become obscured in the mathematical manipulations. However, there is an FM noise analysis available which is suggested specifically by experimental measurements. This is S. O. Rice's analysis (Reference 14), leading to the FM noise threshold in terms of the expected number of "clicks" per second at the output of an FM demodulator. It is found experimentally that as the input noise begins to increase, individual clicks are observed at the demodulator output. When a television signal is transmitted by FM, the upward clicks appear as white spots on the screen and the downward clicks as black spots, or vice versa, depending on the polarity of the connections. As the carrier-to-noise ratio continues to decrease, the number of clicks rapidly increases. It is at this point that the FM threshold is found to appear experimentally (usually in the vicinity of CNR = 8-10 dB for modulation indices greater than 10).

Following the analysis of Rice, the assumption is made that the total

noise spectrum at the output of an FM discriminator, with unmodulated
carrier plus Gaussian noise at the input, is the sum of the spectrum in
the high carrier-to-noise case (Gaussian distribution and a parabolic
spectrum) plus that due to the noise clicks. Thus, assuming a symmetrical
rectangular IF filter of width B_{IF} centered on f_c to simplify the analysis,
it is postulated that the total one-sided noise spectral density is

$$N(f) = \frac{4\pi^2 f^2}{B_{IF} \, CNR} + \frac{4\pi^2}{\sqrt{3}} \, B_{IF} \; erfc \; \sqrt{CNR} \qquad (C-1)$$

which holds only for $0 \leq f \leq B_{IF}/2$ with erfc x = 1-erf x, the complemen-
tary error function. N(f) is approximately 0 for $f > B_{IF}/2$. Equation
(C-1) is particularly valid in the important region in which the CNR is
large and f is small. It is the additional second term assumed due to
the clicks that gives rise to the threshold effect. As noted by Rice, and
as has also been verified experimentally, the rather simple form of Equa-
tion (C-1) leads to noise spectral-density curves that agree quite well
with those found using the more cumbersome, although perhaps more rigorous,
approaches to FM noise analysis.

From Equation (C-1) it is readily apparent that the clicks are assumed
to have a flat or white noise spectrum. This is valid providing the band-
width f_M of the low-pass filter following the demodulator is much less
than the spectral width of the noise clicks. Another way of stating this
is - since the width of the noise clicks is on the average much less than
$1/f_M$, where f_M is the video bandwidth, the noise pulses may be approximated
as delta functions of weight 2π. Note that Equation (C-1) introduces a
nonzero value for N(0), as is found in the exact analyses of others includ-
ing S. O. Rice.

As an example, N(f) (the one-sided noise spectral density) is sketched
in Figure C-2 for the rectangular IF filter and input noise spectral density
of Figure C-1. Values of CNR = 2 and CNR = 10 have been assumed. For
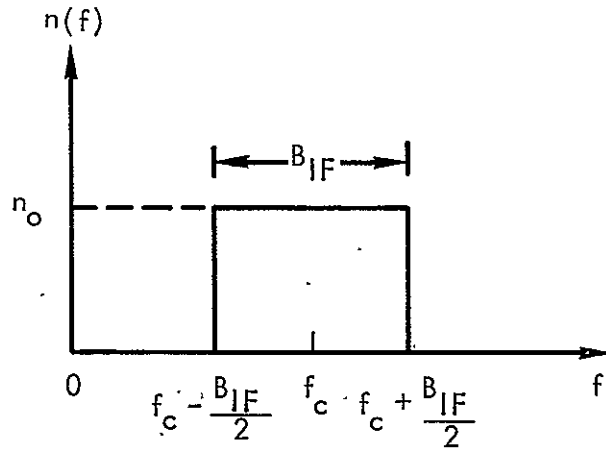this special case of a rectangular IF filter,

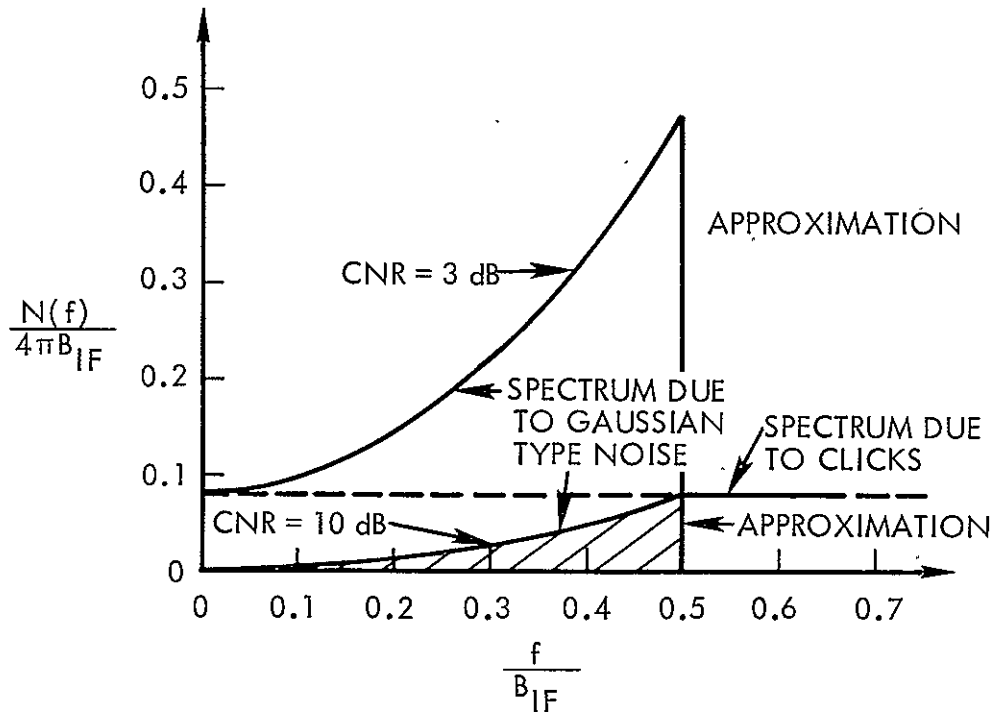Figure C-1. One-sided Noise Spectral Density,
Rectangular Bandpass Filter

Figure C-2. Approximate Output Noise Spectra Using "Clicks" Approach,
FM Discriminator, Rectangular IF Spectrum

$$\frac{N(f)}{4\pi \, B_{IF}} = \frac{\pi}{CNR} \left(\frac{f}{B_{IF}}\right)^2 + \frac{\pi}{\sqrt{3}} \; erfc \; \sqrt{CNR} \; . \qquad (C-2)$$

The above results for the noise spectrum at the output of an FM detector have been verified experimentally by others. They note that although the exact and approximate spectra differ substantially in the case of low carrier-to-noise ratio (for example, CNR = 1.5), there are some conspicuous similarities. For larger values of CNR the agreement between exact and approximate noise spectra improves markedly (Reference 14).

The signal-to-noise ratio improvement through emphasis is defined to be [Equation (3-8)]

$$\mathscr{R} \equiv \frac{(S/N)_{o \; emp}}{(S/N)_{o \; no \; emp}} = \frac{N_o}{N_{oD}} \qquad (C-3)$$

where N_{oD} represents the channel mean noise power when using the deemphasis network and N_o represents the mean noise power with no deemphasis network.

The average noise power in the output channel without emphasis is

$$N_o = \int_o^{f_M} N(f) \; df \qquad (C-4)$$

where f_M is the cutoff frequency of the output baseband filter. From Equations (C-1) and (C-4) with $f_M < B_{IF}/2$ and CNR >> 1,

$$N_o = \int_o^{f_M} \frac{4\pi^2}{B_{IF}} \frac{f^2}{CNR} \; df + \int_o^{f_M} \frac{4\pi^2}{\sqrt{3}} B_{IF} \; erfc \; \sqrt{CNR} \; df \qquad (C-5)$$

$$= \frac{4\pi^2}{B_{IF} \; CNR} \frac{f_M^{\;3}}{3} + \frac{4\pi^2}{\sqrt{3}} \; B_{IF} \; f_M \; erfc \; \sqrt{CNR} \qquad (C-6)$$

.The average noise power in. the output channel with emphasis is .

$$N_{oD} = \int_0^{f_M} \frac{N(f)}{|H_p(f)|^2} \, df \tag{C-7}$$

where $\quad |H_p(f)|^2 = k^2 \, [1 + (f/f_1)^2] \tag{C-8}$

is the square of the absolute magnitude of the preemphasis network response (the inverse of the deemphasis network response) and f_1 is the frequency break point with k the network coefficient. From Equations (C-7) and (C-8),

$$N_{oD} = \int_0^{f_M} \frac{N(f)}{k^2[1 + \left(\frac{f}{f_1}\right)^2]} \, df \tag{C-9}$$

$$= \frac{4\pi^2}{k^2 \, B_{IF} \, CNR} \int_0^{f_M} \frac{f^2 \, df}{1 + \left(\frac{f}{f_1}\right)^2}$$

$$+ \frac{4\pi^2 \, B_{IF} \, erfc \, \sqrt{CNR}}{\sqrt{3} \, k^2} \int_0^{f_M} \frac{df}{1 + \left(\frac{f}{f_1}\right)^2} \tag{C-10}$$

$$= \frac{4\pi^2}{k^2 \, B_{IF} \, CNR} \, f_1^3 \left(\frac{f_M}{f_1} - \tan^{-1} \frac{f_M}{f_1}\right)$$

$$+ \frac{4\pi^2 \, B_{IF} \, erfc \, \sqrt{CNR}}{\sqrt{3} \, k^2} \, f_1 \, \tan^{-1} \frac{f_M}{f_1} \tag{C-11}$$

Recall from Section 3.2.1 and Appendix B that the expression for the coefficient k satisfying the power constraint of Equation (B-3) for a video type signal is

$$k^2 = \frac{f'}{f_M} \tan^{-1} \frac{f_M}{f'} \tag{C-12}$$

$$\frac{f_1}{f_M} \tan^{-1} \frac{f_M}{f_1} \tag{C-13}$$

when assuming that the preemphasis network has been adjusted so that its break point frequency f_1 equals the -3 dB frequency f' of the video spectral density envelope. Inserting Equation (C-13) into Equation (C-11) yields the average noise power in the output channel with emphasis,

$$N_{oD} = \frac{4\pi^2}{B_{IF} \, CNR} f_1^2 f_M \left[1 - \frac{f_1}{f_M} \tan^{-1} \frac{f_M}{f_1} \right] \frac{1}{\frac{f_1}{f_M} \tan^{-1} \frac{f_M}{f_1}}$$

$$+ \frac{4\pi^2}{\sqrt{3}} B_{IF} \, f_M \, \text{erfc} \sqrt{CNR}$$

$$= \frac{4\pi^2}{B_{IF} \, CNR} f_1^2 \, f_M \left[\frac{f_M/f_1}{\tan^{-1}(f_M/f_1)} - 1 \right]$$

$$+ \frac{4\pi^2}{\sqrt{3}} B_{IF} \, f_M \, \text{erfc} \sqrt{CNR} \tag{C-14}$$

Using Equations (C-6) and (C-14) and recalling the definition of $\mathscr{R}$, the SNR improvement which results from preemphasis and subsequent deemphasis,

$$\mathscr{R} \equiv \frac{N_0}{N_{0D}}$$

$$= \frac{\dfrac{4\pi^2}{B_{IF}\,CNR} \cdot \dfrac{f_M^3}{3} + \dfrac{4\pi^2}{\sqrt{3}}\,B_{IF}\,f_M\,\text{erfc}\,\sqrt{CNR}}{\dfrac{4\pi^2}{B_{IF}\,CNR}\,f_1^2\,f_M\left[\dfrac{f_M/f_1}{\tan^{-1}(f_M/f_1)} - 1\right] + \dfrac{4\pi^2}{\sqrt{3}}\,B_{IF}\,f_M\,\text{erfc}\,\sqrt{CNR}}$$

(C-15)

$$= \frac{\dfrac{f_M^2}{3\,B_{IF}\,CNR} + \dfrac{B_{IF}}{\sqrt{3}}\,\text{erfc}\,\sqrt{CNR}}{\dfrac{f_1^2}{B_{IF}\,CNR}\left[\dfrac{f_M/f_1}{\tan^{-1}(f_M/f_1)} - 1\right] + \dfrac{B_{IF}}{\sqrt{3}}\,\text{erfc}\,\sqrt{CNR}}$$

(C-16)

For values of large CNR (CNR greater than 10 dB), where the number of clicks per second is small enough to be negligible and the Gaussian-type output noise dominates, the click noise term

$$\frac{B_{IF}}{\sqrt{3}}\,\text{erfc}\,\sqrt{CNR}$$

becomes negligible and Equation (C-16) reduces to the familiar form [Equation (3-45)],

$$\mathscr{R} = \frac{f_M^2}{3f_1^2}\;\frac{1}{\left[\dfrac{f_M/f_1}{\tan^{-1}(f_M/f_1)} - 1\right]}$$

(C-17)

$$= \frac{\tan^{-1}\left(\frac{f_M}{f_1}\right)}{3\left(\frac{f_1}{f_M}\right)\left[1 - \frac{f_1}{f_M}\tan^{-1}\left(\frac{f_M}{f_1}\right)\right]} \qquad (C-18)$$

For values of CNR below 10, the intensity of the clicks increases markedly, dominating the noise at the discriminator output and resulting in a sharp increase in output noise, as evidenced by the approximate noise spectrum for CNR = 2 sketched in Figure C-2. Due to the added presence of the flat noise spectrum due to clicks, which is nòt affected by the emphasis process, the signal-to-noise ratio improvement through emphasis decreases in the threshold region.

This fact becomes apparent from an inspection of the sketches of Figure C-3. The top curve, Figure C-3 (a), is an approximate output noise spectrum corresponding to a CNR = 2, whereas the bottom curve, Figure C-3 (b), is an approximate output noise spectrum corresponding to a CNR = 10. For the case of the bottom curve (large CNR), the percentage of noise passed through the deemphasis filter (ratio of transmitted noise power to input noise power) is considerably less than for the case of the upper curve (small CNR). The smaller the percentage of noise passed (or the greater the reduction in output noise power), the greater the signal-to-noise ratio improvement. A rectangular IF filter of width 4.2 MHz and a deemphasis filter with a breakpoint at 250 kHz was assumed for both cases.

Figure C-4 is a plot of the signal-to-noise ratio improvement factor $\mathscr{R}$ through emphasis versus input carrier-to-noise ratios, as derived in Equation (C-16).

(a) CNR = 2 (3 dB)
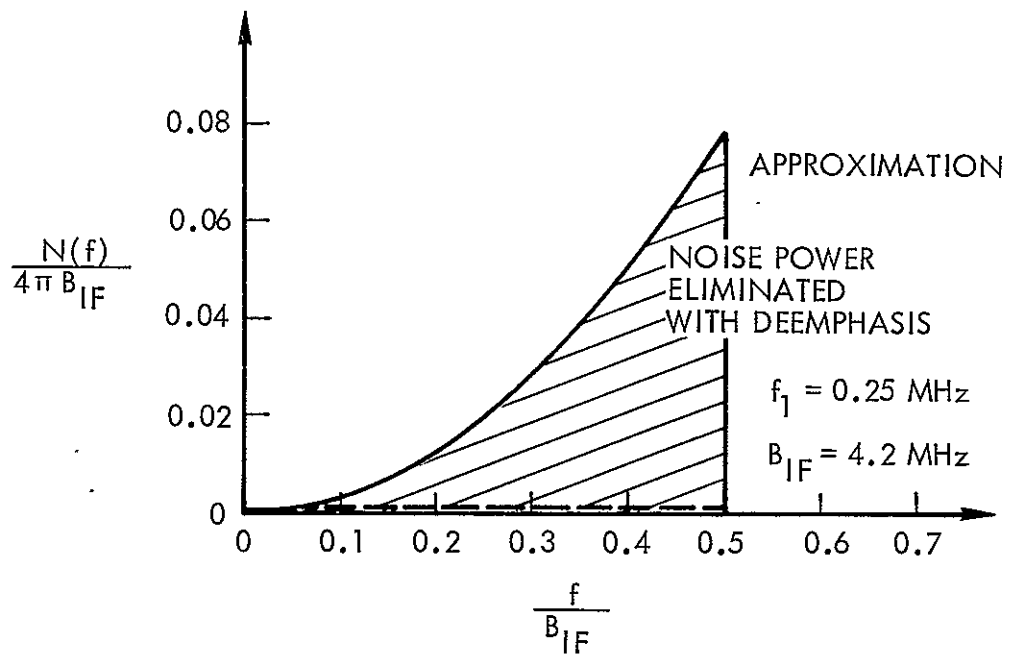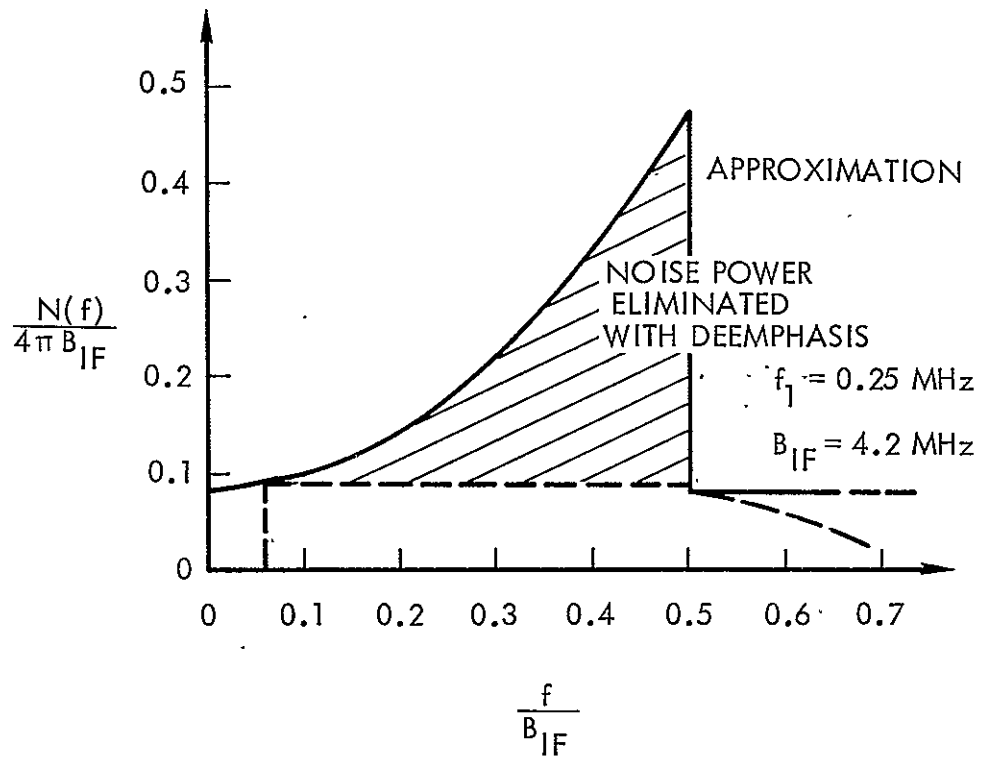

(b) CNR = 10 (10 dB)

Figure C-3. Effect of Deemphasis Upon Output Noise Spectra,
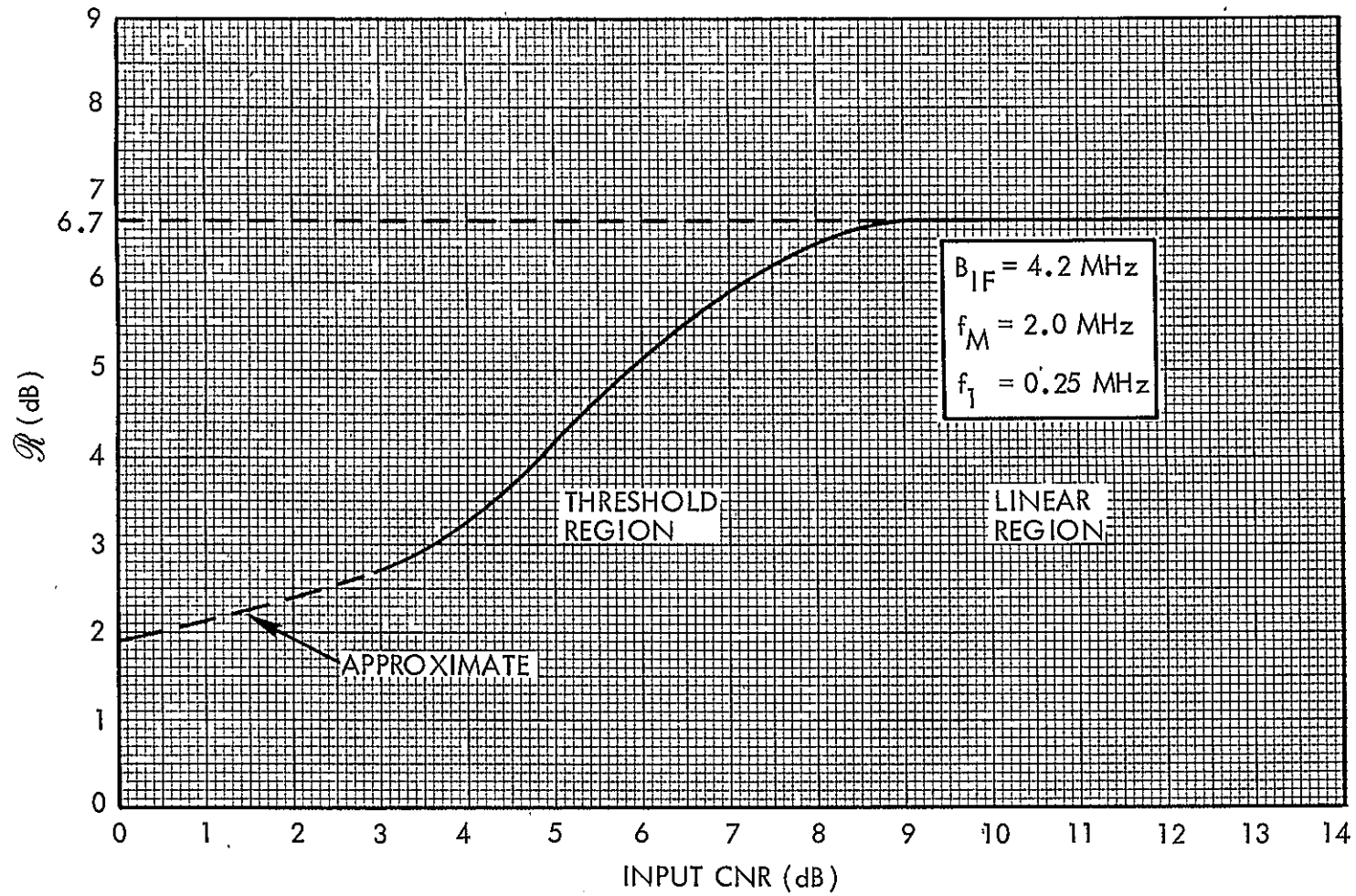FM Discriminator, Rectangular IF Spectrum

Figure C-4. Theoretical Non-Weighted SNR Improvement Factor
Through Emphasis versus Input CNR

.REFERENCES

1. J. D. Drummond, "Color-TV.Wheel Takes a Spin in Space," Electronics, Pages 114-117, July 1969.

2. L. E. Franks, "A Model for the Random Video Process," Bell System Technical Journal, Pages 609-630, April 1966.

3. P. Mertz and F. Gray, "A Theory of Scanning and Its Relation to the Characteristics of the Transmitted Signal in Telephotography and Television," Bell System Technical Journal, July 1934.

4. D. G. Fink, Television Engineering Handbook, McGraw-Hill Book Company, Inc., New York, New York, Page 8-59, 1957.

5. E. R. Kretzmer, "Statistics of Television Signals," Bell System Technical Journal, Pages 751-763, July 1952.

6. F. Carden, W. Osborne, and G. Davis, "Advanced Study of Video Signal Processing in Low Signal-to-Noise Environments," NASA Research Grant NGR-32-003-037, Page 10, December 1967.

7. M. Schwartz, Information Transmission, Modulation, and Noise, McGraw-Hill Book Company, Inc., New York, New York, Pages 305-309, 1959.

8. P. F. Panter, Modulation, Noise, and Spectral Analysis, McGraw-Hill Book Company, Inc., New York, New York, Pages 443-448, 1965.

9. D. L. Schilling, "Noise in Frequency-Modulation Systems" in Principles of Modern Communication Systems, Chapter 9, course notes, June 1969.

10. D. J. Sakrison, Communication Theory : Transmission of Waveforms and Digital Information, John Wiley & Sons, Inc., New York, New York, Pages 187-192, 1968.

11. P. Mertz, "Perception of Television Random Noise," Journal of the SMPTE, Volume 54, Pages 8-34, January 1950.

12. J. M. Barstow and H. N. Christopher, "The Measurement of Random Video Interference to Monochrome and Color Television Pictures," AIEE Transactions, Pages 313-320, November 1962.

REFERENCES (Continued)

13.   J. Jansen, P. L. Jordan, et al., "Television Broadcast Satellite
       Study," TRW No. 08848-6002-RO-00, NASA CR-72510, 24 October 1969.

14.   S. O. Rice, "Noise in FM Receivers" in Proceedings, Symposium on
       Time Series Analysis, M. Rosenblatt, Editor, John Wiley & Sons,
       Inc., New York, New York, Chapter 25, 1963.